College of Engineering Design and Physical Sciences
Department of Electronic and Computer Engineering

Detection of Abnormal Situations and Energy Efficiency Control in Heating Ventilation and Air Conditioning (HVAC) Systems

A thesis submitted for the degree of
Doctor of Philosophy

by

Dimitris C. Sklavounos
Bsc, Beng, Msc, MIEEE

Brunel University

September 2015

Brunel University
Uxbridge
College of Engineering Design and Physical Sciences
Department of Electronic and Computer Engineering

Dimitris C. Sklavounos

Detection of Abnormal Situations and Energy Efficiency Control in Heating Ventilation and Air Conditioning (HVAC) systems

September 2015

A thesis submitted for the degree of
Doctor of Philosophy

Detection of Abnormal Situations and Energy Efficiency Control in Heating Ventilation and Air Conditioning (HVAC) Systems

Abstract

This research is related to the control of energy consumption and efficiency in building Heating Ventilation and Air Conditioning (HVAC) systems and is primarily concerned with controlling the function of heating. The main goal of this thesis is to develop a control system that can achieve the following two main control functions: a) detection of unexpected indoor conditions that may result in unnecessary power consumption and b) energy efficiency control regarding optimal balancing of two parameters: the required energy consumption for heating, versus thermal comfort of the occupants. Methods of both orientations were developed in a multi-zone space composed of nine zones where each zone is equipped with a wireless node consisting of temperature and occupancy sensors while all the scattered nodes together form a wireless sensor network (WSN). The main methods of both control functions utilize the potential of the deterministic subspace identification (SID) predictive model which provides the predicted temperature of the zones. In the main method for detecting unexpected situations that can directly affect the thermal condition of the indoor space and cause energy consumption (abnormal situations), the predictive temperature from the SID model is compared with the real temperature and thus possible temperature deviations that indicate unexpected situations are detected. The method successfully detects two situations: the high infiltration gain due to unexpected cold air intake from the external surroundings through potential unforeseen openings (windows, exterior doors, opened ceilings etc) as well as the high heat gain due to onset of fire. With the support of the statistical algorithm for abrupt change detection, Cumulative Sum (CUSUM), the detection of temperature deviations is accomplished with accuracy in a very short time. The CUSUM algorithm is first evaluated at an initial approach to detect power diversions due to the above situations caused by the aforementioned exogenous

factors. The predicted temperature of the zone from the SID model utilized appropriately also by the main method of the second control function for energy efficiency control. The time needed for the temperature of a zone to reach the thermal comfort zone threshold from a low initial value is measured by the predicted temperature evolution, and this measurement bases the logic of a control criterion for applying proactive heating to the unoccupied zones or not. Additional key points for the control criterion of the method is the occupation time of the zones as well as the remaining time of the occupants in the occupied zones. Two scenarios are examined: the first scenario with two adjacent zones where the one is occupied and the other is not, and the second scenario with a multi-zone space where the occupants are moving through the zones in a cascade mode. Gama and Pareto probability distributions modeled the occupation times of the two-zone scenario while exponential distribution modeled the cascade scenario as the least favorable case. The mobility of the occupants modeled with a semi-Markov process and the method provides satisfactory and reasonable results. At an initial approach the proactive heating of the zones is evaluated with specific algorithms that handle appropriately the occupation time into the zones.

Acknowledgments

I wish to express my deepest acknowledgements to my supervisor *Professor John Stonham, Director of International Admissions, ECE Senior Tutor, Brunel University,* for his perceptive guidance, support, and encouragement throughout my research. Also, for his valuable advises regarding the structure and format of this Thesis.

I wish to express my deepest thankfulness to *Professor Evangelos Zervas, Electronic Department of Technological Education Institute of Athens,* for his valuable guidance and contribution to my research direction.

My deepest thanks and love to my family. To my wife *Annie* for her patience, love, faith, and support that generously offered me throughout the duration of this research, and to my beloved children *Alexandros* and *Stephanos* for the optimism and strength they mentally offered me every day and every moment.

September 2015

Contents

List of figures

List of tables

List of abbreviations

AHU	Air Handling Units
ARMA	Autoregressive Moving Average Model
ASHRAE	American Standard for Heating Refrigerating Air conditioning
BMC	Blended Markov Chain
BEMS	Building Energy Management Systems
CIBSE	Chartered Institution of Building Services Engineers
CUSUM	Cumulative Sum
FDD	Fault Detection
GAM	Generalized Additive Models
GMM	Gaussian Mixture Models
HVAC	Heating Ventilation & Air Conditioning
MC	Markov Chain
MIMO	Multiple Input Multiple Output
MPC	Model Predictive Control
PCA	Principal Component Analysis
PI	Proportional and Integral
PIR	Pyroelectric Infra Red
PSO	Particle Swarm Optimization
SCOPES	Smart Camera Occupancy Position Estimation Systems
SID	Subspace Identification
SVD	Singular Value Decomposition
SVM	Support Vector Classifier
VAV	Variable Air Volume
WSN	Wireless Sensor Network

List of nomenclature

Abnormal situations

Unexpected situations regarding power consumption in HVAC systems due to exogenous reasons such as high infiltration gains or high heat gains.

Comfort

The thermal comfort

Comfort zone

The range of the indoor temperatures that the human body feels thermal comfort.

Comfort cost

A value that represents the loss of thermal comfort per unit time

Comfort gain

A value that represents the gain of thermal comfort per unit time

Discomfort

The lack of thermal comfort

Discomfort cost

A value that represents the discomfort per unit time

Energy cost

The consumed energy

Full-proactive heating

Function when the heating of all zones in a multi-zone HVAC system is activated concurrently when occupancy is detected in one zone.

Full-reactive heating

Function when the heating of each zone in a multi-zone HVAC system is activated only when occupancy is detected into the zone.

Proactive heating

Function when the heating of a zone is activated in advance before the occupants enter into a zone.

Reactive heating

Function when the heating of a zone is activated only when the occupants enter into the zone.

Thermal Comfort

Thermal comfort is the condition of mind that expresses satisfaction with the thermal environment.

Chapter 1

Introduction

1.1 Scope of the Thesis

The present research work falls within the scope of energy efficiency in buildings, focusing on the energy consumption control in Heat Ventilation and Air Conditioning (HVAC) Systems. Since HVAC systems represent worldwide one of the most widespread energy supporting ways for buildings and homes, the control of their energy consumption remains nowadays one of the most important issues for the total energy savings. According to the U.S. Energy Information Administration from 2013 through 2040 the electricity consumption in the commercial and residential sectors will be increasing by 0.5% and 0.8% per year [1]. It's widely accepted through research studies that the main energy consumers in the commercial and residential buildings are the HVAC systems, as well as the lighting systems. Commercial and residential buildings consumed the 41% (or 40 quadrillion btu) of the total U.S. energy consumption in 2014. On the average of about 43% of the energy consumption of these building is due to HVAC systems [2]. HVAC systems of the commercial and residential buildings consume about 57% of the required energy and they are wasting more than 20% of energy due to various faults, insufficient control or improper positioning [52]. This technological area includes a wide range of topics and technologies with challenging research interest, where several valuable research studies have been elaborated and published and a number of them is presented in Chapter 2.

Since the energy consumption control at all levels is nowadays a very important issue, the energy control in HVAC systems is a challenging direction as they constitute a great energy consumer. Into this direction much of the global research community has been shifted. The objective of the research works is the development of innovative technologies capable to contribute towards this direction.

As stated in Chapter 2 the initial form of the control mechanism of the HVAC systems was centralized, i.e. a thermostat in a central point of the conditioned area controlled the temperature of the whole space, even if that was partitioned into rooms. This form of control resulted to a poor management of the energy efficiency due to the issues of temperature variability between the rooms, as well as the lack of occupancy in a number of the zones.

A more modern way of control is the multi-zone model which is extensively applied is space with many individual areas (rooms) i.e. large homes, and buildings. The rationale of the multi-zone control model is to provide an independent control of the air-conditioning system in all of the individual areas (zones). This concept has been the basis for the development of the demand-driven HVAC systems, which have already led to much more effective control, with significant rates of reduction of unnecessary energy waste.

All methods of this thesis are based on the multi-zone control model of nine zones, utilizing the functionality of a wireless sensor network (WSN), which consists of wireless nodes placed in each zone containing temperature and occupancy sensors. The nodes are programmable and cable to implement the functionality of the proposed algorithms. The control of the energy consumption concerns only the energy spent for heating and it's not related to any of the other functions of the HVAC systems (cooling, humidifying etc). The dynamics of the temperature of the zones are based on a lumped capacity model applied in discrete time state space form. For the outside temperature the Walter's model is applied which provides the variations of the temperature during the period of one day. The comfort zone thresholds used for the energy efficiency control are according to ASHRAE 55 standard. The method is adaptable to accept also the thresholds of the European standard EN15251 according to Chartered Institution of Building Services Engineers (CIBSE).

1.2 Aims and Objectives

The motivation of this research relies on the contribution to energy control of the HVAC systems in buildings, which remains one of the most significant energy consumers worldwide.

This research aims to the development of a heating energy control system in a nine-zone HVAC space system, equipped with a WSN as described above. The control system will be able to achieve two control functions. The first function is the detection of unforeseeable indoor conditions that may directly affect the normal operation of the heating, concerning the normal required energy spent and this case is referred as "abnormal situations". The second function is to provide an optimum possible balance between the total energy cost and the total discomfort cost, by utilizing the occupancy information of the zones as well as the occupation times into the zones.

The first objective for the detection of abnormal situations is the evaluation of the statistical Cumulative Sum (CUSUM) algorithm as a change detection mechanism for the detection of power deviations due to exogenous factors that may affect the indoor temperature, such as high infiltration gain and extra heat gain. High infiltration gains may be caused by openings that allow air entry with lower temperature, while extra heat gains may be caused by fire events.

The second objective is the detection of the preservation of lower levels of temperature due to the above exogenous factors, resulting to an aimless energy waste. The third objective is an initial stage of the energy efficiency control and constitutes the development of algorithms aiming to apply proactive heating to the zones, which take into account the parameters of the occupancy information of the zones in binary manner and the occupation time of the zones, with the task to achieve an optimum energy consumption alongside with a satisfactory level of thermal comfort. The term "proactive heating" states the situation where the heating of a zone is activated before the occupants enter a zone..

The fourth objective of the same control function which aims to contribute to the overall energy efficiency is the decision based activation of the heating in the unoccupied zones proactively, according to a criterion that compares the risk of

the energy cost versus the risk of the discomfort cost. This control function will result to the reduction of the total energy consumption alongside with the maintenance of the total thermal comfort to satisfactory levels.

The methodology for the achievement of the first objective is based on a lumped capacity model as a heat transfer dynamic model, which is run by the node of each zone providing the ideal power profile. By comparing the ideal power profile with the real controlled power produced by a PI controller the CUSUM algorithm is expected to detect changes in the distribution of the power profile when an extra heat gain or leakage will be applied in a zone.

The methodology for the achievement of the second objective is based on the utilization of the deterministic SID predictive model, as the key mechanism for the temperature prediction of the zones. The detection mechanism relies on the comparison of the predicted temperature with a real one and when the same exogenous factors are applied, possible divergences of the predicted temperature behaviour, are expected to be indicated. With the support of the CUSUM algorithm the detection is expected to be accurate as it will detect changes in the mean of the rate change of the prediction error.

Two methods are proposed to satisfy the objectives of the second control function concerning the energy efficiency.

For the achievement of the third objective as an initial stage for energy efficiency control, three algorithms are developed. The algorithms are aiming to a proactive heating of the zones according to the occupation time into the zones, with the logic that the longer is the mean of the occupation time into the zones the less is the need of the proactive heating to the adjacent zones. The algorithms are compared with the full-proactive as well as the full-reactive heating modes. The term “reactive heating” states the fact that the heating in a zone activates when occupants enter the zone while the term “full-proactive” heating means that when occupants enter one zone of the nine-zone model the heating activates in all zones. For the achievement of the fourth objective a novel technique is proposed which aims to balance the comfort and energy costs in the nine-zone HVAC system. Aiming to a proactive heating, the proposed method periodically computes the risk of activating the heater or not and decides in favor of the

action that produces the smaller risk. The computation of the risks relies on the relative weights of the energy and discomfort costs so that the balance between the total energy consumed and the total discomfort cost may be regulated. The decision process itself relies on two kinds of predictions: a) temperature-time predictions for the zones and b) the zones' occupancy profile. The emphasis is on the zones' temperature predictions and to this end a deterministic SID method is also used to model the thermal dynamics of each zone. Two scenarios are examined: a two zone scenario with only the one zone occupied and the cascade scenario when occupants are moving through the zones following a certain path. The method is expected to achieve an optimum balance between the aforementioned costs.

1.3 Organization of the Thesis

The structure of the Thesis is as follows: Chapter 1, contains the introduction including the scope, the aims and objectives and the organization of the Thesis. Chapter 2 contains a concise review of the Heat Ventilation and Air-Conditioning (HVAC) systems technology, the state of the art of the HVAC control systems, and related work of both the aforementioned directions. In Chapter 3 the fundamental theoretical models are presented: the multi-zone model including the single zone model as a part of it, as well as the weather model for the outside temperature estimation. Chapter 4 presents the utilized detection mechanism (CUSUSM) and the system predictive model (SID). In Chapter 5, the two proposed methods for detection of abnormal situations are analytically presented, while Chapter 6 contains the results of the methods. Chapter 7 presents the two proposed methods for the energy efficiency control and in Chapter 8 the results of the two methods are outlined. Finally, Chapter 9 initially presents the summary and conclusions of the Thesis evaluating the novelties and the outcomes of the research. Furthermore, directions of the future work are outlined.

Chapter 2

Review of the HVAC systems technology and related work

2.1 Introduction

Heat ventilation and air conditioning (HVAC) systems have been established for a long time, as one of the most widespread energy support ways, mainly in homes, buildings, public transport vehicles and even spacecrafts. The design of HVAC systems should include all possible requirements and complexity, always aiming to the best possible energy efficiency. Sophisticated control systems have been developed and implemented contributing to a more efficient energy consumption control of the HVAC systems, by taking into account parameters such as occupancy and thermal comfort. These control systems have been evolved through several valuable research works carried out, providing significant results towards this direction. In this Chapter the evolution of the HVAC systems is concisely presented in Section 2.2, the HVAC technology features related to this work are presented in section 2.3, the state of the art of the control systems technology is presented in Section 2.4, while the related work of both directions of this Thesis is presented in Sections 2.5 and 2.6.

2.2 The evolution of the HVAC systems

While with the use of fire, people were using heating since antiquity, the cooling function was invented in 1851 by Dr John Gorrie and came into use in 1880 in the USA mainly for industrial purposes. Initially the use of cooling applied to preserve food and also for creating and transporting ice, while from the beginning of the 20th century it began to be implemented for air conditioning in building sites, starting with the building of the New York Stock Exchange in 1902. Nowadays this technological sector is determined by the term "Heat Ventilation and Air Conditioning Systems" (HVAC). Also the term "Air

Conditioning", while in the past meant primarily only the cooling operation, now includes a set of functions that determine Temperature, Moisture in the air (humidity), Supply of outside air for ventilation, Filtration of airborne particles and Air movement in the occupied space.

The evolution of the HVAC systems technology was based on the progress and technological achievements of several science and engineering sectors, such as thermodynamics, fluid mechanics, electrical engineering, medicine, construction and materials engineering and more.

The spreading and implementation of the HVAC systems has been based on technological breakthroughs such as cooling, (initially applied in food preservation), computerization and networking applied for advanced control of large installations of HVAC systems in buildings and medical discoveries such as the effects of passive smoking on humans, affecting the ventilation methods.

Despite the great progress and state of the art technology of HVAC systems, there are still areas of their scope that need optimizations and thus, they remain challenging research fields. Indicatively, such areas are: the quality of the indoor air, the gases emitted, and the energy consumption control [3]. On the last research area (energy saving) focuses the present research thesis.

2.3 Technology features of the HVAC systems

2.3.1 The functionality of the Air-conditioning

The main processes that must coexist in order to achieve a full and adequate air conditioning are seven: The heating, cooling, adding moisture (Humidifying), the removal of moisture (Dehumidifying), the air-cleaning (Cleaning), the ventilation (Ventilating) and the movement of air. A full air-conditioning system must be able to achieve proper control of temperature, humidity, external air supply, the cleaning process and the air moving in the conditioned area. The functions of the air conditioning system can be summarized as follows [3]:

1. *Heating* - the process of adding thermal energy (heat) in the space in order to maintain the desired temperature.
2. *Cooling* - the process of removing heat from the space to reduce the temperature or maintaining a temperature less than the outside.
3. *Humidifying* - adding water vapor to the air of a conditioned space in order to increase or maintain the required air humidity.
4. *Dehumidifying* - the reverse process of humidifying. Removal of moisture from the air of a conditioned space.
5. *Cleaning* - removing harmful particulate matter (dust, pollen, etc.) to clean air space.
6. *Ventilating* - Air exchange between the outdoor and indoor air-conditioned area for the renewal and freshness of indoor air; Naturally or by means of holes created during installation, or mechanically by fans who absorb outside air and the channel via the airways.
7. *Air movement* - The process of circulation and mixing of air between the conditioned spaces to achieve proper ventilation and to facilitate heat transfer between sites.

2.3.2 Muli-zoned HVAC systems

Traditional air conditioning systems were designed in such a way as to treat the whole conditioned space as a single entity, even though it has been partitioned into smaller areas (rooms etc) as it usually done. The air-conditioning system was based on an air source for the whole area of certain dimensions, where the temperature of the entire space was controlled by one thermostat. Since the building areas have a diversity in size and thermal loads the previous design logic of the HVAC systems was ineffective and, furthermore, exhibited high energy consumption rates. The need to amend these systems was imperative in order to create HVAC systems that provide independent sources of heating or cooling in each area and therefore independent control. Each separate area in this type of HVAC systems is called "zone" and usually each zone has independent air-conditioning requirements. A zone is an independent part of a large building space (a room or a hall) and can consist of a single open space or more than one

premises with common air-conditioning requirements. Based on the multi-zoning and how the HVAC systems provide heating and cooling, there are four categories of HVAC systems which are [3]:

1. All-air systems
2. Air-and-water systems
3. All-water systems
4. Unitary, refrigeration-based systems.

2.3.3 Thermal Comfort

A very important parameter included in the study and design of air-conditioning systems is the thermal comfort. The term 'thermal comfort' 'reflects the mental state in which the human mind is satisfied with the thermal environment in which it is located. It is very important to maintain the level of thermal comfort in air-conditioned building spaces and that is a very challenging objective in the design of HVAC systems. Thermal comfort in the human body can be maintained when the heat, generated due to metabolism, diffuses in the environment and so the body is maintained in thermal equilibrium [3].

Factors that directly influence the thermal comfort of the occupants are individual (due to functions of the human body) and environmental. The first category includes factors such as the metabolic rate and clothing insulation, while in the second category are the air temperature, the operative temperature, the air speed and the relative humidity. These factors will not be described in full details throughout this thesis because they aren’t included in the proposed methods in terms of thermal comfort. The proposed methods evaluate thermal comfort based on the adaptability or accessibility model of the human body.

The adaptability of the human body at different temperatures and the influence of the ambient temperature on the indoor temperature are the basis of the adaptive comfort model of ASHRAE (standard 55-2010). This model incorporates the results of a study of 160 buildings which showed that the occupants in buildings with natural ventilation accept a wider range of temperatures than those in sealed air-conditioned buildings.

This is because the required temperature depends on the temperature conditions of the external environment. The diagram of the adaptive model (Fig. 2.1) shows the interior comfort temperature at prevailing external environment temperatures and identifies the zones of 80% and 90% satisfaction.

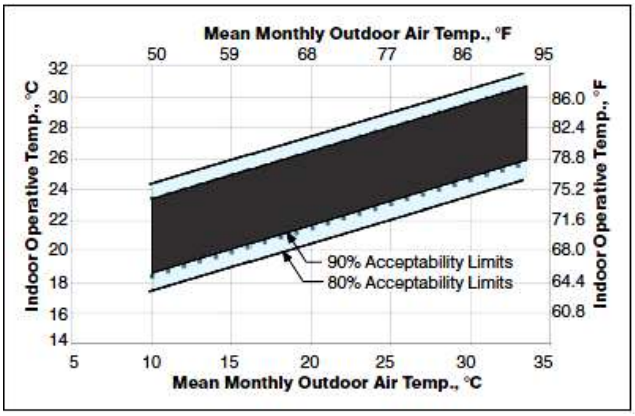

Figure 2.1 Acceptable operative temperature ranges for naturally conditioned spaces [4]

Based on the average of daily outdoor temperatures, the standard ASHRAE 55-2010 introduced the prevailing average outside temperature as an input variable in the adaptive model. This average temperature was calculated at samples of 7 to 30 days prior to the day in question. The adaptive model applies to rooms with natural air conditioning where the outside temperature directly affects the internal and therefore the comfort zone of the occupants.

Also, in order to apply the adaptive model there should be a cooling system in the conditioned space and the occupants will be engaged in sedentary activities with metabolic rates 1 - 1,3 met and an average temperature of 10^{o} (50^{o}F) to 33,5^{o}C (92,3^{o}F). Studies of de Dear and Brager showed that occupants have greater tolerance to a wider range of temperatures when they are in places that are air-conditioned with natural air rather than in spaces with manual air conditioning. This is due to adaptive processes by both physiology and by behaviour. The thermal adjustment categories are three: the behavioural, the physiological and the psychological.

2.3.4 Energy consumption control in HVAC systems

In this research field, innovative methods is attempted to be proposed that will contribute in the reduction of the total energy consumption in new and existing buildings. Two are the key parameters taken into account: the thermal comfort and the air quality of the indoors environment. To this end, several valuable research studies *(Sections 2.5 & 2.6)* propose innovative methods by taking seriously into account the overall costs, further to the aforementioned parameters. Some of these studies are trying to exploit the existing infrastructure, such as Wi-Fi networks or mobile telephones etc. in their methods. Various disciplines are combined in this sector to generate innovative methods based on existing mechanisms. A typical example is the utilization of a WSN consisting of wireless nodes of temperature and occupancy sensors for controlling the use of the HVAC system on demand. Here a combination of two technological sectors is taking place: the sector of the air conditioning systems and the sector of electronics and computer networks. In this particular case of technological combination falls the present research work. All the proposed control methods are based on the parallel functionality of a WSN and a HVAC system. The WSN which consists of wireless nodes installed in each zone provides information concerning temperature measurements as well as occupancy detections. This information is utilized appropriately according to the specific proposed algorithm so that, the desirable control function is provided. Also the ASHRAE 90.1-2004 standard for buildings and homes, developed by the American Society of Heating, Refrigerating and Air Conditioning (ASHRAE) and the Illuminating Engineering Society of North America (IESNA) associations, in order to cover the interaction of electric lighting elements and air conditioning, since the first produces heat energy.

2.4 Review on the energy control systems of HVAC

The energy consumption control in buildings is an indispensable process with high complexity. This complexity may be due to the way in which current technology manages the issue of energy control, on the one hand from the energy source (oil, electricity, RES) and on the other hand from the management of the individual loads of energy consumption (heating, lighting etc).

The evolution of the research and technology over the years has brought significant improvements in the reduction of total energy consumption in buildings, since several innovative methods *(Sections 2.5 & 2.6)* have been invented and implemented for this purpose. Modern building energy management systems (BEMS), which form an integral part of intelligent building, exploit the technology of wireless sensor networks, which is constantly evolving.

Wireless sensor networks have widely replaced old fashioned wired control systems or are used in addition, due to their flexibility and low costs of installation, expanding existing plants. Several building energy control technologies, which have been implemented in previous decades, have a distinctive name of identification. For example: Energy Management Systems (EMS) or else Building Automated Systems (BAS) belong back in the 1970s, and they were implemented aiming to improve energy efficiency by controlling the total power of the heating and lighting systems. As the form of the building units evolved in terms of size and overall design, from the next decade (1980s) an effort began to consolidate the various applied technologies and to form more integrated systems for the energy control in buildings.

In the early 1990s, a new type of thermostats based on PID control and artificial intelligence techniques was developed for the control of temperature, while towards the end of that decade, the technology of Predictive control began to be applied which is still in place and research. This technology utilizes environmental factors as input data for the control of HVAC systems.

2.4.1 Wireless Sensor Networks (WSNs) in HVAC energy control

Nowadays, a significant number of advanced automation and control systems find application in buildings, which utilize the technology of wireless sensor networks (WSNs). Such systems have been proposed and developed by numerous very important research works and subsequently they entered the commercial production for their implementation. Nevertheless, research continues to evolve in the field of energy saving, aiming to improve areas with existing research challenges.

A general design framework of such energy control systems usually consists of three layers (Figure 2.2).

The first layer namely the "sensor layer" deals with the collection of information and it contains all the proper systems and devices for this purpose. Such systems are typically sensor nodes that can communicate with each other or with a central computing unit thus forming a sensor network (wireless or wired).

The second layer (the computation layer) is responsible for the collection and management of the information data and at this layer typically belong central computing units such as servers.

The third layer is responsible for the regulation and control of the various electrical devices and includes a set of intelligent control units such as smart thermostats, smart outlets, relays and more.

The information provided from the sensor layer to the computation layer are utilized by the second in an appropriate way and in combination with other types of information such as statistical or weather condition data, so that it would form proper input data for more complex mechanisms. These mechanisms are usually sophisticated algorithms derived from research studies, for handling various energy consuming building systems (HVAC, lighting, etc) in such a way as to result in energy savings.

The logic of the proposed methodology of this thesis, as described in Chapter 3, has been based on the above architecture of energy control systems.

The simulating algorithms are utilizing a wireless node network of temperature and occupancy sensors functioning appropriately for energy efficiency as well as detection of possible aimless energy consumption. The mode of the WSN

operation is either decentralized when there is communication among the nodes or centralized when the nodes are communicating with a central computing unit.

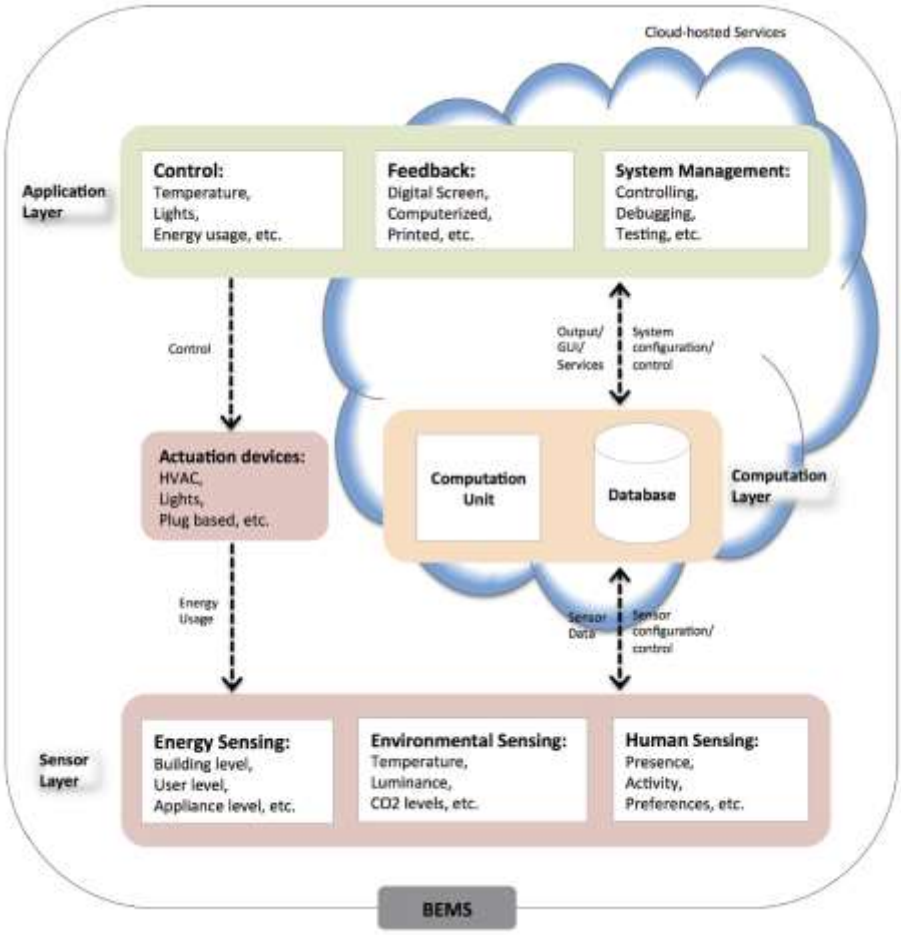

Figure 2.2 Building Management System Architecture [5]

2.4.2 Autonomous Energy Control Systems

Autonomous energy control systems are do not require human intervention. Such systems are mainly used for the control of HVAC and lighting systems in buildings because both of them belong to the category of the highest energy consuming sectors. Autonomous systems utilize several types of sensors as temperature, passive infrared (PIR) or carbon dioxide (CO_2) sensors, sensors for the occupancy detection in various areas as well as light and sound control

sensors, which inform the central server unit for monitoring the indoor space as well as the external surroundings of the building.

The algorithm determines the activation of various actuators to implement the required function of the certain units. For example, the deactivation of the heating system or the reduction of the temperature to a desired level and also the switching on/off of the lighting system. For the HVAC systems control, the modern autonomous systems execute algorithms that exploit the occupancy of the zones and the thermal comfort level as two significant parameters for control.

2.4.3 State of the art technology of sensor units

The state of the art technology of HVAC systems control has been evolved sufficiently to provide integrated sensor system units extensively programmable with communication capabilities, which form the basis for further development and research of control mechanisms.

2.4.3.1 Wireless temperature sensors and controllers

Nowadays, various types of sensor modules like temperature, humidity, occupancy etc sensors, with wireless capability, are commercially available. These units have become widely applied in homes, commercial buildings, industrial sites, museums etc providing basic control functionality in usually binary (on/off) mode like activating the lighting when occupancy is detected and deactivating on departure of the occupants. Individual sensor devices would be capable to provide a basic control with no special demands and they come under a limited use in places where a more advanced control is not necessary. Moreover, commercially available more integrated sensor units consist of a number of different sensors and thus combing a number of detection functions that provide a more accurate, demanding and effective control.

Such units constitute sophisticated controllers for HVAC systems because they combine the operation of various sensors in an integrated device and thus they are capable to carry out a more comprehensive control compared with one type of individual sensor. For example, one sensor detects the opening or closing of the door, while another sensor (PIR sensor) detects the presence or absence of

people as well as the entrance or the departure of the occupants from the zone. By utilizing this information from the sensor unit as input, the controller executes a program of an algorithm concerning occupied or unoccupied zone, enabling or disabling the thermostat HVAC system.

The industry also manufactures controller systems with the capability of learning. This type of controllers requires a time period of approximately one week to learn how the occupancy schedule is formed during this period. After they have built a fixed occupancy schedule, they are able to proactively heat or cool the zones, as well as trigger deactivation. In cases of inactivity (no occupancy) they can either choose to set the target temperature to a comfortable level or deactivate the heating / cooling system. This depends of the next scheduled occupancy time. Moreover, they provide the adjustability service via mobile phones though the appropriate software application. Finally, fully programmable controller systems have been manufactured, which provide network connectivity and capability to cooperate with other sensor units that can be adapted with them [6,7,8,9].

2.4.3.2 Wireless occupancy sensors

In recent years the occupancy sensor units have become a very important tool in research on energy saving in HVAC systems, since they greatly contribute in detecting occupants in different ways, and this information is properly utilized by various control mechanisms. Nowadays, there are various occupancy sensor technologies which are applied appropriately, with significant detection capabilities. Occupancy sensor types regarding their technology that may be utilized for the purposes of the proposed control techniques of this work are described below.

For example, the turnstile sensors, although they accurately record the occupants due to contact, they cannot be implemented to spaces of large commercial buildings where the occupants' swarming is huge, because that way, it will cause a funnel situation, large accumulation of people in the traffic flow. Their application may be limited to specific areas such as specific entrances where there is a special requirement of occupants' detection or record.

Wider implementation for occupants' detection in commercial buildings and generally in large areas, use types of sensors that do not require human contact. Such types are the infrared, ultrasonic, microwave sensors, as well as camcorders equipped with special software for counting occupants, and pyroelectric infra red (PIR) motion sensors, which can also detect and count occupants in a particular area in addition. PIR sensors are usually used in pairs so that they can also determine the direction of the occupants' motion, for example if someone is entering or exiting the door of a room. The implementation of PIR sensors may be limited due to certain weaknesses: for example they cannot make effective detection in large rooms and also, they cannot do effective accounting when there're many people passing through the detection range of a sensor [10]. Microwave sensors work similarly with the ultrasonic sensors and, their functionality is based on the Doppler shift principle. A microwave sensor sends high frequency microwave signals throughout the area, and receives their reflected patterns. If a reflected pattern is changing continuously then it is interpreted as the existence of occupancy. Otherwise, if the reflected pattern is the same for a preset time then the sensor interprets no occupancy. A microwave sensor has high sensitivity as well as detection range, compared to other types of sensors [11].

Video cameras can provide information regarding the number of occupants' as well as the direction of their movement. The proper installation and configuration are very important, for the avoidance of significant errors, arising from three main factors. First, the lighting conditions may affect the video sensors, since low light levels can lead to single persons being counted multiple times. Also, turning a light switch on or off may trigger a sensor count. Second, multiple people crossing the viewing area concurrently, may be undercounted. Finally, the video system may count several crossings, at times when occupants are frequently standing unnecessarily within the recording area [12].

2.5 Review of related work on the detection of abnormal energy consumption in HVAC systems

Several methods have been proposed for the detection of abnormal energy consumption or fault detection diagnosis (FDD) in HVAC systems and they are divided in two main categories: the statistical methods and the computational approaches.

The statistical methods are mainly based on fault detection algorithms that compare data under normal operation conditions with the data under current conditions in order to detect any abnormal behaviour. The authors in [13] proposed a method that is based on the principal component analysis (PCA) detection of sensor faults in air handling units (AHU). The Q-statistic method is used for the sensor fault detection, and furthermore with the use of the Q contribution plot, the faulty sensors can be isolated. In [14], a statistical based method of detecting abnormal energy consumption in buildings is proposed, including the detection of HVAC abnormalities causing outliers. In a first stage, features like the average daily energy consumption or peak demands for a day are determined using data like the total energy consumption of the building. Then these features are sorted according to similar energy consumption and thus groups of days with similar energy consumption are formed. Thereafter, an outlier identifier is applied to determine features of the same day type with significant difference from the normal ones and if detected, a modified z-score is used to determine the amount and direction of the variation. In [15], the authors estimated the appropriate power consumption by approximating the minimum cooling demands of a building (National Taiwan University) and comparing them with the real cooling supply. The results showed a high discrepancy and the authors proposed two types of statistical methods to reduce the energy consumption: polynomial regression and feature based regression are the methods used to model the behaviour in the building and a Hampel identifier is applied to test the consistency of the data.

In the category of the computational approaches earlier works have introduced computer simulations as embedded mechanisms within the control methods of energy consumption of HVAC systems. In [16] the authors, based on the idea of encapsulating simulation programs within building energy management systems (BEMs), proposed a prototype simulation-assisted controller with an embedded simulation program in order to provide real time control decisions. In the same category also falls the work in [17], where a WSN was utilized for the abnormal situation detection. Each node of the WSN, covering a single zone, act as a controller (PI), tuning the heating supply to a predetermined temperature value. A lumped capacity model was used to predict the hypothetical normal operation and the CUSUM sequential algorithm detected possible divergences of the energy consumption from the anticipated one. In [18] a method using a multilevel fault detection diagnosis (FDD) algorithm is proposed, with an energy description of all units in a HVAC and a spatial temporal partition strategy, as the two main elements of the method. The energy performance signals of the HVAC units are becoming the inputs to the FDD algorithm, and possible hardware faults within the HVAC system are captured. The work in [19] proposes a method that detects actuator faults in a HVAC system. It is a software based on fault detection diagnosis mechanism with a two-tiered detection approach. At the first tier, the method utilizes a quantitative model-based approach, which relies on a simple thermodynamic model and it does not require full knowledge of the system model. At the second tier, a qualitative model-based approach is utilized which, based on the air temperature, provides a quick decision whether an actuator is working properly or not. In [20] a Model Predictive Controller is presented which uses both weather forecasts as well as the thermal model of a building in order to maintain indoor temperature independent of the outdoor conditions. An accurate model of the building was indispensable and thus they created a simplified model of the crittall type ceiling of radiant heating and applied a subspace identification algorithm giving the appropriate inputs. In [21] a strategy is presented consisting of two schemes, the FDD of HVAC systems and the sensors fault detection. In the first scheme the indication of each system performance is taken by one or more performance

indices (PIs) which are validated from the actual measurements by the use of regression models. The detection and diagnosis of faulty sensors are achieved with the use of a PCA method. In [22] the authors have combined the benefits of the model predictive control (MPC) technique as well as of building simulation software such as TRNSYS, Energy plus, and so forth, in order to create a physical model, as close as possible to a real building. To achieve this, they applied a subspace identification method which is appropriate to identify a multiple input multiple output (MIMO) system. In [23] the authors have focused on the preventive maintenance of the HVAC systems and they proposed a fault detection method that combines the model FDD method and a support vector machine classifier (SVM). The authors worked on the detection of components sensitive to faults. Using computer simulations they investigated three major faults such as recirculation damper stuck, the block of the cooling coil, and the decreasing of the supply fan.

The Authors in [49] presented a diagnosis method of detecting abnormal energy use in buildings which is based on the hierarchy of the building's submeters and on generalized additive models (GAM). In this method the classification of the energy use as normal is provided by the computation of the GAM model of the main meter, and the computation of the upper and lower bounds of an ARMA model. If abnormality is detected for a period of time, the GAM models of all submeters are computed as well as the ARMA models to determine if they show abnormal behaviour, and the process terminates when all the abnormal submeters are diagnosed. The method provided satisfactory results for detection abnormal energy use in the HVAC system and the lighting system. A temperature based approach to detect abnormal building energy consumption is introduced in [50] which is called Days Exceeding Threshold –Toa (DET-Toa). The method detects small changes (increase or decrease) of the normal building energy consumption. When a greater deviation than the standard between the measured and simulated consumption is detected, then abnormal energy consumption is identified. This deviation must be persisted for at least 20 consecutive days and ordered according to outside air temperature. The DET-Toa method was conducted on a dual-duct VAV as well as a single-duct VAV HVAC system. In [51] a control-

oriented modeling method is presented for multi-zone buildings with mixed-mode cooling. The detailed prediction model of a multi-zone building is established by a state-space representation with time-varying system matrices. The subspace identification algorithm is utilized to develop data-driven linear time-invariant state space models, to represent the linear time-variant state-space (LTV-SS) model which is considered as a true representation of a building.

2.6 Review of related work on the energy efficiency control in HVAC systems

The necessity of demand driven HVAC systems for energy efficient solutions, has orientated the researchers to the direction of occupancy based activated systems. In multi-zone spaces the reactive and pro-active activation of the heating / cooling of the zones contributes to significant energy saving and improves the thermal comfort for the occupants. Several research works with valuable results in energy saving have utilized the occupancy detection and prediction, in order to control the HVAC system appropriately. For the occupancy detection several types of sensors are used (i.e. PIR, CO_2, motion) while for the prediction, combinational systems are usually applied, utilizing mathematical predictive models (etc Markov chains) alongside with detected real data. The authors in [24] developed a heating control algorithm, which uses occupancy sensing data as well as historical occupancy data, and it is called "PreHeat". It is actually an occupancy-based heating control system which reacts when a space is occupied using an Occupied set point. In addition, when a space is not occupied, it predicts the next occupancy of it, by matching historical data with the occupancy data of the current day. In [25] a controller system that optimizes the HVAC system energy consumption for cooling is proposed, by enabling the airflow only into the occupied zones. The control algorithm utilizes the value of the “Total Occupancy” (TO), which is a combination of the current and adjacent room occupancies, as well as the Occupancy pattern of the room. The proposed algorithm quantized the airflow in three levels (0, 0.5 & 1) depending on the TO value. The authors in [26] proposed an automatic

thermostat control system which is based on an occupancy prediction scheme, that predicts the destination and arrival time of the occupants in the air-conditioned areas, in order to provide a comfortable environment. For the occupants' mobility prediction the cell tower information of the mobile telephony system is utilized and the arrival time prediction is based on historical patterns and route classification.

For the destination prediction of locations very close to each other (intra-cell), the time-aided order-Markov predictor is used. The authors in [27] proposed a closed-loop system for optimally controlling HVAC systems in buildings, based on actual occupancy levels named the Power-efficient Occupancy-based Energy Management System (POEM). In order to accurately detect occupants' transition, they deployed a wireless network comprising of two parts: the occupancy estimation system (OPTNet) consisting of 22 camera nodes and a passive infrared (PIR) sensors system (BONet). By fusing the sensing data from the WSN (OPTNet & BONet) with the output of an occupancy transition model in a particle filter, more accurate estimation of the current occupancy in each room is achieved. Then, according to the current occupancy in each room and the predicted one from the transition model, a control schedule of the HVAC system takes over the pre-heat of the areas to the target temperature. In [28] the authors used real world data gathered from a wireless network of 16 smart cameras called Smart Camera Occupancy Position Estimation System (SCOPES) and in this way, they developed occupancy models. Three types of Markov Chain (MC) occupancy models were tested: the Single MC, the Closest distance, and finally the Blended (BMC).

The authors concluded that BMC is the most efficient and thus they embodied it as the occupancy prediction method in their proposed "OBSERVE" algorithm, which is a temperature control strategy for HVAC systems. The authors in [29] have developed an integrated system called SENTINEL that is a control system for HVAC systems, utilizing occupancy information. For the occupancy detection and localization, the system utilizes the existing Wi-Fi network and the clients' smart phones. The occupancy localization mechanism is based on the access point (AP) communication with a client's smart phone, so that if an

occupant's phone sends packets to an AP then he is located within the range of the AP. By classifying the building areas into two main categories, namely the personal and the shared spaces, the proposed mechanism activates the HVAC system when an owner of a personal space (eg. office) has been detected within an area where his/her office is located, or when occupants are detected within shared spaces. In [30] an integrated heating and cooling control system of a building is presented aiming to reduce energy consumption. The occupancy behaviour prediction as well as the weather forecast, as inputs to a virtual (software based) building model, determines the control of the HVAC system. The occupancy detection technique utilizes Gaussian Mixture Models (GMM) for the categorization of selected features, yielding the highest information gain according to the different number of occupants. This categorization was used for observation to a Hidden Markov Model for the estimation of the number of occupants. A Semi-Markov model was developed based on patterns comprised by sensory data of CO2, acoustics, motion and light changes, to estimate the duration of occupants in the space. The work in [31] proposes a model predictive control (MPC) technique aiming to reduce energy consumption in a HVAC system while maintaining comfortable environment for the occupants. The occupancy predictive model is based on the two-state Markov chain, with the states modelling the occupied and occupied condition of the areas. The authors in [32] propose a feedback control algorithm for a variable air volume (VAV) HVAC system for full actuated (zones consisting of one room) and under-actuated (zones consisting of more than one room) zones. The proposed algorithm is called MOBSua (Measured Occupancy-Based Setback for under-actuated zones) and it utilizes real time occupancy data, through a WSN, for optimum energy efficiency and thermal comfort of the occupants. Moreover, the algorithm can be applied on conventional control systems with no need of occupancy information and it is scalable to arbitrary sized buildings.

2.7 Summary

In this Chapter, a concise review of the current technology of the HVAC systems took place initially, without any extensive reference to deeper elements of their technology, as this is not relevant to the research scope of this thesis. Subsequently, a review was made on the currently applied control systems of the HVAC, which formed the basis of the proposed mechanisms of the Thesis. This kind of control systems are based on the Wireless Sensor Networks (WSN) utilizing the functionality of appropriate types of wireless sensors: temperature and occupancy.

The state of the art technology of temperature sensors is on a satisfactory level. Smart thermostats are an indicative sample of the evolution of this kind of sensors. Perhaps the most evolved type of the programmable smart thermostats is the one that provides a learning property. Its functionality is based on an algorithm that provides the capability of recording the occupancy schedule of the zones for a certain period of time, and based on that leading on the activation or deactivation of the HVAC system. Further optimization of this type of thermostats may be achieved by applying more sophisticated functionality algorithms, utilizing their programmability.

The state of the art technology of the occupancy sensors is not capable to provide accurate record of the occupants within a zone. The accurate information of the occupants' exact number could be possibly used by statistical recording systems and further utilized by sophisticated HVAC control algorithms. This point may be considered as an issue of optimization of this type of sensors.

Several valuable research studies related with the research directions of this thesis have been published as they were presented in Chapter 2 (Sec. 2.5 & 2.6).

In the scope of detection of faults and anomalies, almost all referenced works are focused on the detection of faults due to technical reasons or unit failures (i.e. faulty thermostat). In the field of energy efficiency control, several works propose methods for demand driven HVAC systems based on statistical data concerning the occupancy of the zones, while a number of other works propose

more computational methods that utilize mainly probabilistic mathematical models. The difference and unity of the work of this thesis is distinguished by the following points:

- The detection of abnormal behaviour due to environmental situations in a HVAC space constitutes a field which has not been extensively investigated. Abnormal environmental situations i.e. continues cold air intake during winter period causing undesirable energy waste, as well as fire events may be detected with the proposed methods, and hence play an important role to the total energy consumption control.
- The utilization of the Subspace Identification (SID) as a temperature predictive model. The significance and the potential of the model are utilized in this work, on one extreme for the detection of abnormal situations (2^{nd} method) and on the other extreme for the improvement of the energy efficiency (2^{nd} method). Significant role for the detection mechanisms played the utilization of the statistical CUSUM algorithm for accurate and reliable detection of abrupt changes of the power consumption, as well as the temperature deviations from the anticipated ones.
- Finally, the novel technique aiming to balance the comfort and energy costs in a multi-zone system leading to a proactive action. The proposed method periodically computes the risk of activating the heater or not and decides in favor of the action that produces the smaller risk. The computation of the risks relies on the relative weights of the energy and discomfort costs so that the balance between the total energy consumed and the total discomfort cost may be regulated.

Chapter 3

Fundamental models utilized in the proposed methods

3.1 Introduction

All methods of this Thesis have utilized the models presented in this chapter. The first model is the multi-zone. As mentioned in Chapter 2 (Section 2.3.2) the most predominant scenario of the HVAC system design is the muli-zone one, where each area (zone) is independently heated or cooled and thus, more efficient energy control may be provided. The second model is the weather model on which the outside temperature has been based taking the temperature values during the period of one day (24h). Section 3.2 presents the properties of the theoretical multi-zone space model containing the characteristics and the dynamics of the single zone model as a part of it. Section 3.3 presents the weather model (Walter's model) that is utilized for the estimation of the outside temperature (T_o) involved in the proposed mechanisms.

3.2 The theoretical multi-zone space model

This section presents the theoretical multi-zone space model used for all the involved simulations of the proposed methods. In section 3.2.3 the form of the multi-zone space model is described, as far as the logic of the arrangement of the zones is concerned. First, the single-zone model is presented below, as an individual part of the multi-zone model, including the involved equipment and the thermal dynamic model of the energy balance equations.

3.2.1 The single-zone model

Isolating a single zone of the theoretical multi-zone space model its form is depicted in Figure 3.1 and as it's shown every single zone is theoretically equipped with a wireless node as well as a heater.

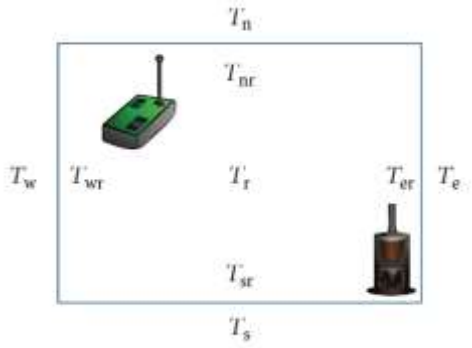

Figure 3.1 The single zone model consisting of a heat source and a wireless node [45].

This section presents the dynamic model used for the heat propagation into the space of each zone. Due to the complexity of formulating the zone dynamic model, a theoretical approach has been avoided. Specifically, they are six state variables which characterize the zone model: the zone's temperature (T_r) , the east-room wall temperature (T_{er}), the west-room wall temperature (T_{wr}), the north-room wall temperature (T_{nr}), the south-room temperature (T_{sr}), and the roof temperature (T_R). In order to have a uniform temperature distribution, the air in the zones is supposed to be fully mixed so that the dynamics of the zone can be expressed by the lumped capacity model. The following assumptions should be made to form the energy balance equations of the zone: The North and South walls of the zone should have the same effect on the room's temperature as well as the East and West walls must also have the same effect. Furthermore, no effect on the temperature of the zone has the ground of each zone, so there is no influence on the temperature change. Moreover, people, lights, and extreme weather conditions are the uncontrolled inputs [33].

According to these assumptions, the present zone model is characterized by six state variables, the room's temperature T_r, the east-room wall temperature T_{er}, the west-room wall temperature T_{wr}, the north-room wall temperature $T_{nr,}$ the

south-room wall temperature T_{sr} and the roof temperature T_R. The energy balance equations of the zone's temperature behaviour are [33]:

$$C_r \frac{dT_r}{dt} = U_{ew}A_{ew}(T_{er} - T_r) + U_{ew}A_{ew}(T_{wr} - T_r) + U_{ns}A_{ns}(T_{nr} - T_r) + U_{ns}A_{ns}(T_{sr} - T_r) + U_R A_R(T_R - T_r) + q(t) \quad (3.1)$$

$$C_{ew} \frac{dT_{er}}{dt} = U_{ew}A_{ew}(T_r - T_{er}) + U_{ew}A_{ew}(T_e - T_{er}) \quad (3.2)$$

$$C_{ew} \frac{dT_{wr}}{dt} = U_{ew}A_{ew}(T_r - T_{wr}) + U_{ew}A_{ew}(T_w - T_{wr}) \quad (3.3)$$

$$C_{ns} \frac{dT_{nr}}{dt} = U_{ns}A_{ns}(T_r - T_{nr}) + U_{ns}A_{ns}(T_n - T_{nr}) \quad (3.4)$$

$$C_{ns} \frac{dT_{sr}}{dt} = U_{ns}A_{ns}(T_r - T_{sr}) + U_{ns}A_{ns}(T_s - T_{sr}) \quad (3.5)$$

$$C_R \frac{dT_R}{dt} = U_R A_R(T_r - T_R) + U_R A_R(T_O - T_R) \quad (3.6)$$

The parameters used in the previous equations are:

A_{ew} *: Area of the east-west wall*
A_{ns} : *Area of the north-south wall*
A_R *: Area of the roof*
C_r *: Thermal capacity of the room*
C_{ew} *: Thermal capacity of the east-west wall*
C_{ns} *: Thermal capacity of the north-south wall*
C_R *: Thermal capacity of the roof*
U_{ew}*: Heat transfer coefficient of east-west walls*
U_{ns} *: Heat transfer coefficient of north-south walls*
U_R *: Heat transfer coefficient of roof*
$q(t)$*: Heat gain due to heating sources*
T_r *: Temperature of the room*
T_{er} *: Temperature of the east-room wall*
T_{wr} *: Temperature of the west-room wall*
T_n *: Temperature of the north-room wall*
T_{sr} *: Temperature of the south-room wall*
T_R *: Temperature of the roof*
T_o *: Outside temperature*

Equation (3.1) states that the rate change of energy in the zone is equal to the difference between the energy transferred to the zone by either conduction or convection and the energy removed from the zone. In equations (3.2) – (3.6) the rate change of energy through walls is equal to the energy transferred through walls due to temperature difference between indoor and outdoor air [33].

However, because in this case the only energy type is the heat energy, equation (3.1) expresses the fact that the difference between the heat transferred to the zone and the heat removed from the zone is equal to the rate change of heat in the zone. Similarly, equations (3.2) - (3.6) state that the heat transferred through the walls due to difference of temperatures between the outside and inside air is equal to rate change of heat through walls. In this simple model we neglected the effects of moisture, doors, windows and pressure losses across the zone [33]. To take into account the infiltration gain we should add the term

$$q_i = mV(T_o - T_r)/3 \tag{3.7}$$

to the right hand of equation (3.1). V is the room volume and m is an index that indicates the air changes per hour. A conservative value of m (that we used in the simulations) is 1/4 which is a value used when there are conditions to prevent infiltration (e.g. double glassing) [48]. Thus, the detection is examined with a small amount of infiltration gain. Equations (3.1) - (3.6) can be written compactly using the state space model

$$\frac{d}{dt}x(t) = Ax(t) + Bu(t) \tag{3.8}$$

$$y(t) = Cx(t) \tag{3.9}$$

Where

$$x(t) = (T_r \;\; T_{er} \;\; T_{wr} \;\; T_{ns} \;\; T_{sr} \;\; T_R)^T \tag{3.10}$$

$$u(t) = \left(T_e \;\; T_w \;\; T_n \;\; T_s \;\; T_o \;\; q(t)\right)^T \tag{3.11}$$

$$y(t) = T_r \tag{3.12}$$

The matrices B and C are the following:

$$C = (1 \quad 0 \quad 0 \quad 0) \tag{3.13}$$

$$B = \begin{pmatrix} 0 & \frac{1}{C_{ew}} U_{ew} A_{ew} & \frac{1}{C_{ns}} U_{ns} A_{ns} & \frac{1}{C_R} U_R A_R \\ \frac{1}{Cr} & 0 & 0 & 0 \end{pmatrix}^T \tag{3.14}$$

and A is a 4x4 matrix with elements $a_{i,j}$ is given by

$$A = \begin{pmatrix} \frac{1}{C_r}(-2U_{ew}A_{ew} - 2U_{ns}A_{ns} - U_R A_R) & \frac{1}{C_r} 2U_{ew}A_{ew} & \frac{1}{C_r} 2U_{ns}A_{ns} & \frac{1}{C_r} U_R A_R \\ \frac{1}{C_r} 2U_{ns}A_{ns} & -\frac{1}{C_{ew}} 2U_{ew}A_{ew} & 0 & 0 \\ \frac{1}{C_{ns}} U_{ns}A_{ns} & 0 & -\frac{1}{C_{ns}} 2U_{ns}A_{ns} & 0 \\ \frac{1}{C_R} U_R A_R & 0 & 0 & -\frac{1}{C_R} 2U_R A_R \end{pmatrix} \tag{3.15}$$

The zone model parameter values are taken from [33], and are summarized in the table 3.1.

Table 3.1
Simulation parameters [17]

$A_{ew}: 9m^2$	$C_{ns}: 70KJ/℃$
$A_{ns}: 12m^2$	$C_R : 70KJ/℃$
$A_R : 9m^2$	$U_{ew}: 2W/m^2$
$C_r : 47.1\ KJ/℃$	$U_{ns} : 2W/m^2$
$C_{ew}: 70\ KJ/℃$	$U_R : 1W/m^2$

3.2.2 The Proportional Integral (PI) controller

The Proportional-Integral (PI) controller is used by each zone's node in the initial first method, to control the power source $q(t)$. This controller type is a combination of two types of controllers, the proportional (P) controller and the Integral (I) controller connected in parallel. The relationship between the input u and the error signal e in a PI controller is

$$u(t) = K_c e(t) + \frac{K_c}{T_i} \int_0^t e(t)dt \tag{3.16}$$

The transfer function of a PI controller is

$$G_c(s) = K_c(1 + \frac{1}{T_i s}) \tag{3.17}$$

where K_c is proportional gain and T_i is the integral constant. The block diagram of a PI controller is as follows (Fig. 3.2):

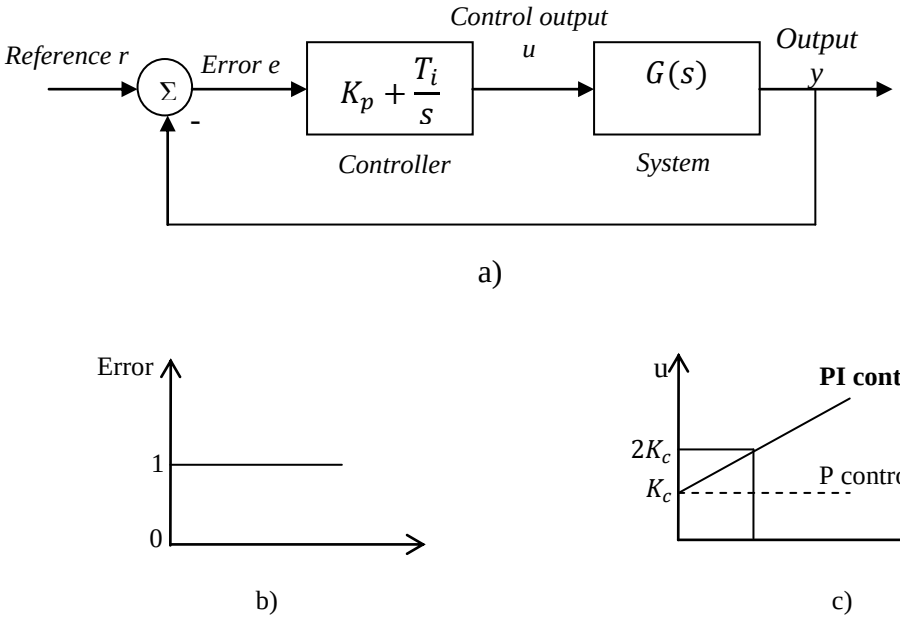

Figure 3.2 a) Proportional – Integral (PI) controller diagram, b) Error, c) PI response

The Proportional – Integral (PI) controller used to control the power source $q(t)$ is of the following form

$$H(s) = K_p + \frac{K_i}{s} \tag{3.18}$$

The controller is driven by the error function

$$e(T) = T_r - T \tag{3.19}$$

where T is the target temperature value of the zone.

The discrete version of the model with sampling period T_s is given by the following equations

$$x_{k+1} = A_d x_k + B_d u_k \tag{3.20}$$

$$y_k = C x_k \tag{3.21}$$

Where

$$A_d = e^{AT_s} \tag{3.22}$$

and

$$B_d = A^{-1}(A_d - 1)B \tag{3.23}$$

In this case the controller is expressed by the difference equation

$$q_k = K_p e_k + K_i \sum_{i \le k} e_i \tag{3.24}$$

3.2.3 The multi-zone model

The theoretical multi-zone model consists of nine zones as depicted in figure 3.3. In each single zone the factors described in the above section (3.2.1) have effect, with the dimensions and surface areas of table I. The arrangement of the zones was decided to have the form depicted in Figure 3.3, so that there is symmetry as far as the indoor temperature behaviour is concerned, according to the influence of the outside temperature T_o (i.e. zones I-III, I-VII, III-IX). All the peripheral zones may be considered as the peripheral frontage rooms of a real building, while the internal zone (zone V) may be considered as an interior area like a corridor. This symmetry facilitates the general evaluation of the simulation results with respect to the behaviour of the thermal dynamic model. Also the existence of the internal zone (zone V) is necessary, because the outside temperature of it, is provided by the influence of the temperatures of the surrounding zones (i.e. I, II, III, IV, VI, VII, VIII, IX).

In simulations the multi-zone model has been treated as a unique system with forty two (42) states and nine (9) outputs which are the temperatures of the nine zones. This consideration comes out from the fact that variables like the wall temperatures are common to the individual systems (single zones). The 42 states are provided from the following logic (Figure 3.4): nine (9) states are the heat balance of the nine zones denoted with (•), twenty four (24) states are the heat balance of the walls denoted with (X) and another nine (9) states are the heat balance of the nine roofs denoted with (↗). Adding all these states together, we have 42 states.

As mentioned in the section above, each single zone is equipped with a wireless node as a part of the whole WSN. Each one of the methods utilizes the WSN of the nine-zone model appropriately, according to the specific algorithm and each utilization mode is analytically described in each method.

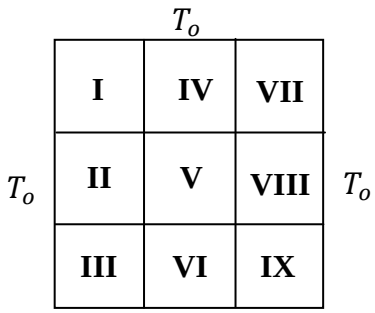

Figure 3.3 The multi-zone model arrangement [45]

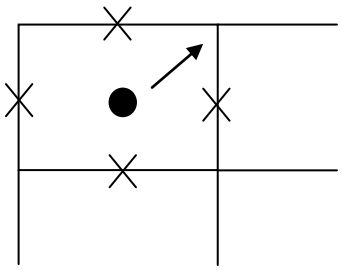

Figure 3.4 Schematic depiction of the 42 states calculation of the multi-zone model. 24 (X), 9 (•) and 9 (↗)

3.3 The weather model for the outdoor temperature estimation

In Figure 3.5, T_o denotes the outside temperature which is assummed to be uniform with no loss of generality. For simulation purposes daily outside temperature variations are obtained using Walters' model [34]. This model provides the "average unit curve" given by

$$X_a(h) = 0.463\,sin(B + 232^o38') + 0.121\,sin(2B + 55^o21') + 0.031sin(3B + 73^o19') \quad (3.25)$$

Where $X_a(h)$ is the unit ordinate at time h (Local Apparent Time, LAT), B is angular measure of the time of day, h (LAT), $0 < B < 360^o$, $B = 15h$. Using this formula along with

$$X_a(h) = \frac{T_o - T_m}{T_{max} - T_{min}} \quad (3.26)$$

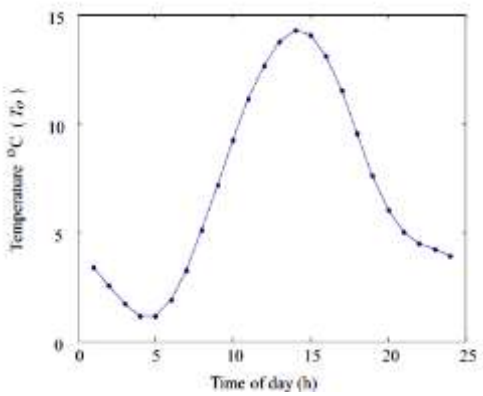

Figure 3.5 Empirical estimation of T_o [17]

the screen temperature T_o at time h is estimated. T_{max} is the maximum temperature, T_{min} is the minimum temperature of the day and T_m is the mean of the 24 hourly temperatures approximated by the daily mean temperature plus a correction factor of $-0.054(T_{max} - T_{min})$. For example if $T_{max} = 15℃$, $T_{min} = 2℃$ and $T_m = 7℃$ the daily variations of temperature of Figure 3.4 are obtained, which shows that temperature is highest at 2:00-3:00 pm [17].

3.4 Summary

In this chapter the fundamental theoretical models utilized by all the proposed methods were presented. As a multi-zone space model, a model of nine zones with the depicted arrangement (Fig. 3.2) was utilized for all the simulated methods (algorithms). The single-zone model, as a part of the "nine-zone" one, was subsequently presented including the installed equipment (wireless node & heater) as well as the dynamic model for the heat propagation into the single zone. This dynamic model of the single zone was expressed with the lumped capacity model, in order to achieve a uniform temperature distribution where the air in each zone was supposed to be fully mixed. The model in the continuous time form, consists of six energy balance differential equations (3.1 – 3.6), which expressed into the discrete time state-space form in order to be processed by the computer simulation platform.

The arrangement of the nine-zone model was presented which is based on the symmetry of the zones as far as the behaviour of the temperature is concerned, according to the influence of the outside temperature T_o, as well as the existence of frontage and internal zones. Moreover, because the nine-zone model has been considered as a single model of forty two states, the way of this calculation has been described.

Finally, a model was presented on which the outside temperature (T_o) estimation during the day period was based, in order to be provided an outside temperature behaviour as natural as possible. This weather model was the Walter's model and the temperature behaviour of it was depicted in Figure 3.5.

Chapter 4

Detection mechanism *(CUSUM algorithm)* and system predictive model *(SID)*

4.1 Introduction

In this Chapter the change detection mechanism as well as the System Identification predictive model is presented. The change detection mechanism which is the Page's CUSUM algorithm is utilized in both proposed methods for detection of abnormal situations in HVAC systems. The system identification predictive model that is the SID model is utilized in the second of the two detection methods and as will be mentioned in Chapter 7, it is also utilized in the second method for energy efficiency. In Section 4.2 a review in the change detection method is presented, starting with an introduction to change detection concept, continuing with a reference on the tools and concepts of the change detection and finalizing with the presentation of the CUSUM algorithm as a change detection mechanism. Section 4.3 contains an analytical presentation of the Subspace Identification predictive model as a discrete system identification mechanism.

4.2 Review of the change detection mechanism (CUSUM algorithm)

4.2.1 Introduction to change detection

The analysis of time series and identification was a very challenging research area. The fundamental notion underlying this research field is that the properties or parameters that describe the data either remain constant throughout the time period or changing very slowly. However, in many cases, problems arise that

could be modeled using parametric models in which the parameters showed abrupt changes in unknown times.

By the term ‘’abrupt changes’’, changes in the characteristics are meant, which occur very quickly, if not immediately, in relation to the measurement sampling period. The detection of abrupt changes could be possible with the aid of mechanisms which help a decision to be taken whether such a change in the characteristics of the considered object occurred. An abrupt change occurs at a time instant where before and after that, the properties are constant. This characteristic is fundamental, on one hand, for the statement of the mathematical problem and, on the other hand, for the change detection algorithms derivation [34].

4.2.2 Basic tools and concepts of the change detection

In this work the CUSUM sequential detection algorithm is utilized which is analytically presented in the following section (4.1.3). In order to make the algorithm understandable, some basic tools and elements must be presented. First of all let’s consider a sequence of independent random variables $(y_k)_k$ with probability density$P_\theta(y)$. The probability is depending on only one scalar parameter θ. If a change occurs at the unknown time t_o, the parameter θ will undergo a change so that if it was equal to θ_0 before change, it will be equal to $\theta_1 \neq \theta_0$ after change. The task now is to detect and estimate this change in the parameter assuming that the parameter before change (θ_0) is unknown. A very important concept in Mathematical statistics is the logarithm of the likelihood-ratio and it is defined as

$$S(y) = ln\frac{P_{\theta_1}(y)}{P_{\theta_0}(y)} \tag{4.1}$$

This ratio is based on the following key statistical property: if E_{θ_1} and E_{θ_0} denote the expectations of the random variables of the probability distributions $P_{\theta_1}(y)$ and $P_{\theta_0}(y)$ respectively then,

$$E_{\theta_0}(s) < 0 \text{ and } E_{\theta_1}(s) > 0 \tag{4.2}$$

This means that if a change occurs in the parameter θ, a change in the sign (from negative to positive or vice-versa) of the mean value of the log-likelihood ratio will also occur [36].

4.2.3 The Cumulative Sum (CUSUM) Algorithm

The Cumulative sum algorithm (CUSUM), developed by E. S. Page of the University of Cambridge in 1954. CUSUM algorithm is a statistical analysis mechanism for monitoring change detection in statistical quality control. A fundamental element for the mechanism is the "quality number" θ (referred by Page). θ may be a parameter of the probability distribution i.e. the mean or variance. Let's consider θ as the mean of a distribution; then CUSUM algorithm is the actual method to determine changes in θ and thus, in the mean of the distribution [35, 36].

The cumulative sum provides the sequential functionality characteristic of the algorithm. As a simple case to understand the cumulative sum, and how it is calculated, let's consider a process with sample data X_n and the average of all samples ω. Initially, the difference between the 1st sample (X_1) and ω is calculated and the result (positive or negative) is added to the difference between the 2nd sample (X_2) and ω and so on, as follows:

$$\begin{aligned} S_1 &= X_1 - \omega \\ S_2 &= (X_1 - \omega) + (X_2 - \omega) = S_1 + (X_2 - \omega) \\ S_3 &= S_2 + (X_3 - \omega) \\ &\vdots \\ S_n &= S_{n-1} + (X_n - \omega) \end{aligned} \tag{4.3}$$

When the value of S exceeds a certain threshold value h, a change in value has been found. Changes in the positive direction detect the formula (4.5) while changes in the negative direction are detected by the formula (4.6)

$$S_0 = 0 \tag{4.4}$$

$$S_n = max(0, S_{n-1} + X_n - \omega) \tag{4.5}$$

$$S_n = min(0, S_{n-1} + X_n - \omega) \tag{4.6}$$

CUSUM algorithm is a sequential detection process and it gives an optimal solution to the following problem:

Assuming that $X(n)$ is a discrete random signal with independent distributed samples. Each sample follows a probability density function (PDF), $p(x[n], \theta)$. The PDF depends on a deterministic parameter θ that may be, for example, the mean value μ_X or the variance σ_X^2 of $X[n]$. An abrupt change of the signal might have occurred at the time n_c. At this time (n_c) there is an instantaneous modification of the value of the parameter θ, so that $\theta = \theta_0$ before n_c and $\theta = \theta_1$ after n_c to the current sample. According to these assumptions the observed signal PDF (p_X) from the first to the current sample ($x[0]\ to\ x[k]$) can have two forms.

1. The form with no change hypothesis (H_0) will be given by:

$$P_{X|H_0} = \prod_{n=0}^{k} p[n], \theta_0 \tag{4.7}$$

2. The form with one change hypothesis will be given by:

$$P_{X|H_1} = \prod_{n=0}^{n_c-1} (p[n], \theta_0) \prod_{n=n_c}^{k} (p[n], \theta_1) \tag{4.8}$$

In the problem above, the values of the parameter θ before (θ_0) and after (θ_1) the abrupt change are supposed to be known as well as the PDF of each sample $p([n], \theta)$. The unknown factors to be determined are: a) the occurrence or not of an abrupt change between $n = 0$ and $n = k$, and b) the value of the change time (n_c).

4.2.4 The intuitive derivation of the CUSUM algorithm

A typical behaviour of the log-likelihood ratio S_k is a negative drift before change and a positive one after change.

The difference between the log-likelihood ratio value and its current minimum value provides the information of the change. So, if at each time instant the difference is compared to a threshold h, the decision rule is then as follows:

$$g_k = S_k - m_k \tag{4.9}$$

Where

$$S_k = \sum_{i=1}^{k} s_i \Longrightarrow s_i = ln \frac{p\theta_1(y_i)}{p\theta_0(y_i)} \tag{4.10}$$

is the cumulative sum and

$$m_k = min_{1 \le j \le k} S_j \tag{4.11}$$

The stopping time t_a is

$$t_a = min\{k: g_k \ge h\} = min\{k: S_k \ge m_k + h\} \tag{4.12}$$

Equation (4.12) states that the detection rule is the actual comparison between the Cumulative sum S_k and the adaptive threshold $m_k + h$. The factor m_k, influences the threshold to be modified on-line and keep complete memory of the entire information contained in the past observations [36].

The general logic of the detection mechanism that followed by the detection methods of this work is the following: As equation (4.3) stated, the difference of a parameter ω and a sample data X_1 is added to the difference between ω and the second sample X_2 and this process continues until the sample X_n. In the case of this detection process the parameter ω corresponds to the mean value of the normal operation (null hypothesis) q while the samples X_n corresponds to the

random variable Z_k which specifies the difference of the sequence of the prediction error ($E_k - E_{k-1}$). The error E_k specifies the difference between the predicted values and real ones. According to the proposed methods, these values may be temperature values. A new random variable Q_k is produced which is the sequential difference of $Z_k - q$ (for $k \geq 1$). Thus the sum

$$S_k = \sum_{i=1}^{k} Q_i \tag{4.13}$$

constitutes the cumulative sum. If the random variable $Z_k = E_k - E_{k-1}$ has a density function $f(Z_\kappa; q, \sigma)$ for $k \geq 1$ where the mean q is known or it may be observed and σ is a nuisance parameter and it is unknown, the using of Combay's adaptation of nuisance parameter on the CUSUM algorithm is necessary as presented in the next Section.

4.2.5 Nuisance parameter adaptation on the CUSUM technique

Combay [37] utilized CUSUM algorithm taking into account a nuisance parameter σ. That is, when Y_i are independent random variables, exponentially distributed with density function $f(\theta_i, \theta, \sigma)$, where θ is the parameter of interest and σ is an unknown nuisance parameter. The statistics proposed by Combay are based on the following elements: the efficient score (Rao's statistics), the maximum likelihood estimator (Wald's statistics), or on the log likelihood ratio. Thus, the efficient score vector is defined as

$$V_k(\theta, \sigma) = \sum_{i=1}^{k} \nabla_v \, log f(\theta_i; \theta, \sigma) \qquad v = (\theta, \sigma) \tag{4.14}$$

Assuming that $v = (\theta, \sigma)$ is a point in an open subset $\Omega \subset \mathbb{R}^{d+p}$ then equation (4.13) is valid under some regularity conditions. If the density $f(\cdot)$ belongs to the exponential family, i.e. Gaussian, there exists a Wiener process $W(t)$ if the above regularity conditions hold under the null hypothesis (normal operation). $W(t)$ approximates

$$W_k = \Gamma^{-\frac{1}{2}}(\theta, \sigma) V_k(\theta, \hat{\sigma}_k) \tag{4.15}$$

where $\hat{\sigma}_k$ is the maximum likelihood estimation of σ and $\Gamma^{-1/2}(\theta, \sigma)$ is the Fisher information matrix. When monitoring the mean $\theta = 0$ the equation (4.15) takes the form [37]

$$k^{-1/2} W_k = k^{-1/2} \frac{1}{\sqrt{\frac{1}{k}\sum_{i=1}^{k} Q_i^2}} \sum_{i=1}^{k} Q_i \tag{4.16}$$

4.3 Deterministic Subspace Identification (SID) predictive model

4.3.1 General system model

A dynamic model of the form shown in Figure 4.1 can meet a multitude of system models such as: industrial, technical, biological, economical etc. In this work the interest is mainly directed on mathematical models which are usually described by differential equations, when presented in continues time and with difference equations when presented in discrete time. The mathematical present the dynamic behaviour of a system as a function of time and they are used for simulations, analysis, fault detection, system control etc.

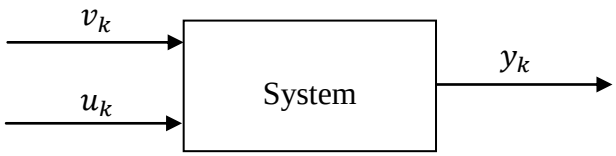

Figure 4.1. Schematic diagram of a dynamic system with inputs u_k, outputs y_k and noise v_k [39]

4.3.2 State space model

Consider the following discrete time model that is described by the difference equations of the form

$$x_{k+1} = Ax_k + Bu_k + w_k \tag{4.17}$$

$$y_k = Cx_k + Du_k + v_k \tag{4.18}$$

where $u_k \in \mathbb{R}^m$ and $y_k \in \mathbb{R}^i$are the input and output measurement vectors respectively at time k. $x_k \in \mathbb{R}^n$ is the state vector containing the values of the states of the process in a discrete time k.

The matrix $A \in \mathbb{R}^{nxn}$is the dynamical matrix and describes the dynamics of the system. $B \in \mathbb{R}^{nxm}$ is the input matrix and it represents the linear transformation of the deterministic inputs that influences the next state. $C \in \mathbb{R}^{ixn}$ is the output matrix which describes the transformation of the internal state to the outside world. $D \in \mathbb{R}^{ixm}$ is the direct feedthrough term which is most often (0) in continues time systems. In discrete time systems is not (0) due to sampling.

In Figure 4.2, a graphical representation of the system is shown

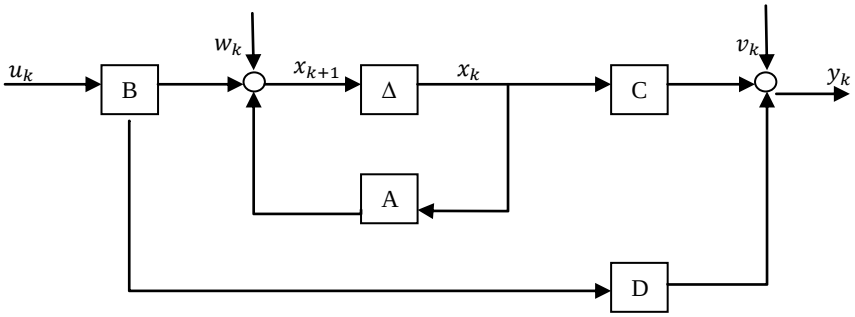

Figure 4.2 Graphical more detailed representation of the system [39]

where the vector input signals u_k as well as the output signals y_k are known (could be measured) while the disturbances w_k and v_k are unknown.

The Δ symbol represents a delay. According to above description of the system model the problem of the system identification can be stated as follows:

Given input u_k and output y_k measurements ($k = 1,2 \ldots . s$), how the system matrices A, B, C, D and the order n can be found? The answer to this question is presented in the following subsection.

4.3.3 Subspace Identification Analysis

One of the solutions to the above stated problem is the subspace identification process. In order to express the problem in a more comprehensible way let's consider the system of the state space form of (4.17) and (4.18) where the only known elements are: the given inputs u_k, and the measured outputs y_k. The states x_k of the system are unknown and hidden. The matrices A, B, C & D and the noises (v_k, w_k) are also unknown as well as the dimensions of the hidden states x_k. The task is to estimate the "best" possible system parameters A, B, C & D so that given the inputs u_k, the outputs y_k are observed. There is not a unique solution to this problem and this can be shown as follows: from the system described in (4.17) and (4.18) without noise, suppose that the true parameters A, B, C & D and the initial state x_1 are known

$$\begin{bmatrix} x_2 & x_3 & \cdots & x_{p+1} \\ y_1 & y_2 & \cdots & y_p \end{bmatrix} = \begin{bmatrix} A & B \\ C & D \end{bmatrix} \begin{bmatrix} x_1 & x_2 & \cdots & x_p \\ u_1 & u_2 & \cdots & u_p \end{bmatrix} \tag{4.19}$$

where matrices $x_i = nx1$, $y_i = 0x1$, $A = nxn$, $B = nxm$, $C = 0xn$, $D = 0xm$ and $u_i = mx1$

If both sides will be multiplied with some arbitrary invertible matrix T, then:

$$\begin{bmatrix} T & 0 \\ 0 & I \end{bmatrix} \begin{bmatrix} x_2 & x_3 & \cdots & x_{p+1} \\ y_1 & y_2 & \cdots & y_p \end{bmatrix} = \begin{bmatrix} T & 0 \\ 0 & I \end{bmatrix} \begin{bmatrix} A & B \\ C & D \end{bmatrix} \begin{bmatrix} x_1 & x_2 & \cdots & x_p \\ u_1 & u_2 & \cdots & u_p \end{bmatrix}$$

$$\begin{bmatrix} Tx_2 & Tx_3 & \cdots & Tx_{p+1} \\ y_1 & y_2 & \cdots & y_p \end{bmatrix} = \begin{bmatrix} TA & TB \\ C & D \end{bmatrix} \begin{bmatrix} x_1 & x_2 & \cdots & x_p \\ u_1 & u_2 & \cdots & u_p \end{bmatrix} \tag{4.20}$$

where $T = nxn$, and $I = 0x0$ (Identity matrix)

and by multiplying (4.20) with the identity matrix (4.21)

$$I = A \cdot A^{-1} = \begin{bmatrix} T & 0 \\ 0 & I \end{bmatrix} \begin{bmatrix} T^{-1} & 0 \\ 0 & I \end{bmatrix} \tag{4.21}$$

$$\begin{bmatrix} Tx_2 & Tx_3 & \cdots & Tx_{p+1} \\ y_1 & y_2 & \cdots & y_p \end{bmatrix} = \begin{bmatrix} TA & TB \\ C & D \end{bmatrix} \begin{bmatrix} T^{-1} & 0 \\ 0 & I \end{bmatrix} \begin{bmatrix} T & 0 \\ 0 & I \end{bmatrix} \begin{bmatrix} x_1 & x_2 & \cdots & x_p \\ u_1 & u_2 & \cdots & u_p \end{bmatrix}$$

$$\begin{bmatrix} Tx_2 & Tx_3 & \cdots & Tx_{p+1} \\ y_1 & y_2 & \cdots & y_p \end{bmatrix} = \begin{bmatrix} TAT^{-1} & TB \\ CT^{-1} & D \end{bmatrix} \begin{bmatrix} Tx_1 & Tx_2 & \cdots & Tx_p \\ u_1 & u_2 & \cdots & u_p \end{bmatrix} \tag{4.22}$$

as it is shown from (4.22), if the unknown axis (x) is multiplied by an unknown matrix T, the same outputs from the same inputs will be precisely generated but with different A, B, C,and D parameter matrices.

The outputs (y_i) are a linear combination of the states (x_i) and the inputs (u_i) of the current time and all the previews times. If the observed outputs (y_i) could have been projected in such a way that the influence of the inputs u_i is eliminated, then the generated system will be proportional to the hidden states x_i. This is the objective of the SID analysis. The SID analysis states that a system could be identified by the projection of the measured data (y_i) matrix onto a matrix that is perpendicular to the space of the inputs (u_i).

4.3.3.1 Block Hankel matrices

Hankel matrices are matrices of a special form that they are used in SID process and can be easily constructed from the input and output data. The input Hankel matrices are defined as

$$U_{0|2i-1} \equiv \left[\begin{array}{cccc} u_0 & u_1 & \cdots & u_{j-1} \\ u_1 & u_2 & \cdots & u_j \\ \vdots & \vdots & \cdots & \vdots \\ u_{j-1} & u_i & \cdots & u_{i+j-2} \\ \hline u_i & u_{i+1} & \cdots & u_{i+j-1} \\ u_{i+1} & u_{i+2} & \cdots & u_{i+j} \\ \vdots & \vdots & \cdots & \vdots \\ u_{2i-1} & u_{2i} & \cdots & u_{2i+j-2} \end{array}\right] \begin{array}{l} \text{“past”} \\ \\ \\ \\ \text{“future”} \\ \\ \\ \end{array}$$

$$\equiv \left(\frac{U_{0|i-1}}{U_{i|2i-1}}\right) = \left(\frac{U_p}{U_f}\right) \tag{4.23}$$

$$\equiv \left[\begin{array}{cccc} u_0 & u_1 & \cdots & u_{j-1} \\ u_1 & u_2 & \cdots & u_j \\ \vdots & \vdots & \cdots & \vdots \\ u_{j-1} & u_i & \cdots & u_{i+j-2} \\ \hline u_i & u_{i+1} & \cdots & u_{i+j-1} \\ u_{i+1} & u_{i+2} & \cdots & u_{i+j} \\ \vdots & \vdots & \cdots & \vdots \\ u_{2i-1} & u_{2i} & \cdots & u_{2i+j-2} \end{array}\right] \begin{array}{l} \text{“past”} \\ \\ \\ \\ \\ \text{“future”} \\ \\ \\ \end{array}$$

$$\equiv \left(\frac{U_{0|i}}{U_{i+1|2i-1}}\right) = \left(\frac{U_p^+}{U_f^-}\right) \tag{4.24}$$

where

- The number of rows (i) is a used –defined index which it should at least be larger than the largest observability index or else larger that the order of the system to be identified $(i > n)$.
- The number of columns (j) is typically equal to $s - 2i + 1$ since all given data samples are used.
- The subscripts "p" and "f" stand for “past” and “future” respectively and the subscripts of $U_{0|2i-1}$, $U_{0|i-1}$, $U_{0|i}$ denote the first and last element of the first column of the block Hankel matrix. The matrices U_p and U_f (the past and the future inputs respectively) are defined by splitting $U_{0|2i-1}$ in two equal parts of i block rows. By shifting the border between past and future one row down, the matrices U_p^+ and U_f^- are defined. The subscripts “+” and “-“ stand for “add one block row” and “delete one block row” respectively.

Similarly the output block Hankel matrices $Y_{0|2i-1}, Y_p, Y_f, Y_p^+, Y_f^-$ are defined as

$$Y_{0|2i-1} \equiv \left[\begin{array}{cccc} y_0 & y_1 & \cdots & y_{j-1} \\ y_1 & y_2 & \cdots & y_j \\ \vdots & \vdots & \cdots & \vdots \\ y_{i-1} & y_i & \cdots & y_{i+j-2} \\ \hline y_i & y_{i+1} & \cdots & y_{i+j-1} \\ y_{i+1} & y_{i+2} & \cdots & y_{i+j} \\ \vdots & \vdots & \cdots & \vdots \\ y_{2i-1} & y_{2i} & \cdots & y_{2i+j-2} \end{array}\right] \begin{array}{l} \text{“past”} \\ \\ \\ \\ \\ \text{“future”} \\ \\ \\ \end{array} \equiv \left(\frac{Y_{0|i-1}}{Y_{i|2i-1}}\right) = \left(\frac{Y_p}{Y_f}\right) \tag{4.25}$$

$$\equiv \left[\begin{array}{cccc} y_0 & y_1 & \cdots & y_{j-1} \\ y_1 & y_2 & \cdots & y_j \\ \vdots & \vdots & \cdots & \vdots \\ y_{i-1} & y_i & \cdots & y_{i+j-2} \\ \hline y_i & y_{i+1} & \cdots & y_{i+j-1} \\ y_{i+1} & y_{i+2} & \cdots & y_{i+j} \\ \vdots & \vdots & \cdots & \vdots \\ y_{2i-1} & y_{2i} & \cdots & y_{2i+j-2} \end{array}\right] \begin{array}{l} \text{“past} \\ \\ \\ \\ \\ \\ \\ \text{“future”} \end{array} \equiv \left(\frac{Y_{0|i}}{Y_{i+1|2i-1}}\right) = \left(\frac{Y_p^+}{Y_f^-}\right) \tag{4.26}$$

The block Hankel matrices consisting of inputs and outputs are defined as

$$W_{0|i-1} = \begin{pmatrix} U_{0|i-1} \\ Y_{0|i-1} \end{pmatrix} = \begin{pmatrix} U_p \\ Y_p \end{pmatrix} = W_p \tag{4.27}$$

and as before

$$W_p^+ = \begin{pmatrix} U_p^+ \\ Y_p^+ \end{pmatrix} \tag{4.28}$$

The deterministic state sequence matrix is

$$X_i \equiv [x_i \quad x_{i+1} \quad \cdots x_{i+j-2} \quad x_{i+j-1}] \tag{4.29}$$

Similarly and analogous to the past inputs/outputs, the past (X_p^d) and future (X_f^d) state sequences are

$$X_p^d = X_0^d, \qquad X_f^d = X_i^d$$

Each row vector in $Y_{0|2i-1}$ can be written as a linear function of the row vector in X_i and the row vectors in U_i. Therefore from (4.25) the row vectors in $Y_{0|2i-1}$ exist in the subspace defined by the row vectors of U_i and X_i.

$$Y_{0|2i-1} = \begin{bmatrix} Cx_0 + Du_0 & Cx_1 + Du_1 & \cdots \\ CAx_0 + CBu_0 + Du_1 & CAx_1 + CBu_1 + Du_2 & \cdots \\ CA_1x_0 + CABu_0 + CBu_1 + Du_2 & CA_1x_1 + CABu_1 + CBu_2 + Du_3 & \cdots \\ \vdots & \vdots & \ddots \end{bmatrix}$$

4.3.3.2 Additional system matrices

According to the above matrix ($Y_{0|2i-1}$) and assuming that the pair $\{A, C\}$ to be observable and the pair $\{A, B\}$ to be controllable, the extended observability matrix (Γ_i) can be defined as

$$\Gamma_i = \begin{bmatrix} C \\ CA \\ CA_2 \\ \vdots \\ CA_{i-1} \end{bmatrix} \in \mathbb{R}^{l_i x n} \tag{4.30}$$

(The subscript i denotes the number of block rows for Γ_i).

The controllable modes can be either stable or unstable and the matrix H_i^d can be defined as a lower block Toeplitz matrix of the form

$$H_i^d = \begin{bmatrix} D & 0 & 0 & \cdots & 0 \\ CB & D & 0 & \cdots & 0 \\ CAB & CB & D & \cdots & 0 \\ \vdots & \vdots & \vdots & \ddots & \vdots \\ CA_{i-2}B & CA_{i-3}B & CA_{i-4}B & \cdots & D \end{bmatrix} \in \mathbb{R}^{l_i x m_i} \tag{4.31}$$

and so the output matrix $Y_{1|i}$ can have the following form

$$Y_{1|i} = \Gamma_i [x_1 \quad x_2 \quad x_3 \quad \cdots] + H_i \begin{bmatrix} u_1 & u_2 & \cdots \\ u_2 & u_3 & \cdots \\ u_3 & u_4 & \cdots \\ \vdots & \vdots & \ddots \end{bmatrix} \tag{4.32}$$

From (4.27) the state sequence equations are defined as

$$\begin{aligned} x_2 &= Ax_1 + Bu_1 \\ x_3 &= A^2x_1 + ABu_1 + Bu_2 \\ x_4 &= A^3x_1 + A^2Bu_1 + ABu_2 + Bu_3 \\ x_{i+1} &= A^ix_1 + A^{i-1}Bu_1 + A^{i-2}Bu_2 + \cdots Bu_i \end{aligned} \tag{4.33}$$

and from the above the reversed extended controllability matrix (Δ_i^d) is defined as

$$\Delta_i^d = [A^{i-1} \; A^{i-2} \; \cdots \; AB \; B] \in \mathbb{R}^{nxmi} \tag{4.34}$$

(the subscript i denotes the number of block columns)
and so the past and the future input-output equations can be written as

$$Y_p = \Gamma_i X_p + H_i U_p \tag{4.35}$$

$$Y_f = \Gamma_i X_f + H_\iota U_f \tag{4.36}$$

$$X_f^d = A^i X_p^d + \Delta_i^d U_p \tag{4.37}$$

In equations (4.35), (4.36) and (4.37) the matrices Y and U are known while the rest of the matrices are unknown. The row vectors of Y exist in a subspace defined by the row vectors of U and the row vectors of X. If a subspace that is perpendicular to the subspace defined by U is found and Y will be projected onto this subspace, then the influence of U and Y will be eliminated and only the influence of X will remain.
Matrix (X_f^d) is a linear combination of the past inputs U_p and outputs Y_p as it is shown from the equations (4.35) and (4.37)

$$\begin{aligned} X_f^d = A^i X_p^d + \Delta_i^d U_p &= A^i\left[\Gamma_\iota^* Y_p - \Gamma_i^* H_i^d U_p\right] + \Delta_i^d U_p \\ &= \left[\Delta_i^d - A^i \Gamma_i^* H_i^d\right] U_p + \left[A^i \Gamma_i^*\right] Y_p \\ &= L_p W_p \end{aligned} \tag{4.38}$$

where

$$L_p = (\Delta_i^d - A^i \Gamma_i^* H_i^d | A^i \Gamma_i^*) \tag{4.39}$$

By substituting the equation (4.38), the equation (4.36) can be written as

$$Y_f = \Gamma_i L_p W_p + H_i^d U_f \tag{4.40}$$

If Y_f will be projected onto the subspace which is perpendicular to the subspace defined by U_f

$$Y_f \,/U_f^\perp = \Gamma_i L_p W_p \,/U_f^\perp \tag{4.41}$$

$$[Y_f\ /U_f^{\perp}][W_p/U_f^{\perp}]^* W_p = \Gamma_i L_p W_p \tag{4.42}$$

and if in the above equation (4.42)

$$[Y_f\ /U_f^{\perp}][W_p/U_f^{\perp}]^* W_p = O_i \quad \text{and} \quad L_p W_p = X_f^d \quad \text{then}$$

$$O_i = \Gamma_i X_f^d \tag{4.43}$$

which is equal to

$$O_{i+1} = \Gamma_i X_{i+1} = \begin{bmatrix} C \\ CA \\ \vdots \\ CA^{i-1} \end{bmatrix} \begin{bmatrix} x_{i+1}\ x_{i+2}\ \cdots\ x_{i+j} \end{bmatrix}$$

$$= \begin{bmatrix} Cx_{i+1} & Cx_{i+2} & \cdots & Cx_{i+j} \\ CAx_{i+1} & CAx_{i+2} & \cdots & CAx_{i+j} \\ CA^2x_{i+1} & CA^2x_{i+2} & \cdots & CA^2x_{i+j} \\ \vdots & \vdots & \vdots & \vdots \end{bmatrix}$$

Here there is the important stage where a matrix (O_i) has been produced, with row vectors that exist in the subspace defined by the hidden state matrix X_i. Also the row vectors of the matrix (O_i) are linearly dependent, therefore the dimensioning of matrix (O_i) is equal to the dimensioning of matrix (X_i) which is equal to the dimensions of vector x. So, although the value of the hidden states is unknown, the dimensions of the vector x is known.

4.3.3.3 Singular Value Dicomposition (SVD)

By performing the Singular Value Decomposition (SVD) of matrix O_i the hidden states X_i will be estimated.

$$O_{i+1} = \quad U_1 S_1 V_1^T$$

$$= [U_1 \quad U_2] \begin{bmatrix} S_1 & 0 \\ 0 & 0 \end{bmatrix} \begin{bmatrix} V_1^T \\ V_2^T \end{bmatrix} \tag{4.44}$$

Where the columns of U_1 are the orthonormal eigenvectors of OO^T, the columns of V_1 are orthonormal eigenvectors of O^TO, and S is a diagonal matrix containing the square roots of eigenvalues from U or V in descending order. Thus:

$$\Gamma_i X_{i+1} = U_1 S_1 V_1^T \tag{4.45}$$

where

$$U_1 = (\Gamma_i X_{i+1})(\Gamma_i X_{i+1})^T \tag{4.46}$$

$$V_1 = (\Gamma_i X_{i+1})^T (\Gamma_i X_{i+1}) \tag{4.47}$$

The dimensions of matrix U_i are equal to the dimensions of matrix Γ_i, the dimensions of matrix S_i are $(n\ x\ n)$ where n is the dimension of the vector x and the dimension of each vector v of matrix V_i is $(n\ x\ 1)$ where n is the dimension of vector x. So, from equation 4.45, if we multiply twice with the square root of S_1 as well as with an arbitrary non-singular (nxn) matrix T as below

$$\Gamma_i X_{i+1} = \quad U_1 S_1 V_1^T = \quad U_1 {S_1}^{1/2} T T^{-1} {S_1}^{1/2} V_1^T \tag{4.48}$$

then the extended observation matrix Γ_i is identified as

$$\Gamma_i = U_1 S_1^{1/2} T \tag{4.49}$$

and the state vector X_{i+1} is also identified as

$$X_{i+1} = \quad T^{-1} {S_1}^{1/2} V_1^T \tag{4.50}$$

The number of singular values in equation (4.44) that are different from zero determines the order of the system (4.17) – (4.18).

4.3.3.4 Determination of the system matrices A, B, C and D

One way for the determination of the matrices A, B, C and D could be made with the following method [39]:

First the oblique projections of equation (4.51) and (4.52) must be calculated

$$O_i = Y_f /_{U_f} W_p \tag{4.51}$$

$$O_{i-1} = Y_f^- /_{U_f} W_p^+ = \Gamma_{i-1} X_{i+1} \tag{4.52}$$

next, the SVD of the weighted oblique projection of equation (4.53) must be calculated, with the determination of the order by inspecting the values in S.

$$W_1 O_i W_2 = USV^T \tag{4.53}$$

subsequently, the extended observation matrix Γ_i and Γ_{i-1} must be determined as:

$$\Gamma_i = W_1^{-1} U_1 S_1^{1/2}, \quad \Gamma_{i-1} = \underline{\Gamma_i} \tag{4.54}$$

then, the system states X_i^d and X_{i+1}^d must be also determined as:

$$X_i^d = \Gamma_i^\dagger O_i \text{ and } \quad X_{i+1}^d = \Gamma_{i-1}^\dagger O_{i-1} \tag{4.55}$$

and finally the set of equations of equation (4.56) may be solved in a least square sense for A, B, C and D.

$$\begin{pmatrix} X_{i+1}^d \\ Y_{i|i} \end{pmatrix} = \begin{pmatrix} A & B \\ C & D \end{pmatrix} \begin{pmatrix} X_i^d \\ U_{i|i} \end{pmatrix} \tag{4.56}$$

4.4 Summary

Initially in this Chapter the logic of the sequential CUSUM detection algorithm was presented, which has been utilized as the basic detection mechanism in the proposed methods for the detection of abnormal situations in HVAC systems. As pointed out, the CUSUM detection algorithm is a statistical analysis mechanism for monitoring change detection in statistical quality control. The fundamental parameter of the algorithm is θ, which may be the mean or variance of a probability distribution and if an abrupt change occur at some unknown time t_o and cause changes in θ, the CUSUM algorithm is capable to immediately detect

these change and possibly trigger an alarm. This mechanism utilized in both the detection methods as the appropriate detection algorithm for the abnormal power consumption.

Subsequently, the Subspace Identification predictive model was analytically presented which has been utilized as the temperature prediction model of the zone's temperature. The fundamental principle of the SID model is the prediction of the unknown states x_k of a state space model, if the inputs u_k are given and the outputs y_k are observed. In order to obtain the prediction of the unknown states x_k and result to the identification of the system, the identification of the matrices $A, B, C,$ and D that are the system parameters is essential. This may be achieved by the projection of the observed output data (y_k) matrix onto a matrix that is perpendicular to the space of the inputs u_k. Then by performing the singular value decomposition (SVD) process, the hidden states x_k will be identified.

Chapter 5

Methodology for the detection of abnormal situations in HVAC systems

5.1 Introduction

The first direction of this thesis concerning the first control function includes the methods for the detection of abnormal situations in HVAC systems which are presented in this Chapter. The detected abnormal situation by the proposed methods is the unexpected power consumption due to exogenous reasons. The methods are distinguished as follows:

The first method is an initial approach proposing the first algorithm that utilizes a WSN of nodes consisting of a temperature sensor as well as a proportional integral (PI) controller for tuning. The method provides detection of possible divergences of the power consumption than the anticipated one, by applying the CUSUM change detection algorithm.

The second method is also based on a WSN of temperature sensors, as well as a central computer unit and it's utilizing the SID predictive model as the temperature prediction mechanism for the prediction of zones' temperature. The detection of a change in temperature behaviour is achieved by the CUSUM test, when a divergence between the predicted and the normal temperature behaviour is indicated.

5.2 Methodology Overview

The first control function is focusing on the detection of abnormal situations in multi-zone HVAC systems and suggests two methods of detection. The term "abnormal situations", concerns situations resulting to undesirable divergences from the normal operation of the HVAC system, concerning the power consumption of the system. The high infiltration gain causes unexpected power

consumption and may be caused by several undesirable openings (i.e. windows, doors), which allow the entry of possible cold air. Especially during the winter period, the continuous entry of freezing air may induce a non-stop heating in an air-conditioned area and thus, cause a significant energy waste. Moreover, fire events are also included, where the temperature is rising in an unexpectedly fast rate. Such situations could arise in any HVAC system and result to a considerable amount of energy consumption when cooling, or the maintenance of the high level temperature on heating.

All methods of the first control function are based on a nine-zone theoretical model where in each zone a temperature lumped capacity dynamic model is utilized to provide the temperature behaviour as presented in Chapter 3.

The first approach utilizes a theoretical wireless sensor network (WSN) of nodes on a decentralized control mode. Each node is installed in each zone of the multi-zone model and acts as a temperature sensor as well as a controller that tunes the room's temperature to a predetermined value. The controller type is the Proportional - Integral (PI) as described in Chapter 3. Temperature measurements of the surrounding nodes to each zone's node can be transmitted to it and provide the temperature values external to the room. These values act as inputs to the detection system which utilizes the above temperature dynamic model to detect possible divergences from its normal operation and the CUSUM sequential algorithm (Chapter 4) as the detection mechanism to isolate possible divergences of the energy consumption from the anticipated ones.

The second method for the detection of abnormal situations is based on the SID as described in Chapter 4, and uses a hybrid scheme of operation. The method comprises two phases of operation. The first phase is the "training phase". During the training phase the nodes transmit their readings to a central computing unit, which organizes the data to input-output form in order to be used by the SID process which will be run in the node system of each zone. As it is extensively described in section (X) in this chapter, the SID model needs the inputs $u(t)$ and the outputs $y(t)$ of a system, in order to be able to produce the hidden states $x(t)$. The temperature measurements of the adjacent zones to each

zone as well as the power profile of the zones' heater are the inputs $u(t)$ for each zone's SID process while the output is the zone's temperature itself. Also the central computing unit identifies a linear state space system for each zone and its parameters are communicated back to the wireless sensor node that monitors the zone. At this point the first phase (training phase) has been completed and the second phase of the system starts. The second phase is the "detection phase" which operates in a decentralized fashion. During this phase each node collects the temperature measurements by its adjacent sensor nodes and the power measurements of the zone's heater. Then the identified state space subsystem predicts the zone's temperature based on the collected measurements. The detection of possible deviations of the predicted values from the real ones is achieved by applying a suitable detection algorithm. The CUSUM algorithm is utilized to detect possible deviations from the normal operation and this second phase is split into several cycles. As the CUSUM sequential detection algorithm has been utilized to both detection methods, is presented in the following section.

5.3 Initial detection approach for abnormal power consumption based on a WSN

As it has been already mentioned, each wireless node is capable to control a heat source located into the zone using a PI controller as mentioned in Chapter 3. Moreover, the nodes have the functionality to detect abnormal operation, for example higher power consumption than the anticipated one, due to open windows during winter or lower power consumption due to the onset of a fire, and signal it to an operation center. The detection mechanism relies on knowledge of the surrounding zones' temperatures and the dynamics of the covered zone. To be more specific, the assumption is made that each node runs a model of the form

$$\dot{x}(t) = F[x(t), u(t), q(t)] \quad (5.1)$$

$$y(t) = G[x(t)] \quad (5.2)$$

$$q(t) = H[y(t) - T] \quad (5.3)$$

where $x(t)$ is the state vector, $u(t)$ is a vector of external inputs, $y(t)$ is the room temperature, T is the target room temperature, and $q(t)$ is the ideal heat gain tuned by the PI controller. This gain is a function of the error $e(t) = y(t) - T$. Knowing the dynamics of the system, that is the functions $F[.]$ and $G[.]$, and the external inputs $u(t)$, which in our case are the temperatures of the surrounding zones and possibly the outdoor temperature, the node is able to specify the ideal power profile $q(t)$. During operation the node compares the real controlled power q_r(t) with the hypothetical $q(t)$ and detects possible deviations. To this end let us consider a discrete time system ($t = iT_s$, where T_s is the sampling period) and the sequence of random variables $\{Z_i\}$, i.e. a sequence of independent measurements of the heat gain. We assume that Z_i has density $f(z_i; q, \sigma)$ for $i = 1, \dots \tau - 1$ and density $f(z_i; q_r, \sigma)$ for $i \geq \tau$, where parameter q is known and q_r and σ are generally unknown. The time index τ signals an event that changes the distribution of the measurements. In terms of the proposed algorithm, q is the ideal mean heat gain as it is estimated by the zone's model and σ^2 is the variance of the estimation due to uncertainties of $u(t)$, the presence of lamps or other heat sources. σ is a nuisance parameter and it is generally unknown. The parameter q_r denotes the mean temperature in case of an abnormal situation, i.e. high heat leakages or high heat gains due to a fire, and it is considered unknown. The parameter τ is the time index that a change of densities occurs and sequential tests deal with this detection of change. Although, $q(t)$ and $q_r(t)$ are functions of time, we will apply the detection algorithm using the random variables $Y = Z - q(T)$. Thus, under normal operation Y has a constant mean value equal to 0, whereas under the alternative hypothesis Y has a non-zero unknown mean value.

5.3.1 The utilization of the multi-zone model

We consider an arrangement of rooms where each room (zone) is equipped with a wireless sensor node that is capable to control a heat source located in the zone. Each node transmits its room temperature in regular periods of time with probability p and therefore the information about zones' temperature is spread in an "epidemic" fashion. In general the probability p varies from node to node. In power constrained environments this probability may depend on the battery energy stock. A node with limited power supply transmits with small probability in order to elongate its life. In the proposed application it is more meaningful to adjust the transmission probability depending on the difference of successive measurements. Thus, a node that senses a noticeable difference of its measurements increases p in order to communicate faster this change to its neighbors. Moreover, we assume that nodes are aware of the network topology (static routing) and they piggyback information in cases they act as relay nodes. The transmitted data are time stamped in order for the nodes to utilize updated information. Nodes that do not transmit are in a receiving mode "listening" for possibe transmissions by neighbor nodes. We may relax the power constraints of the nodes since in indoor environments nodes can be mounted close to power supply sockets. Thus, the processing, transmission and reception power consumption does not limit the operation of the nodes. We further assume that each node is able to resolve n simultaneous transmissions with n being a variable in the range [1, 4]. A value of $n = 4$ suggests that each node has at most four neighbors and a multiple access scheme with no collisions is involved i.e., a TDMA approach with synchronized nodes. On the other extreme, the value of $n = 1$ suggests that nodes transmit independently and only in the case of no collisions a packet is correctly received by a node. There is a tradeoff between p and n. The largest the value of p the more transmissions occur and thus the more susceptible is a packet to collisions.

5.3.2 The detection mechanism based on the CUSUM algorithm

One of the most promising algorithms to sequentially detect the change is the CUSUM test [33]. Gombay [35] adapted Page's CUSUM test for change detection in the presence of nuisance parameters. Gombay proposed statistics based on the efficient score (Rao's statistics), on the maximum likelihood estimator (Wald's statistics), or on the log likelihood ratio. The efficient score vector as defined in equation (3.13) will be

$$V_k(\mu,\sigma) = \sum_{\iota=1}^{\kappa} \nabla_{\nu} \log f(Z_i ; q, \sigma) \quad \nu=(q,\sigma) \tag{5.4}$$

As it can be proved, if the density f(.) belongs to the exponential family, i.e. Gaussian, then if some regularity conditions hold under the null hypothesis (normal operation), there exists a Wiener process W(t) that approximates

$$W_k = \Gamma^{-1/2}(q,\sigma) V_k(q,\sigma_\kappa) \tag{5.5}$$

where σ_k is the maximum likelihood estimation of σ, and $\Gamma(q,\sigma)$ is the Fisher information matrix.

The test statistic W_k in (5.5) can be used to check if a change in densities has occurred at some time instant $\tau \leq k$. Under the alternative hypothesis (abnormal energy consumption) this statistic drifts for $k \geq \tau$ with the size of the drift proportional to the rate at which the test statistic moves in the direction of the alternative density. Moreover, in order to make decisions after n observations have been obtained, we use the following result (Darling, Erdos [36])

$$exp(-e^{-s}) = lim_{n\to\infty} P\{a(log(n))\, max_{1<k\leq n}\, k^{-1/2}\, W_k \leq s + b(log(n))\} \tag{5.6}$$

where

$$a(x) = (2\, log(x))^{1/2} \tag{5.7}$$

and

$$b(x) = 2\,log(x) + 0.5\,log(log(x)) - 0.5log(\pi) \tag{5.8}$$

To make use of this result a false alarm rate f is set, i.e. $f = 0.001$, where $1 - f = exp(-e^{-s})$ and the threshold is computed

$$T(f) = (2\,log(log(n)))^{-1/2}[-log(-log(1-f)) + 2\,log(log(n)) + 0.5\,log(log(log(n))) - 0.5\,log(\pi)] \tag{5.9}$$

Then, the alternative hypothesis (abnormal operation) is supported by the data at the first k when

$$k^{-1/2}W_k \geq T(f) \tag{5.10}$$

If no such k exists for $k \leq n$ the hypothesis of normal operation is not rejected. For $n = 300$ (that is 5 min with sampling period 1 sec) and the two indicative values of $f = 0.01$ and $f = 0.001$ $T(f) = 4.17$ and $T(f) = 5.42$ are obtained respectively. In what follows an assumption is made that all measurements Z_i, $i \geq 1$ are independent normal distributed random variables. In this case the test statistic in (18) is considerable simplified. Under this assumption

$$f(z_i; q, \sigma) = \frac{1}{\sqrt{2\pi}} e^{-(z_i - q)^2/2\sigma^2} \tag{5.11}$$

and under the alternative hypothesis (abnormal operation)

$$f(z_i; q_r, \sigma) = \frac{1}{\sqrt{2\pi}} e^{-(z_i - q_r)^2/2\sigma^2} \tag{5.12}$$

Let Y_i and q_d be defined as $Y_i = Z_i - q$ and $q_d = q - q_r$ respectively. It is clear that in normal operation $Y_i \sim N(0, \sigma^2)$, whereas under the alternative hypothesis $Y_i \sim N(q_d, \sigma^2)$. In this case the test statistic is

$$k^{-1/2}W_k = k^{-1/2}\frac{\sum_{i=1}^{k} Q_i}{\left(\sum_{i=1}^{k} {Q_i}^2/k\right)^{1/2}} \tag{5.13}$$

Under the alternative, the drift of $k^{-1/2}W_k$ after change is

$$k^{-1/2}\frac{(k-(\tau-1))q_d}{\left(\sigma^2+\frac{k-(t-1)}{k}{q_d}^2\right)^{1/2}} \tag{5.14}$$

Figure 5.1 shows the drift for $\tau = 1, n = 300, \sigma = 5, q_d = 1$ (blue), q_d = 2 (green), and q_d = 3 (red). As it is observed the greater the excess power difference ($q_d = q - q_r$) the largest the slope of the drift.

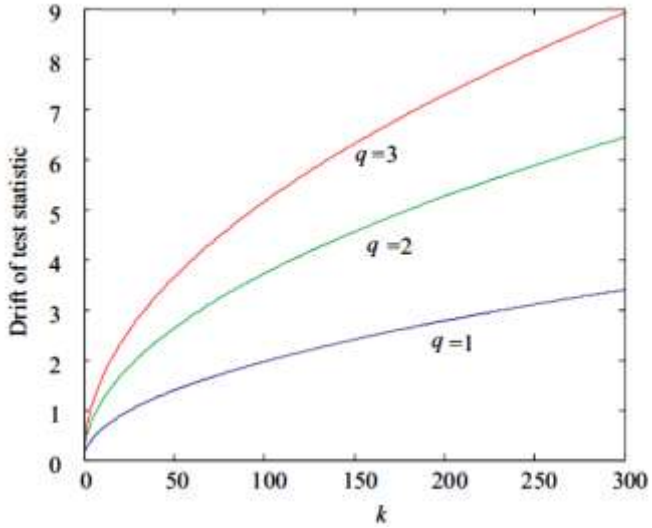

Figure 5.1 Drift of test statistic for σ = 5 and q_d = 1,2 and 3 [17, 45]

The only parameter needed to run the detection algorithm is q. This parameter is estimated by each node using the model described by equations (5.1) - (5.3). The external inputs $u(t)$, which are the surrounding temperature values, are conveyed to the node through the WSN. Depending on the multiple access technique, a node may not receive updated values of $u(t)$ due for example to transmission collisions. In this case, the node runs the detection algorithm with the latest received values of $u(t)$. As it will be shown in Chapter 6, this does not affect much the detection process.

5.4 The Subspace Identification method for the detection of abnormal power consumption

5.4.1 System modeling

5.4.1.1 Detection of abnormal system behaviour

As it has been already mentioned, we consider a nine-zone system with a WSN deployed consisting of temperature sensor nodes. Each wireless node measures the temperature of the zone and it covers and conveys this information to its neighboring nodes. Additionally, the nodes have the functionality to detect abnormal operation, for example slower temperature rising than the anticipated one due to open windows during winter, or high temperature values due to the onset of a fire, and signal it to an operation center. The detection mechanism relies on knowledge of the temperatures of the surrounding zones and the dynamics of the covered zone. The dynamics of each zone are learned during a training period using the subspace identification procedure presented in the next subsection.

In general, the assumption is made that each zone is represented by a discrete model of the form

$$x_{k+1} = F\left[x_{k,}u_k, \psi\right] \tag{5.15}$$

$$y_k = G\left[x_{k,}u_{k,}\zeta\right] \tag{5.16}$$

where x_k is the state vector at discrete time k, u_k is a vector of external inputs, y_k is the predicted zone temperature and ψ, ζ are specific parameters to the systems $F[\cdot]$ and $G[\cdot]$ respectively. Knowing the dynamics of the system and the external inputs u_k, the node is able to predict the temperature of the zone y_k. The inputs u_k in this case are the temperatures of the surrounding zones, the outdoor temperature and the power of heaters located in the zone. Comparing the predicted values to the actual ones, as measured by the temperature sensors, possible changes in the dynamics of the system can be detected, which signal an abnormal operation. Optimal detection theory deals with the problem of

detection of changes in the distribution of measurement data. Control charts [40] and the CUSUM algorithm [35] are some of the simplest and most applied solutions. Alternatively, the subsystem model can be periodically re-identified looking for possible changes in the parameter space $\{\psi, \zeta\}$. However, such a detection process is computationally demanding and overloads the wireless nodes. Moreover, more data are needed to be processed to draw safe conclusions and thus large delays are unavoidable. On the contrary CUSUM charts can detect easily small systematic shifts but their response to large shifts is relatively slow. For all these reasons, in this work the CUSUM technique is used as the basic change detection algorithm since even small deviations from strict operating requirements should be detected. The detection process will be based on the rate of variation of the prediction error between the real and the predicted temperature. To this end the sequence of prediction errors $E_k = Y_k^r - Y_k$ is defined where Y_k denotes the predicted temperature process and Y_k^r is the "real" temperature process of the zone. The derivative of this discrete process is the random variable Z_k, where

$$Z_k = E_k - E_{k-1} \tag{5.17}$$

The assumption is made that Z_k have density $f(z_k; q_n, \sigma)$ for $k = 1, \dots \tau - 1$ and density $f(z_k; q_a, \sigma)$ for $k \geq 1$ where the parameter q_n is known (or it is estimated) and q_a and σ are generally unknown. The time index τ signals an event that changes the distribution of the measurements. In terms of the proposed algorithm, q_n is the mean of the rate of the prediction error in normal operation and σ^2 is the variance of the rate due to uncertainties of the measurement devices. σ is a nuisance parameter and it is generally unknown. The parameter q_a denotes the mean of the rate of the prediction error in case of an abnormal situation, and it is considered unknown. The parameter τ is the time index when a change of densities occurs and sequential tests deal with the detection of this change. Although, q_a is in general a function of time k, the detection algorithm will be applied using the random variables $Q_k = Z_k - q_n$. Thus, under normal operation (null hypothesis) Q_k has a constant mean value equal to 0, whereas

under the alternative hypothesis Q_k has a non-zero unknown mean value $q = q_a - q_n$. Note that the measurement noise is only due to the sensors and not due to exogenous factors such as lamps, the presence of people etc that may influence the detection process. These sources of noise affect both the estimate of q_n, the mean of the rate of the prediction error on normal operation, and the drift of the test statistic (see below) so that one cannot draw safe conclusions about an abnormal situation. Nevertheless, in the simulation results presented in Chapter 6 an experiment with such noise processes modeled is included, primarily to demonstrate the effectiveness of the SID method and to provide directions for future research. The efficient score vector based on equation (5.4) is defined as

$$V_k(q,\sigma) = \sum_{i=1}^{k} \nabla_v \, logf(q_i; q, \sigma), \qquad v = (q,\sigma) \tag{5.18}$$

and if the density $f(\cdot)$ belongs to the exponential family, i.e. Gaussian, there exist the Wiener process $W(t)$, and from (5.5) approximates

$$W_k = \Gamma^{-\frac{1}{2}}(q,\sigma) V_k(q,\hat{\sigma}_k) \tag{5.19}$$

where $\hat{\sigma}_k$ is the maximum likelihood estimation of σ and $\Gamma(q,\sigma)$ is the Fisher matrix. The test statistic W_k in (5.19) can be used to check if a change in densities has occurred at some time instant $\tau \leq k$. Under the alternative hypothesis (abnormal behaviour) this statistic drifts for $k \geq \tau$ with the size of the drift proportional to the rate at which the test statistic moves in the direction of the alternative density. Moreover, in order to make decisions after n observations have been obtained, equation (5.6) is used with $a(x)$ and $b(x)$ as in equations (5.7) and (5.8) respectively. A false alarm rate is set to f = 0.001, where $1 - f = exp(-e^{-s})$ and the threshold is computed by equation (5.9).

Then as in the initial approach in Section 5.3 equation (5.10), the alternative hypothesis (abnormal operation) is supported by the data at the first k when

$$k^{-1/2} W_k \geq T(f) \tag{5.20}$$

If no such k exists for $k \leq n$ the hypothesis of normal operation is not rejected. Again as in the initial approach, for $n = 300$ (that is 5 min with sampling period 1 sec) and the two indicative values of $f = 0.01$ and $f = 0.001$, $T(f) = 4.17$ and $T(f) = 5.42$ are obtained respectively.

The assumption is made that all measurements Q_i, $i \geq 1$ are independent random variables. In this case the test statistic in (5.19) based on equation (5.13) takes the form

$$k^{-1/2} W_k = k^{-1/2} \frac{\sum_{i=1}^{k} Q_i}{\left(\sum_{i=1}^{k} {Q_i}^2 / k\right)^{1/2}} \tag{5.21}$$

Under the alternative, the drift of $k^{-1/2} W_k$ after change is based on equation (5.14)

$$k^{-1/2} \frac{(k-(\tau-1))q}{\left(\sigma^2 + \frac{k-(t-1)}{k} q^2\right)^{1/2}} \tag{5.22}$$

The drifts for $= 1$, $\nu = 300$, $\sigma = 5$, $q = 1$ (blue), $q = 2$ (green), and $q = 3$ (red) are as depicted in Figure 5.1 [45].

5.4.1.2 Deterministic subspace identification

The deterministic SID model has been implemented in order to be achieved the temperature prediction for each zone after the completion of the "training phase". According to the SID analysis in Chapter 4 the temperature prediction has been achieved as follows: Each zone is treated separately and is represented by a discrete time, linear, time invariant, state space model (equations 4.17 and 4.18). That is, $F[\cdot]$ and $G[\cdot]$ are linear functions and for a specific zone we can write

$$x_{k+1} = Ax_k + Bu_k + w_k \tag{5.23}$$

$$y_k = Cx_k + Du_k + v_k \tag{5.24}$$

where y_k is the zone temperature at time k and is in general an l-dimensional vector if l temperature sensors scattered in the zone have been deployed. Assuming a uniform zone temperature only one sensor node is needed and thus

y_k becomes scalar. v_k represents the measurement noise due to imperfections of the sensor. u_k is a vector of input measurements and its dimensionality varies from zone to zone. This vector contains the measurable output of sources that influence zone's temperature. Such sources are the power of a heater located in the zone, the air temperature at various positions outside the zone etc. The vector x_k is the state vector of the process at discrete time k. The states have a conceptual relevance only and they are not assigned physical interpretation. Of course a similarity transform can convert the states to physical meaningful ones. The unmeasurable vector signal w_k represents noise due to the presence of humans in the zone, switching lamps on and off etc. The effects of state and output noise are neglected and thus a deterministic identification problem is obtained, which is the computation of the matrices A, B, C and D from the given input-output data. Following the process and the derivation in Chapter 4 the block Hankel matrices are defined

$$U_p = U_{0|i-1} = \begin{pmatrix} u_0 & u_1 \cdots & u_{j-1} \\ u_1 & u_2 \cdots & u_j \\ \vdots & \vdots & \vdots \\ u_{i-1} & \cdots & u_{i+j-2} \end{pmatrix} \tag{5.25}$$

$$U_f = U_{i|2i-1} = \begin{pmatrix} u_i & u_{i+1} \cdots & u_{i+j-1} \\ u_{i+1} & u_{i+2} \cdots & u_{i+j} \\ \vdots & \vdots & \vdots \\ u_{2i-1} & \cdots & u_{2i+j-2} \end{pmatrix} \tag{5.26}$$

which represent the "past" and the "future" input with respect to the present time instant i. Stacking U_p on top of U_f the block Hankel matrix is obtained (eq. 4.23)

$$U_{0|2i-1} = \begin{pmatrix} U_{0|i-1} \\ \hline U_{i|2i-1} \end{pmatrix} = \begin{pmatrix} U_p \\ \hline U_f \end{pmatrix} \tag{5.27}$$

which can also partitioned as (eq. 4.24)

$$U_{0|2i-1} = \begin{pmatrix} U_{0|i} \\ \hline U_{i+1|2i-1} \end{pmatrix} = \begin{pmatrix} U_p^+ \\ \hline U_f \end{pmatrix} \tag{5.28}$$

by moving the "present" time one step ahead to time $i+1$. Similarly, the output block Hankel matrices $Y_{0|2i-1}$,Y_p , Y_f, Y_p^+, Y_f^- and the input-output data matrices are defined (eq. 4.27)

$$W_p = W_{0|i-1} = \left(\frac{U_{0|i-1}}{Y_{0|i-1}}\right) = \left(\frac{U_p}{Y_p}\right) \tag{5.29}$$

and (eq. 4.28)

$$W_p^+ = \left(\frac{U_p^+}{Y_p^+}\right) \tag{5.30}$$

The state sequence X_m is defined as (eq. 4.29)

$$X_m = \left(X_m\ X_{m+1}\ \ldots\ X_{m+j-1}\right) \tag{5.31}$$

and the "past" and "future" state sequences are $X_p = X_0$ and $X_f = X_i$ respectively. With the state space model (4.17), (4.18) the extended observability matrix Γ_i and the reversed extended controllability matrix Δ_i are associated where (eq. 4.30, 4.34)

$$\Gamma_i = \begin{pmatrix} C \\ CA \\ CA^2 \\ \cdots \\ CA^{i-1} \end{pmatrix}, \qquad \Delta_i = \left(A^{i-1}B\ A^{i-2}\ \cdots AB\ B\right) \tag{5.32}$$

The subspace identification method is based on determining the state sequence X_f and the extended observability matrix Γ_i directly from the input-output data u_k, y_k; then based on them, in a next step, extracting the matrices A, B, C and D. To this end the oblique projection of the row space of Y_f along the row space of U_f on the row space of W_p is defined (eq. 4.43)

$$O_i = Y_f\ /_{U_f}\ W_p = \left[Y_f\ /\ U_f^{\perp}\right]\left[W_p\ /\ U_f^{\perp}\right]^{\dagger} W_p \tag{5.33}$$

where † denotes the Moore-Penrose pseudo-inverse of a matrix, and $A/B^{\perp}$ is a shorthand for the projection of the row space of matrix A onto the orthogonal complement of the row space of the matrix B, that is

$$A \,/\, B^{\perp} \;=\; I - AB^{T}(BB^{T})^{\dagger}B \tag{5.34}$$

As it is proved in [19] the matrix O_i is equal to the product of the extended observability matrix and the "future" state vector (eq. 4.43),

$$O_i = \Gamma_i X_f \tag{5.35}$$

Having the matrix O_i its singular value decomposition (SVD) is computed (eq. 4.44)

$$O_i = (U_1\ U_2)\begin{pmatrix} S_1 & 0 \\ 0 & 0 \end{pmatrix}\begin{pmatrix} V_1^T \\ V_2^T \end{pmatrix} = U_1 S_1 V_1^T \tag{5.36}$$

and the extended observation matrix Γ_i and the state vector X_f are obtained

$$\Gamma_i = U_1 S_1^{1/2} T, \quad X_f = T^{-1} S_1^{1/2} V_1^T = \Gamma_i^{\dagger} O_i \tag{5.37}$$

where T is an $n \times n$ arbitrary non-singular matrix representing a similarity transformation.

One method [39] to extract the matrices A, B, C and D uses in addition the oblique projection

$$O_{i-1} = Y_f^{-} \,/_{U_f^{-}}\, W_p^{+} = \Gamma_{i-1} X_{i+1} \tag{5.38}$$

where Γ_{i-1} is obtained from Γ_i by deleting the last l rows ($l = 1$ in our scale). Similar to the previous derivation the equation is obtained

$$X_{i+1} = \Gamma_{i-1}^{\dagger} O_{i-1} \tag{5.39}$$

and the matrices A, B, C and D are obtained by solving (in a least square fashion) the system

$$\begin{pmatrix} X_{i+1} \\ Y_{i|i} \end{pmatrix} = \begin{pmatrix} A & B \\ C & D \end{pmatrix}\begin{pmatrix} X_i \\ U_{i|i} \end{pmatrix} \tag{5.40}$$

5.4.2 The proposed Algorithm

The key ingredients in this proposed algorithm are the deterministic subspace system identification and the CUSUM algorithm as both presented in Chapter 4. The algorithm includes two operation phases: the training phase and the detection phase. During the first phase (training) all the nodes in the structure report their measurements to a central computing system. These measurements consist of the temperature of the zone and the current power of a heater, if the sensor node is in charge of a heated zone, or only the temperature if the sensor node monitors an area immaterial to the detection process but relevant to other zones, i.e, the exterior of a building. The training phase should be performed only once but under controlled conditions, for example no extra sources of heating, closed windows etc. Moreover, the length of this period should be quite large in order that several variations in the input signals to excite the modes of the system are present. In the simulation part a training period of 24 h, that is 86400 samples with sampling period 1 sec are considered. After receiving all the measurements, the central system arranges them to input-output data for each zone. For example, in the case of a zone named A, with neighbors zones named B, C, D and the exterior to the building zone named E, then the temperature values of zone A are considered the output of the system to be identified, whereas the temperatures of the zones B, C, D and E as well as the power profile of the heater of zone A are the input data for the system. Then, a deterministic subspace identification process is run for each zone as described in the previous subsection. The relevant matrices A, B, C and D of the state space model of the equations 4.1 and 4.2 of each zone are communicated back to the sensor node that is responsible for monitoring the zone.

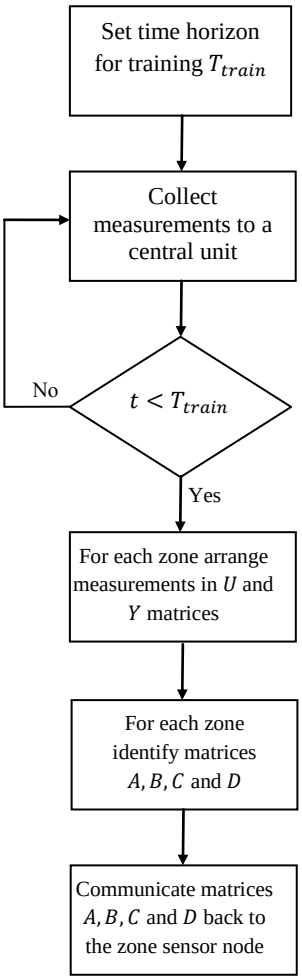

Figure 5.2 Training phase steps of the algorithm

Figure 5.2 depicts the flow diagram of the "training phase". After reception of these matrices, the sensor node enters the detection phase. The detection phase is split into cycles of possibly unequal lengths. In the beginning of each cycle the value q_n, that is the mean of the rate of the prediction error is estimated using a few samples. For the simulation part short periods of 1 min (60 samples) are used to estimate the value q_n. Then, for the rest of the cycle the CUSUM algorithm is run to detect possible deviations from the normal operation.

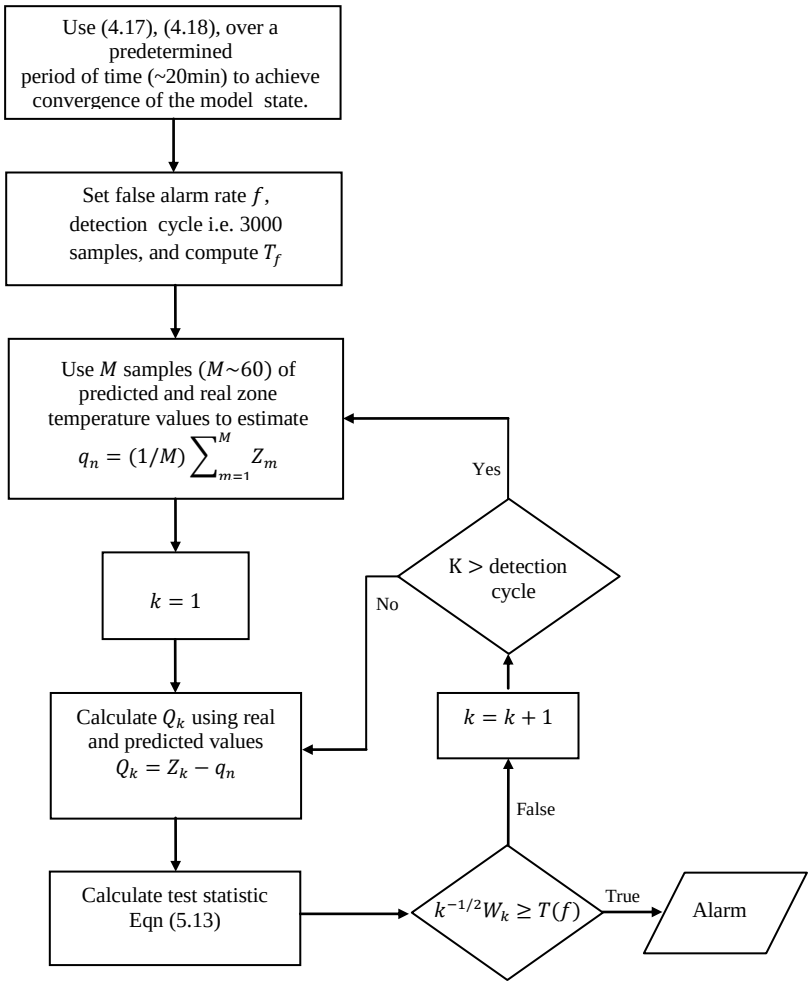

Figure 5.3 Detection phase steps of the algorithm

The length of the detection interval is quite large, in the order of 1 hour, and it should depend on the time of the day. During periods (of the day or night) with small (large) expected changes of the exterior temperature, the detection interval can be increased (decreased).

Note that a positive drift of the test statistic ($q > 0$) designates an abnormal increase of temperature, that may be due to the onset of a fire, whereas a negative drift of the test statistic ($q < 0$) designates leakage of heat, that may be due to open windows during winter, or malfunctioning of the heater. The detection phase flow diagram is depicted in Figure 5.3.

5.5 Summary

In the initial approach of detection of abnormal situations, an HVAC control system based on the multi-zone (nine-zone) principle is proposed. The system utilizes a WSN network of temperature sensors to control independently the heating supply of each zone. Moreover, the system is capable to detect abnormal energy consumption that may be due to heat leakages or other events like fire. To this end, the reference power consumption at each zone is estimated based on a suitable zone lumped capacity model with inputs the surrounding temperatures that are communicated to the node using the means of the WSN. The CUSUM algorithm is used next to detect possible divergences of energy consumption from the reference values.

The second proposed method for the detection of abnormal behaviour in HVAC systems is also based on the multi-zone (nine-zone) principle and utilizes deterministic subspace identification to obtain state space system models that will provide the reference temperatures for each zone. The method consists of two phases of operation: the training phase and the detection phase. During the training phase the nodes of the WSN (installed in each zone) send their temperature readings to a central computer unit in order to be arranged in the input/output form as required from the SID model. After the SID is processed by the central unit the parameter matrices A, B, C & D are communicated back to the nodes of each zone where they are applied on the state space model to predict the temperature behaviour. Then the algorithm enters to the detection phase where the CUSUM algorithm is implemented to detect possible divergences of the rate of change of the difference between the real and the predicted values.

Chapter 6

Results of the methods for the detection of abnormal situations in HVAC systems

6.1 Introduction

This chapter contains the results of the methods presented in Chapter 5. In Section 6.2 the results of the first initial approach for detection of abnormal situations is presented with the results of the single zone simulation *(Subsection 6.2.1)* and the results of the multi-zone simulation *(Subsection 6.2.2).* In Section 6.3 the results of the second detection method based on the SID model are presented including the results of the training and the detection phases.

6.2 Results of the initial detection approach based on a WSN

6.2.1 Single zone simulation results

First, a single zone system was simulated using Walter's model for the outdoor temperature T_o, as it is depicted in Figure 3.4 *(Chapter 3)*. The target temperature is set to 24℃. A tuning technique, like the Ziegler-Nichols method, is utilized to determine the parameters of a PI controller. The values of K_p and K_i that have been used in the simulations were 100 and 0.1 respectively.

The single zone model dynamics and parameter values are taken from [33] as presented in Chapter 3. The parameters are summarized as in Table 3.1 *(Chapter 3).*

A_{ew}: $9m^2$	C_{ns}: 70 KJ/C^o
A_{ns}: $12m^2$	C_R: 70 KJ/C^o
A_R: $9m^2$	U_{ew}: 2 W/m^2C^o
C_r: 47.1 KJ/C^o	U_{ns}: 2 W/m^2C^o
C_{ew}: 70 KJ/C^o	U_R: 1 w/m^2C^o

The system starts in the all zero initial state, and as it is depicted in Figure 6.1, the room temperature reaches its target value in less than 90 min (5400 sec). After that, the room temperature is kept almost constant to 24℃ despite the variations of the outdoor temperature. The duration of the simulation is 24 hours (86400 sec) and the sampling period was set to 1 sec.

Figure 6.2 shows the controlled values of $q(t)$ for a 24 hours simulation period. The graph of this figure (Fig. 6.2) should be compared to that of Figure 3.4 *(Chapter 3)*, which shows the variations of the outdoor temperature T_o. As it is expected, in high temperature hours like 13:00-15:00, the function $q(t)$ takes lower values, whereas in low temperature periods $q(t)$ increases as depicted in Figure 6.3. The estimated energy consumed is 19.8 KWh [17].

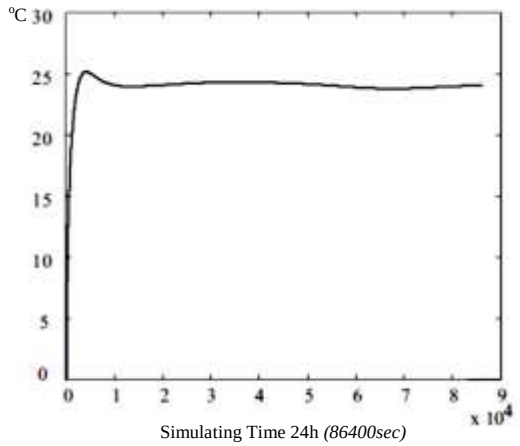

Figure 6.1. Room temperature variation vs time (sec). Target value 24°C

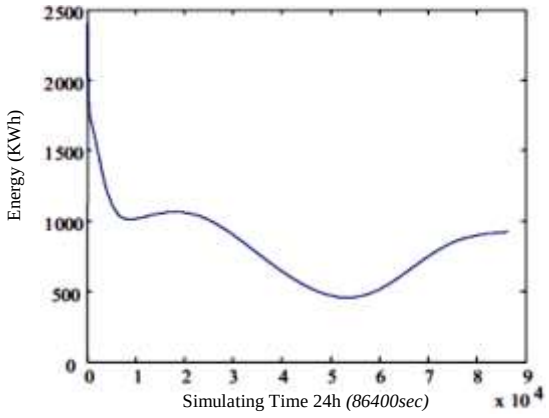

Figure 6.2. Power variation

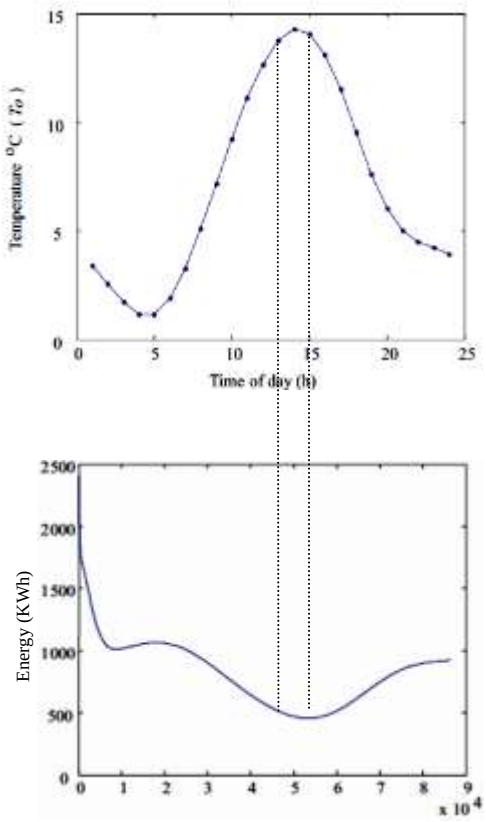

Figure 6.3 Comparison of the outside temperature T_o with the consumed energy

6.2.2 Multi-zone simulation results

Next a multi-zone system was simulated consisting of nine rooms as it is shown in Figure 6.4. The target temperatures for each zone, as shown in this figure, are: 26, 18, 16, 17, 20, 22, 19, 18, 26 (℃).

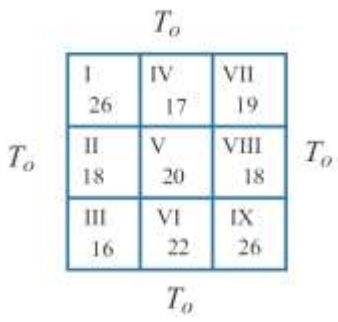

Figure 6.4 Nine-zone model with the target temperatures for each zone

The transmission probability was set to $p = ¼$ and any collision resolution was not allowed. This means that a node having two or more neighbor nodes transmitting simultaneously could not receive their packets. In this case, the node is obliged to use the latest values of received surrounding temperatures. The temperature variations for the five first zones are depicted in Figure 6.5. The outdoor temperature T_o was obtained using Walter's model and each node started in the all zero state. The simulation time was set to 15000 sec (~4h). As it is observed, after 7000 sec (approx. 2h) the temperatures settle to the target values. Figure 6.6 shows the power profile used for the first five zones. The highest energy consumption is due to zone I, which has the highest target temperature and lies in the corner of the floor. This means that two sides of the room are exposed to the outdoor temperature and this demands high heat gains to hold the zone temperature constant. The same reasoning applies to zone III. Although the target temperature for zone III is only 16℃, low outdoor temperatures T_o, causes high energy consumption.

Next we simulated the proposed detection algorithm. To this end we considered the same layout as in Figure 6.4, but now we forced a conservative heat leakage due to infiltration at time $\tau = 10000$. Thus, equations (3.1) - (3.6) *(Chapter 3)* are modified after τ by adding the term q_i (equation 3.7 - *Chapter 3)*. Moreover, we added white zero mean Gaussian noise, $w(t)$ with unit variance to the measurements $y(t)$. Figure 6.8 shows the real power profile $q_r(t)$ for this case. As it is observed the noise is amplified due to the high gain k_p of the PI controller.

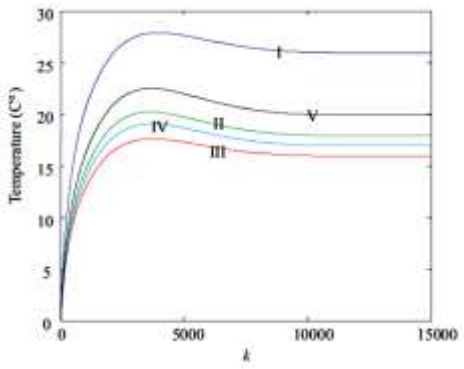

Figure 6.5. Temperature variation of the zones I – V vs time (sec) [17]

Figure 6.7 depicts the drift of the test statistic. After τ = 10000 there is a positive drift which indicates the higher power is needed than the anticipated one. This means that there is a heat loss in the zone. In the case of a heat gain due for example to a fire in the zone, the drift of the test statistic would be negative. Again, for the WSN supporting the transfer of temperatures between zones, we set $p = 1/4$ and no collision resolution.

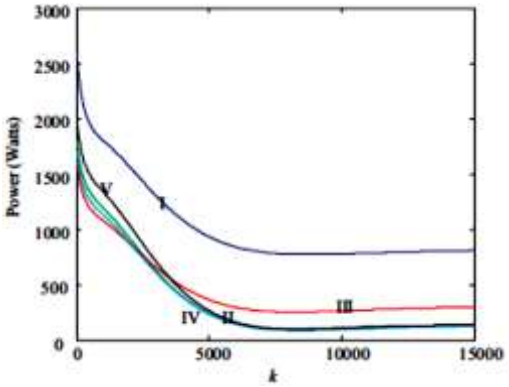

Figure 6.6 Power variation vs time

This means that the zones have partial information of the surrounding temperatures, and they are forced frequently to use previous values to update their models. As it is observed from Figure 6.7, a threshold of value approximately equal to 5, is crossed in 20 min (1200 samples) even for this conservative heat loss. Higher heat losses or gains will lead to faster detection times with small false alarm rates

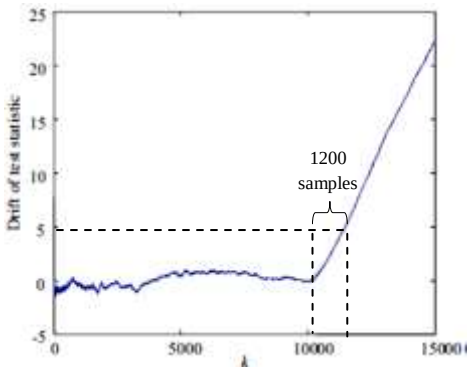

Figure 6.7. Drift of set statistic (change at time 10000 sec)

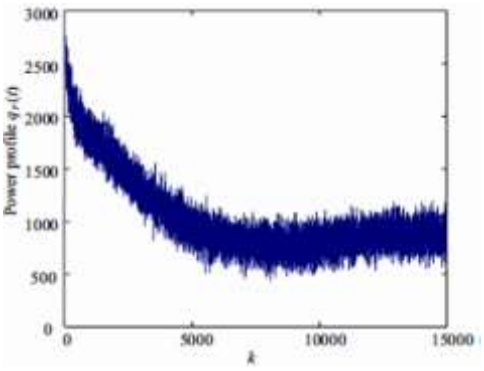

Figure 6.8. Real power profile $q_r(t)$

6.3 Results of the SID detection method

6.3.1 Training Phase

For the deterministic subsystem identification 86400 samples are used with sampling period $T_s = 1sec$. For the outside temperature the Walter's model is used with parameters given in the first row of Table 6.1 and a heater gain equal to 600 W. The target temperatures of the zones T_{tg} are set to those

Table 6.1
Training and Testing Parameters for Outer Temperature Model and Heat Gain

	WALTER'S MODEL TEMPERATURES (℃)			HEAT GAIN (W)
PHASE	TMAX	TMIN	TM	Q(T)
TRAINING	13	2	7	600
TESTING	16	1	6	700

of Table 6.2 (first row) with a margin equal to $T_{mg} = 1$℃. That is, for a specific zone the heater is on until temperature $T_{tg} + T_{mg}$ is reached. After this point the heater is turned off until temperature hits the lower threshold $T_{tg} - T_{mg}$ and the whole process is repeated.

Table 6.2
Training and Testing Zones' Target Temperature

	Target temperatures (℃)								
Zone	**I**	**II**	**III**	**IV**	**V**	**VI**	**VII**	**VIII**	**IX**
Training	16	18	13	15	14	13	12	16	14
Testing	17	20	17	17	17	14	18	19	21

Having collected the data over the period of 24 hours, the measurements of the zones' temperature, the outer temperature and the heat gains of each zone, are arranged into input-output data for the subsystem identification process. For example, for zone I, the outer temperature, the heating gain of zone I, as well as the temperatures of zones II and IV, are the input data to the identification process whereas the temperature of the zone I itself is the output data. Note that the number of input signals differ from zone to zone. Zones I, III, VII and IX use 4 input signals whereas the rest of the zones use 5 input signals. Based on the input-output data the matrices A, B, C and D for each zone as described in Section 3 are identified. During this process the order of the subsystems must be decided. This is achieved by looking at the singular values of the SVD decomposition in (4.57) and deciding on the number of dominant ones. Figure 6.9 depicts the singular values for zones I and V. All subsystems exhibit similar behaviour regarding the profile of their singular values and therefore we set the order of all subsystems is set to 2.

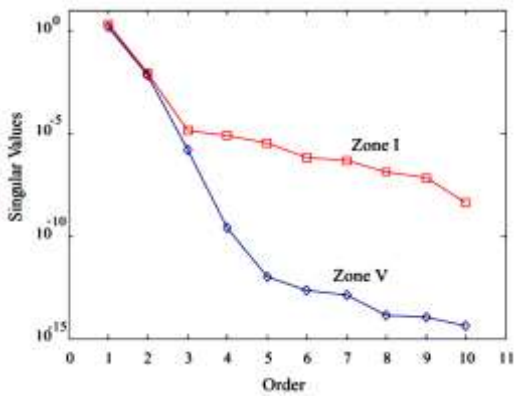

Figure 6.9 Singular values of Zones I and V.

Next a test is run on the obtained state-space models. The outer temperature parameters are set as in the second row of Table 6.1 the heat gain equal to 700 and the target temperatures as in the second row of Table 6.2. The initial state of the subsystem model was set to $[-10 \;\; 0]$, whereas the elements of the 42 state vector of the multizone system were set equal to 5 (the initial output temperature). Figure 6.10 shows the evolution of the actual and predicted temperature for Zone I. As it is observed, after 7000 samples (appox. 2 hours period) the state of the subsystem has converged to one that produces almost the same output as the original system. After this point the WSN nodes can enter in the detection phase.

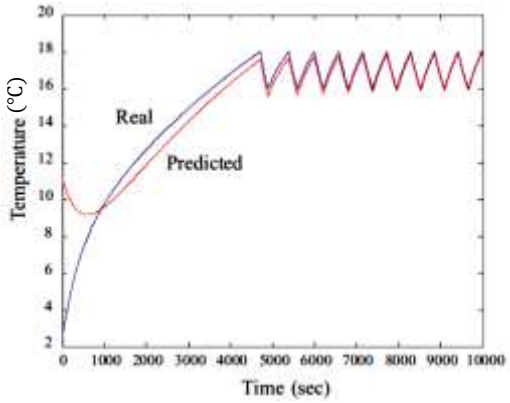

Figure 6.10 Real and Predicted temperature of Zones I

6.3.2 Detection Phase

To demonstrate the detection capabilities of the algorithm two scenarios are used. In the first scenario, there is heat leakage, possibly due to an open window. To take into account the infiltration gain (equation 3.7) the term below is added

$$q_i = mV(T_o - T_r)/3 \tag{6.1}$$

to the right hand of equation (3.1). V is the room volume and m is an index that indicates the air changes per hour. As described in Chapter 3 *(Sec 3.2.1)* the same conservative value of m is used that is $1/4$. Assumption is made that the change

in the dynamics of the system takes place at Zone I, at time instant $n = 8000$. Figure 6.11 shows the real and the predicted temperatures in this case. The target temperature is 17℃ .

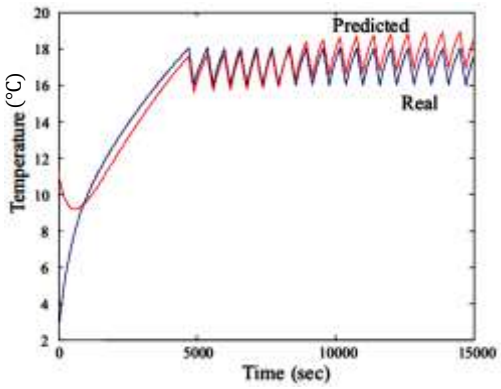

Figure 6.11 Real and Predicted temperature of Zone I, with a heat leakage starting at $n = 8000$.

As it is observed the predicted values deviate from the real ones after time index 8000. In fact the predicted values do not stay in the zone $[16^o, 18^o]$, that is the target temperature $\pm 1^o$. This is due to the fact that in this scenario the heater is turned on more frequently and this forces the prediction model to produce higher temperature values. Crossing the upper limit of the operation zone is an indicator of a heat loss and this information could be fused with the results of the CUSUM algorithm for more reliable detection of the abnormal condition. Figure 6.12 shows the drift of the test statistic of the CUSUM algorithm in case of normal and abnormal operation. The CUSUM algorithm started at time 7000 and 60 samples were used to estimate q_n that is the mean of the rate of the prediction error.

In the second scenario there is an extra source of heat with power 100 W. This source is activated at time instant 8000 and it remains on independently of the zone's heater. Figure 6.13 depicts the real and the predicted temperatures in this case. As it is observed, the predicted values in this case fall below the zone $[16^o, 18^o]$. This is because the heater of the zone is turned on less often since there is an additional heat power in the zone.

However, the prediction model is unaware of this fact and "sees" only the power on-off process of the zone's heater. Similar to the previous scenario, crossing the lower limit of the operation zone is an indicator of an extra heat source in the zone. The CUSUM test results for this scenario are depicted in Figure 6.14. In both scenarios, the drift test statistic crosses the threshold of $T_f = 5.42$ within 300 samples and therefore with a false alarm rate equal to $f = 0.001$ it can be determined that a change has occurred or not within 5 min.

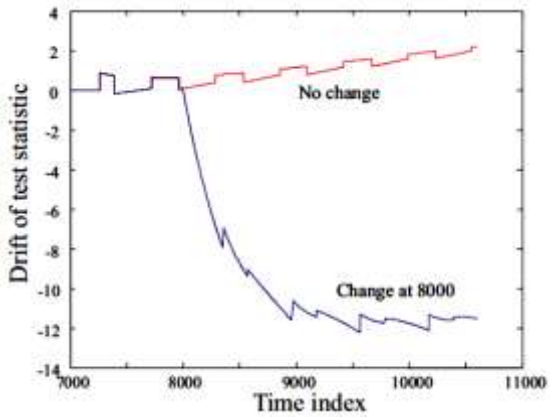

Figure 6.12 Drift of the test statistic for scenario I, under no change and a heat leakage starting at n = 8000.

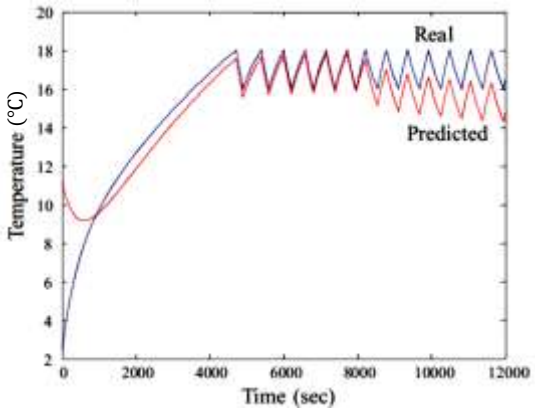

Figure 6.13 Real and Predicted temperature of Zone I, with an extra heat source powered on at n = 8000

It should be noticed at this point that the "original" simulated system (42 state-space model) is also linear and thus the use of linear subspace identification may be questionable for more complex and possibly nonlinear systems. As the

simulation results indicate although the dynamics of each zone are more complex (including the roof temperature for example) a low dimensionality subsystem of order 2 can capture its behaviour. For more complex systems the order of the identified subsystem can be chosen high enough. For nonlinear systems the identification of a time varying system is possible using a recursive update of the model.

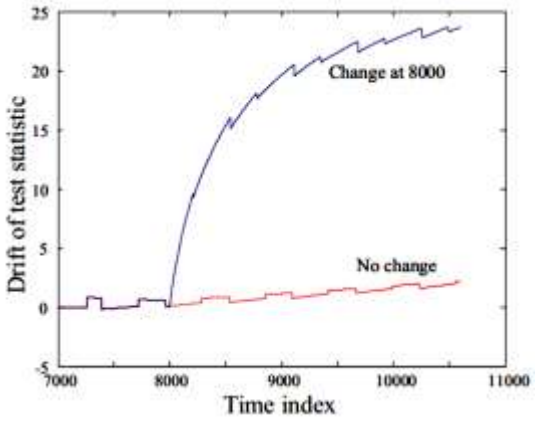

Figure 6.14 Drift of the test statistic for scenario II, under no change and an extra heat source powered on at n = 8000

Next, the SID method is tested when an exogenous heat noise is present. This noise is modelled as

$$n(t) = \sum_i \ a_i w\left(\frac{t-\left(\frac{T_i}{2}+\sum_{j>i} T_j\right)}{T_i}\right) \tag{6.2}$$

where a_i is uniformly distributed in the range [50, 100] Watt, and T_i is exponentially distributed with mean 180 sec. $w(t)$ denotes a rectangular window of unit length and height equal to one. A sample of this process is given in Figure 6.15.

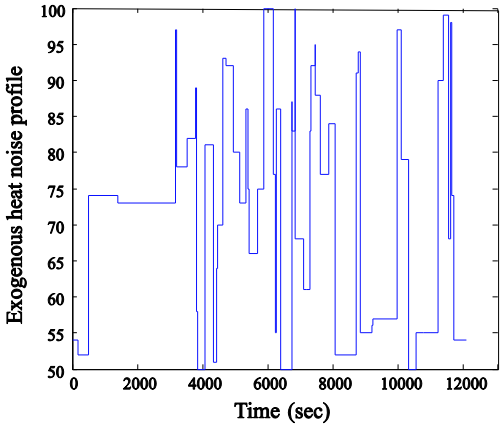

Figure 6.15 Exogenous heat noise profile

The real and predicted temperature values for this case are shown in Figure 6.16. As it is observed the predicted values are always lower than the real ones and this is due to the fact that the SID method ignores the extra source of heat and it bases its predictions solely on the zone's heater on/off periods. This is clearer after time instant 8000 where an extra heat source of 100 Watt is always present. Several techniques can be used in this case to detect the discrepancies from the target operating restrictions. Deviations of the mean predicted values from the anticipated ones, or the number of crossings of a low threshold are some possible solutions [45].

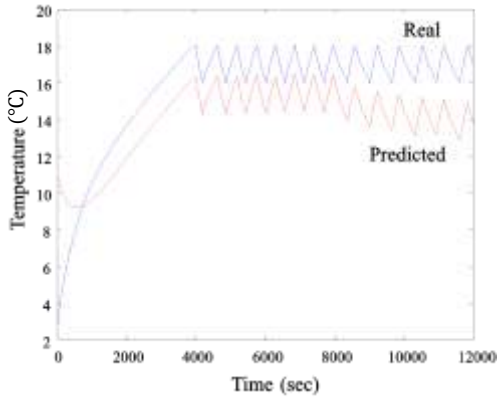

Figure 6.16 Real and Predicted temperature of Zone I, with an exogenous heat noise depicted in Fig. 6.15 and an extra heat source powered on at n = 8000.

6.4 Summary

In this Chapter the results of the methods for detection of abnormal situations in HVAC system were presented. The outlined results of the initial detection approach were as follows:

6.4.1 Simulation of the Single and Muli-zone systems

First, the single zone system was simulated with dynamics and parameter values as presented in Chapter 3, and using the Walter's model for the outside temperature T_o estimation. The evaluation of the results is as follows:

- Initially the temperature behaviour was tested. The system was simulated for 24h and showed a normal behaviour, since the temperature reached the target $T_g = 24℃$ in less than 90 min starting from 0℃. Then, the room temperature was kept almost constant to 24℃ despite the variations of the outdoor temperature.
- Subsequently, the behaviour of the power of the heater $q(t)$ was evaluated compared with the behaviour of T_o, and as it was expected in high temperature hours like 13:00-15:00, the function $q(t)$ took lower values, whereas in low temperature periods $q(t)$ was increasing.

Next, the multi-zone model consisting of nine zones was simulated with certain target temperatures for each zone, and certain probability of the nodes' transmission so that any collision resolution was not allowed. The evaluation is:

- Initially, the temperature behaviour and the power profile of five zones were evaluated for 15000sec (~4h). As it was reasonably observed, the target temperatures were reached after 7000 sec (~2h) and the highest power consumption was due to zones with the highest T_g and two sides of them were exposed to outside temperature.
- Subsequently, the CUSUM detection algorithm was simulated. For the creation of an abnormal situation, a conservative heat leakage was forced due to infiltration, at time $\tau = 10000$. Moreover, white zero mean

Gaussian noise $w(t)$ was added to the energy balance equations in addition to the term q_i (equation 3.7). As it was observed a threshold of value 5 was crossed in 20 min and the detection was made. With a higher heat loss a faster detection could be achieved.

6.4.2 Results of the SID detection method

The results of the second method based on the SID model consisting of two phases of operation (Training & Detection) were as follows:

First, the mechanism of the training phase was simulated where 86400 samples were used (24h) with sampling period $T_s = 1sec$. The Walter's model was utilized for the outdoor temperature and the heater power was 600W. There was a margin equal to $T_{mg} = 1℃$ that was $(T_{tg} + T_{mg})$when the heater was on and $(T_{tg} - T_{mg})$ when the heater was off and this process was repeated until the end of the simulation duration.

- The data collected for the training phase over the period of 24h was the measurements of the zones' temperature, the outer temperature and the heat gains of each zone.
- After collection, this data was arranged to the input/output form as required in order to be processed by the SID model. The adjacent zones' temperatures and the heater gain were arranged as the input data while the temperature of each zone was the output data.
- Based on the input / output data the parameter matrices A, B, C & D were identified. In order this identification to be achieved, the singular value decomposition (SVD) process was simulated to obtain the hidden state vector x_f with the order of 2.
- Finally, a test was run on the obtained state-space models with different outer parameters, heat gain set to 700, and different target temperatures. The temperature of zone I was predicted and produced almost the same output as the original system.

Next, the mechanism of the detection phase was simulated. A heat leakage was created in zone I by taking into account the infiltration gain, and this case caused a change in the dynamics of the zone at time instant $n = 8000$.

- The real and predicted temperatures were simulated and as it was observed, the predicted values deviated from the real ones after time index 8000. The deviation exceeded the target temperature's upper margin and this was due to the fact that the heater was turned on more frequently and so, the prediction model produced higher temperatures.
- This case was an initial indicator for a possible heat loss, but for more reliable detection of this condition the CUSUM algorithm was applied at time 7000 with 60 samples used to estimate the mean of the rate of the prediction error.
- Subsequently, the opposite of the above condition was created where an extra heat source with 100W power was added to zone I. The source was activated at time instant 8000 and it was remaining independently of the zone's heater. As it was observed, the predicted values in this case fall below the lower margin of the target temperature of the zone. The CUSUM algorithm applied, as above, to detect more reliably this abnormal condition.
- Finally, the SID method was tested when an exogenous heat noise is present with power uniformly distributed in the range of [50, 100] Watt and time exponentially distributed with mean 180 sec. Again the SID showed the deviation clearly after time instant 8000 where the extra heat source was activated.

Chapter 7

Methodology for energy efficiency control

7.1 Introduction

In this chapter the two methods for energy efficiency control in a HVAC system are presented. Both methods are focused on two parameters for the energy efficiency: the energy consumption control as well as the satisfactory thermal comfort levels. The methods are distinguished as follows:

The first method is an initial approach to energy control of a HVAC system by utilizing the occupancy status of the zones as well as the occupation time period, aiming to a significant energy saving alongside with a satisfactory thermal comfort level. It is assumed that the WSN consists of temperature and occupancy sensors. The method proposes one integrated algorithm (including two preliminary algorithms) that manages the heating scenarios of the zones: proactive heating of the adjacent zones of 1st and 2nd layer ("1-hop" and "2-hop"), full-proactive (all zone are heated when occupancy is detected), and full-reactive (only the occupied zone is heated), depending on occupants' residence time into the zones. The occupation time has been modeled as exponentially distributed with three discrete mean values.

The second method is a technique aiming to balance the thermal comfort and the energy waste of a HVAC system. This method also utilizes a WSN with temperature and occupancy sensors, as the method above, which are exchanging the information between them. Two types of predictions are provided in this method, on one hand the zones' temperature prediction provided by the SID predictive model, and on the other hand the zones' occupancy profile prediction that is provided by a semi-Markov model where occupants stay into the zones for a random period of time and then move to adjacent zones of each one with given probabilities. The method aims to a proactive zones' heating and manipulates the

risk of activation or not of the heater, relying on the weights of energy and discomfort costs.

7.2 Methods for energy efficiency control in HVAC systems

7.2.1 Methodology Overview

The second direction concerning the second control function is focused on the energy control as far as the appropriate heating timing of the zones is concern, taking into account the occupancy and the thermal comfort condition of the heating space. All methods are based on the same theoretical nine-zone model as presented in section 3.2.2, with the same temperature dynamics to any single zone, as well as the same equipment as far as the WSN is concerned. The functionality of the WSN for both algorithms is described in the next section and, as mentioned, is the appropriate for each algorithm. The initial first method utilizes the occupancy as a key factor to the zones' reactive heating or pre-heating and in addition the mean residence time (occupation time) of the occupants in each zone. The method is an integrated algorithm that comprises two proposed sub-algorithms and two conventional and widely applied heating scenarios. The two sub-algorithms utilize occupancy in the form of binary decision (occupied zone or not) and so they both require minimum information with no prediction about occupancy dynamics. The conventional heating scenarios are: the full-proactive heating scenario on one hand, where the heating is activated in all zones upon the occupants' entry into the whole space, and the full-reactive heating on the other hand, where the heating is activated only to any occupied zone. The integrated algorithm employs the above sub-algorithms as well as the existent heating scenarios in an appropriate way and according to the knowledge of the expected occupants' residence time (occupation time) in each zone. Depending on the occupation time of each zone the algorithm manages the proactive heating or not of the directly adjacent zones.

Towards this direction, a novel technique is proposed as the second method, which aims to balance the comfort and energy costs in a multi-zone system. The decisions of activating the heating of the zones or not, may be taken either centrally or in a distributed manner by wireless sensor nodes scattered in the multi-zone system. In any case temperature and zone occupancy information must be exchanged between a node, responsible for a zone, and its neighboring nodes. The decision process itself relies on two kinds of predictions: a) temperature-time predictions for the zones and b) the zones' occupancy profile. The emphasis is on the zones' temperature predictions and to this end a deterministic subspace identification method is used to model the thermal dynamics of each zone. That is, each zone is modeled by a simple state space model capable to produce accurate predictions based on the surrounding temperatures, the heating power of the zone and the current state that summarizes the temperature history of the zone. For the zones' occupancy predictions a semi-Markov model is considered, where occupants (moving as a swarm) stay in a zone for a random period of time and then move to adjacent zones with given probabilities. What is needed by the decision process is the distribution of the first entrance time to unoccupied zones. Aiming to a proactive action, the proposed method periodically computes the risk of activating the heater or not and decides in favor of the action that produces the smaller risk. The computation of the risks relies on the relative weights of the energy and discomfort costs so that the balance between the total energy consumed and the total discomfort cost may be regulated.

7.2.2 Initial approach for energy efficiency control

The rationale of our proposed algorithms is using the occupancy of the zones as a basic factor to control the heat energy and the thermal comfort condition. The basic characteristic is the proactive heating of the adjacent zones. The algorithms namely the "1-hop" and the "2-hop" require minimum information with no prediction about occupancy dynamics, since they utilize occupancy in the form of binary decisions (occupied zone or not). The third one, namely the

"Adaptive", requires knowledge of the expected residence time of the occupants in each zone. Depending on the occupants' residence time into the zones, either the adjacent zones are not heated or the directly adjacent (1-hop) are proactively heated or, furthermore, the neighbors of the adjacent zones (2-hop) are proactively heated. All the proposed algorithms could be applied to all buildings as an alternative heating method from, a) the centralized heating, where all the zones are heated constantly even if they are not occupied and b) the heating of each individual zone, only when it is occupied, or else, they stay unheated. The goal of our proposed method is the energy control as well as, the maintenance of the comfort condition in areas of the buildings that remain vacant for relatively long time, or they are in use for short time periods during work (conference rooms, meeting rooms, sections of private study in libraries etc). Otherwise, these areas would be normally heated, wasting energy vainly or instead, stay unheated and uncomfortable. The proposed algorithms have been contrasted with the above two heating scenarios.

7.2.2.1 Rationale of the algorithms

A. "1-hop" Algorithm

The functionality of the "1-hop" algorithm is described in a three-zone space model as a part of the nine-zone model and it's the following: In the three-zone space model of Fig.7.1a, when occupants enter the zone 1, the heating in this zone starts until it reaches the target temperature (T_g), and the occupancy sensor sends it's detection information to the wireless actuator nodes of the directly adjacent zones 2 and 3 *(1st hop)*. Hence, the zones 2 & 3 start to be heated concurrently. If the occupants exit zone 1 and visit zones 2 or 3 then the adjacent to zones 2 or 3 (1,4,5,6) will be heated (Fig 7.1b) [46].

"1-hop" Algorithm

for *each zone*
  If *zone occupied* ***then***
  heat zone and its 1-hop neighbors
end

B. "2-hop" algorithm

The rationale of the "2-hop" algorithm is the same as the "1-hop" with the additional characteristic the proactive heating of the neighbors to the directly adjacent zones (4,5&6) (Fig.7.1b). When occupants enter the zone 1, the heating starts in this zone and also starts in the zones 2 and 3 as well as in 4,5 and 6 [46].

"2-hop" algorithm
for *each zone*
  If *zone occupied* ***then*** *heat zone and 1-hop neighbors*
  and 2-hop neighbors
end

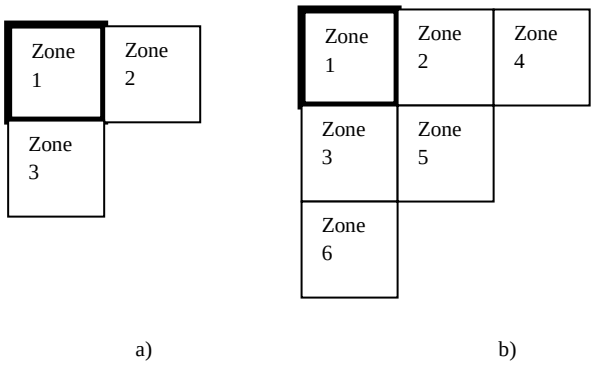

Figure 7.1 a) Occupied zone (zone1) & directly adjacent zones "1st hop" (2&3), b) Occupied, directly adjucent, and neighbor zones "2nd hop" (4,5,6) [46]

C. "Adaptive"algorithm

The third algorithm, namely the "Adaptive", requires knowledge of the expected mean residence time (t_m) of the occupants in each zone. Depending on the occupation time into the zones, either the adjacent zones are not heated or the

directly adjacent (1-hop) are proactively heated or, furthermore, the neighbors of the adjacent zones (2-hop) are proactively heated. The rationale of the third algorithm, takes into account the occupants' mobility rate through the areas of a space. The longer is the mean residence time in an occupied zone the less is the need of a proactive heating to the adjacent zones. The opposite situation where the mobility rate increases, results in the need for proactive heating of the adjacent zones. The mean of the occupation time has been quantized into four states: st= *short time*, mst= *medium-short time*, mlt= *medium-long time* and lt= *long time*. If the occupants' residence time t_m is $0 < t_m <$ st, then the zones will be proactively heated (Full-proactive scheme), because the residence time is too short and the occupants are moving quickly through the areas. If the t_m of the occupants exceeds the short time value until the medium-short time (st < t_m < mst) then the "2-hop" algorithm is applied, where the directly adjacent zones and their neighbors are proactively heated. In this case the mobility-rate of the occupants is in the time range where there is a high probability, to visit both layers of the adjacent zones (directly adjacent & neighbors). The third case is when t_m is in the range between medium-short time and medium-long time (mst < t_m < mlt) and the "1-hop" algorithm is applied, since t_m is in the time range where the occupants stay much longer into the present zone and there is a probability to visit only the directly adjacent zones. The fourth and last case is when t_m is between medium-long time and long time (mlt < t_m < lt) and there is no need for a proactive heating to any of the adjacent zones.

"Adaptive" Algorithm

` ***for*** *each* zone
if zone *occupied* & ***0< t_m <st***
then *full-proactive algorithm*
if *room occupied* & ***st < t_m < mst***
then *2-hop algorithm*
if *room occupied* & ***mst < t_m < mlt***
then *1-hop algorithm*
if *room occupied* & ***mlt < t_m < lt***
then *full-reactive algorithm*
end

7.2.3 Second proposed method for energy efficiency control based on the SID model

We consider a multizone HVAC system consisting of Z zones $z_i, i = 1, 2, \dots, Z$. Each zone equipped with a wireless sensor node capable to convey the zone's temperature and occupancy information to its neighbors or to a central processing unit. The occupancy information may be very simple i.e., binary information indicating the presence or absence of individuals in the zone, or more advanced like the number of occupants in the zone. The objective is to minimize the total energy and discomfort cost defined as

$$E = E_{energy} + E_{discomfort} \tag{7.1}$$

$$= \sum_{i=1}^{Z} \int_{-\infty}^{\infty} W_i I\,(H_i = on) dt + \sum_{i=1}^{Z} \int_{-\infty}^{\infty} C_i I\,(T_i < T_c) dt$$

In equation (7.1), $I\,(A)$ denotes the indicator function which takes the values 1 or 0 depending on whether the condition A is true or false. W_i is the power of a heater that covers zone z_i and H_i is the state of the heater, that is the heater is on or off. Thus, the first term of (7.1) is the total energy consumed by the multizone system. For the discomfort cost we define the cost per unit time C_i and the target comfort threshold T_c. As long as the zone's temperature T_i is higher than T_c the occupants do not feel discomfort. The parameter C_i may depend on the zone, the number of the occupants (e.g. the total system's discomfort cost is proportional to the number of people experiencing discomfort) and the difference of the zone's temperature T_i and the comfort threshold T_c. It is worth noting that there is a tradeoff between energy savings and discomfort cost. All zones may be preheated to the comfort level thus rendering the discomfort cost equal to zero. This policy is inefficient due to the large amount of energy consumed. In the other extreme we could act reactive by heating a zone only upon detecting occupants in it. In this case the energy cost would be as small as possible but the discomfort cost could increase dramatically. In the sequel we will describe a

method that acts proactively by taking periodically decisions on whether to heat on not a zone. If the entrance to a zone is delayed then we postpone heating until the next decision epoch. If on the contrary, it is anticipated that a zone will be occupied before the zone's temperature reaches the comfort level then we pre-heat the zone.

The decision of wheather or not the heater of an unoccupied zone z_i should be turned on depends a) on the current state of the zone, b) the relative value of the energy cost (W_i) and discomfort cost (C_i) per unit time, c) the temperatures of the surrounding zones and d) an estimate of the time that the zone will become occupied. This decision may be taken either centrally from the central processing unit that gathers information by all zones or in a distributed manner by each zone's node after collecting the relative information. There is also the possibility to divine the decision process functionality between the central unit and the wireless sensor network nodes. For example, the prediction of the first entrance times to unoccupied zones may be taken by the central unit, that is aware of the location of people in the multi-zone system, and then the predicted values may be communicated back to the zone's nodes for the final decision. The specific implementation of the decision process is irrelevant to this paper and it will not be further analyzed.

We assume that time is discretized $t = mT_{s,}$ T_s is the sampling period, and that each period, and that each node takes its decisions periodically every D sampling periods. Note that there is no need for the nodes to be synchronized to each other. Let $Y_i(t)$ denote the random variable that models the remaining tine from the current time instant t until entrance to the unoccupied zone z_i . It is obvious that the random variables $Y_k(t)$, for the various unoccupied zone z_k, do not follow the same distribution. We further assume that the node is capable to make predictions for the time it takes to exceed the comfort threshold T_c. To this end, let $S_i^{on}(t)$ denote the time period that is required to exceed T_c if the heater is turned on immediately. Similarly, we define $S_i^{off}(t)$ as the predicted time to reach the comfort threshold if the heater remains off for a period D and then, at

the next decision epoch it is turned on. The relation of the aforementioned parameters is shown in Figure 7.2.

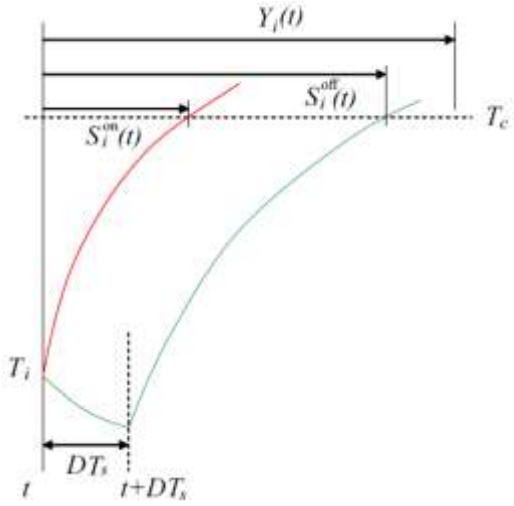

Figure 7.2 Predicted time intervals related to the decision process

Suppose now that at time t the node of the unoccupied zone z_i has to take a decision whether to turn the zone's heater on or remain in the off state. At the decision epoch t the risk to turn the heater on is

$$R_i^{on}(t) = W_i DP\left\{S_i^{off}(t) \le Y_i(t)\right\} + W_i\left(Y_i(t) - S_i^{on}(t)\right)P\{S_i^{on}(t) < Y_i(t) \le S_i^{off}(t)\} \quad (7.2)$$

That is, if $S_i^{off}(t) \le Y_i(t)$ there is plenty of time to reach the comfort threshold even the heating starts at the next decision epoch and therefore we consume unnecessarily $W_i D$ units of energy (this is the case depicted in Figure 7.2). Similarly, if $S_i^{on}(t) < Y_i(t) \le S_i^{off}(t)$ then $W_i(Y_i(t) - S_i^{on}(t))$ units of energy are wasted. Note that there is no risk to turn on the heater if the entrance to the zone happens sooner than it is predicted. In a similar fashion we calculate the risk of keeping the heater off. In this case

$$R_i^{off}(t) = C_i DP\{Y_i(t) \le S_i^{on}(t)\} + C_i \left(S_i^{off}(t) - Y_i(t)\right) P\{S_i^{on}(t) < Y_i(t) \le S_i^{off}(t)\} \quad (7.3)$$

Using (7.2) and (7.3) the decision criterion takes the form

$$R_i^{on}(t) \underset{off}{\overset{on}{\lessgtr}} R_i^{off}(t) \quad (7.4)$$

Consider for the moment that there is no randomness on $Y_i(t)$, that is strict time scheduled occupation of zones. Typical examples are the classrooms in a university campus. In this case, criterion (7.4) takes a very simple from since one of the involved probabilities is equal to one and the rest assume the value of zero. Thus, if $Y_i(t) \le S_i^{on}(t)$ then the heater is turned "ON", if $S_i^{off}(t) < Y_i(t)$ the heater remains "OFF" and if $S_i^{on}(t) < Y_i(t) \le S_i^{off}(t)$ the heater will be turned ON/OFF depending on the values of the relative energy and discomfort cost. The balance between these two costs is regulated by the weights W_i and C_i .

If $Y_i(t)$ is random then criterion (7.4) needs to be slightly modified as the value of $Y_i(t)$ is unknown. In this case we replace Y_i(t) with its conditional expected value given than $S_i^{on}(t) < Y_i(t) \le S_i^{off}(t)$. Therefore, in criterion (7.4) $Y_i(t)$ is substituted by $E[Y_i(t)|S_i^{on}(t) < Y_i(t) \le S_i^{off}(t)]$.

From the previous discussion, it becomes clear that the decision process needs the estimates $S_i^{on}(t)$, $S_i^{off}(t)$ and the distribution of the process $Y_i(t)$. The former is the subject of the next subsection whereas a discussion on the distribution of $Y_i(t)$ is left for subsection 7.2.3.2.

7.2.3.1 Temperature-time predictions based on SID

In order to make predictions about the temperature evolution of a zone, the SID model has been implemented as in the detection method of Chapter 5 *(Section 5.4).* As in the aforementioned method (Chapter 5), each zone is treated

separately and is represented by the discrete time linear, time invariant, state space model of the equations 4.1 and 4.2. The process of the SID model for the temperature prediction of each zone is the same as it has been described in Chapter 5 *(Subsection 5.4.1.2).*

For the estimation of the state-space matrices A, B, C & D of each zone, the "training phase" is needed during which all nodes in the structure, report their relative measurements to a central computer unit. The "training phase" has been presented in Chapter 5 *(Subsection 5.4.3)*

After the completion of the "training phase", the state space model matrices A, B, C and D for each zone are communicated back to the node responsible for the zone. Upon reception of the matrices the nodes enter the "convergence phase", that is starting from an initial state x_o, they update the state equation ($x_{k+1} = Ax_k + Bu_k + \omega_k$) for a predetermined period of time, using the measurements of the surrounding zones and the status of the zone's heater. Note that the "training" and the "convergence phase" need to be executed only once prior to the normal operation of the nodes. After the "convergence phase" the nodes enter to the "decision phase". During this phase the nodes update the state of the model (as in the "convergence phase") and periodically they take decisions on whether to turn the zone's heater "ON" or not. Suppose that at the decision epoch t the state of the tagged unoccupied node is x_t. The node bases its decision on the estimates $S_i^{on}(t)$ and $S_i^{off}(t)$. Recall that, $S_i^{on}(t)$ and is the time needed to reach the comfort level T_c if the heater is "ON". Namely

$$S_i^{on}(t) = \min l: y_{t+l} \geq T_c \tag{7.5}$$

The node "freezes" the input vector u_k to its current value u_t (more recent temperatures of the surrounding zones, and the tagged zone's heater is "ON") and starting from the state x_t repeats equations (4.17) and (4.18) until y_{t+k} exceeds the values T_c. Note that

$$y_{t+k} = CA^k x_t + CA^{k-1}Bu_t + CA^{k-2}Bu_{t+1} + \cdots + CABu_{t+k-2} + CBu_{t+k-1} + Du_{t+k} \quad (7.6)$$

and for $u_t = u_{t+1} = \cdots = u_{t+k}$ it is obtained

$$\begin{aligned} y_{t+k} &= CA^k x_t + C(I + A + \cdots A^{k-1})Bu_t + Du_t \\ &= CA^k x_t + C(I - A)^{-1}(I - A^k)Bu_t + Du_t \end{aligned} \quad (7.7)$$

If y_{t+k} is set to $y_{t+k} = T_c$ and

$$w = T_c - C(I - A)^{-1}Bu_t - Du_t$$

then equation (7.7) takes the form

$$\begin{aligned} w &= CA^k x_t - C(I - A)^{-1}A^k Bu_k \\ &= CV\Lambda^k V^{-1}x_t - C(I - A)^{-1}V\Lambda^k V^{-1}Bu_t \end{aligned} \quad (7.8)$$

where I is the identity matrix and the diagonalization of the matrix A has been considered as $A = V\Lambda V^{-1}$, with Λ the diagonal matrix of the eigenvalues and V the matrix of the corresponding eigenvectors. Numerical methods can be used to solve equation (7.8) for k. In a similar manner the $S_i^{off}(t)$ is computed. In this case however, first equation ($x_{k+1} = Ax_k + Bu_k + \omega_k$) is repeated D times with input vector u_k reflecting the fact that the heater is "OFF", and then starting from the new state x_{t+D}, the time needed to reach T_c is estimated if heater is "ON".

7.2.3.2 On the distribution of $Y_n(t)$

The random variable $Y_n(t)$ expresses the remaining time from the current time instant t until entrance to zone z_n. Namely, the assumption is made that occupants move around as a swarm, visiting zones either in a predetermined order or in a random fashion and finally they end up in zone z_n. Each time the occupants visit a zone z_l they stay in it for a non zero time period which is itself

a random variable with distribution $F_l(x)$. The variable t is used to designate calendar time, the time elapsed since the process started, and τ is used to designate the time elapsed since entry to a zone. The zone occupation time distribution $F_l(x)$ may be given parametically either a priori or interred from examination of historic data by suitable fitting of the distribution's parameters. We may use the empirical distribution function (e.d.f.) instead which is the nonparametric estimate of $F_l(x)$. Namely, if a sample on N occupation periods of zone $z_l, \{x_1, x_2, \dots, x_N\}$ is available, then

$$\hat{F}_{l(x)} = \frac{1}{N}\sum_{m=1}^{N} I(x_m \in [0, x]) \tag{7.9}$$

where $I(\cdot)$ is the indicator function.

Let us consider first the simple case of two adjusting zones $z_l,\ z_n$ with zone z_l being occupied and z_n unoccupied as it is shown in Figure 7.3. We assume that the occupants remain to zone z_l for a random period of time X_l which is distributed according to $F_l(x)$, and then upon departure they enter zone z_n.

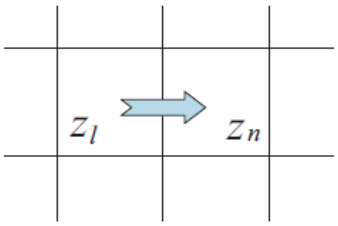

Figure 7.3 Movement of occupants from zone z_l to the adjacent unoccupied zone z_n

In this case $Y_n(t)$ expresses the remaining waiting time to zone z_l and follows the residual life distribution which is defined by

$$\bar{R}_{Y_n(t)}(y) = 1 - R_{Y_n(t)}(y) = P\{X_l > \tau + y | X_l > \tau\} = \frac{\bar{F}_l(\tau+y)}{\bar{F}_l(\tau)} \tag{7.10}$$

Next the case that occupants are currently in a zone z_0 is considered, and upon departure they visit in cascade zones $z_1, z_2, \ldots, z_n$ as it is shown in figure 7.4. Then,

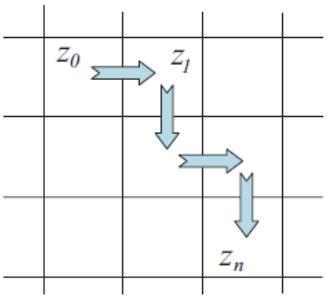

Figure 7.4 Movement of occupants in cascade from zone z_o to zone z_n.

$$Y_n(t) = Y_0 + X_1 + X_2 + \cdots + X_{n-1} \tag{7.11}$$

where Y_0 is the remaining time in zone z_0 and X_i is the occupation period of zone z_i. It is well known that the distribution of $Y_n(t)$ is the convolution of the distributions of the random variables $Y_0, X_1, \ldots, X_{n-1}$. Thus,

$$F_{Y_n(t)}(y) = P\{Y_n(t) \leq y\} = R_0(y) * F_1(y) * F_2(y) * \cdots * F_{n-1}(y) \tag{7.12}$$

with $R_0(y) = 1 - \bar{F}_0(\tau + y)/\bar{F}_0(\tau)$. A more compact form is obtained by considering a transform of the distributions, i.e. the Laplace transform, the moment generating function, or the characteristic function. Using the moment generating function (mfg) which for a distribution $F_X(x)$ of a nonnegative random variable X is defined by

$$F_X(s) = \int_0^\infty e^{sx} dF_X(x)$$

equation (7.12) takes the form

$$F_{Y_n(t)}(s) = R_0(s) \cdot F_1(s) \cdot F_2(s) \cdot \ldots \ldots \cdot F_{n-1}(s) \tag{7.13}$$

In some cases (unfortunately few) equation (7.9) can be inversed analytically in order to calculate the distribution $F_{Y_n(t)}(y)$. For example, if the occupation periods X_i, i=0,….,$n-1$, are exponentially distributed with corresponding parameters λ_i, then Y_o is also exponentially distributed with parameter λ_o due to the memoryless property of the exponential distribution, and the probability density function of $Y_n(t)$ is (assuming that the parameters λ_i are all distinct)

$$f_{Y_n(t)}(x) = \sum_{i=0}^{n-1} \frac{\lambda_0 \cdots \lambda_{n-1}}{\prod_{j=0.j\neq i}^{n-1}(\lambda_j - \lambda_i)} exp(-x\lambda_i) \tag{7.14}$$

(The expression for the general case, of non distinct parameters, is slightly more involved but still exists). If a closed form for the density $f_{Y_n(t)}(x)$ does not exist, or it is difficult to be obtained, we resort to the saddle point approximation [41] to invert $F_{Y_n(t)}(s)$. To this end, for a random variable X with cumulative distribution function (cdf) $F_X(x)$, we define the cumulant generating function (cgf) $K_X(s)$ as the logarithm of the corresponding mfg $F_X(s)$, namely

$$K_X(s) = \ logF_X(s)$$

Then, the saddlepoint approximation of the probability density function (pdf) $f_X(x)$ is

$$f_X(x) \approx \left(\frac{1}{2\pi K_x''(\hat{s}(x))}\right)^{1/2} \exp\{K_X(\hat{s}(x)) - \hat{s}(x)x\} \tag{7.15}$$

where $\hat{s}(x)$ is the solution to the saddlepoint equation

$$K_X'(s) = x \tag{7.16}$$

The estimation (7.15) relies on numerical computations based on the cgf $K_X(S)$, which in turn depends on $F_X(s)$. Note that, we may use the empirical mgf $\hat{F}_X(s)$ instead, so that a nonparametric estimation of the pdf $f_X(x)$ is possible.

The more general case is to model the movement of the occupants in the multi-zone system as a semi-Markov process. The states of the process are the zones of

the system and at the transition times they form an embedded Markov chain with transition probabilities p_{ij}. Given a transition from zone z_i to zone z_j, the occupation time in z_i has distribution function $F_{ij}(x)$. The matrix $Q(x)$ with elements $Q_{ij}(x) = p_{ij}F_{ij}(x)$ is the so called semi-Markov kernel. The occupation time distribution in zone z_i independent of the state to which a transition is made is $F_i(x) = \Sigma_j Q_{ij}(x)$. Consider now the case that at time t occupants exist in zone z_i and the node of zone z_n has to make a decision on whether to start heating the zone or not. For the decision process the distribution of time until entrance to zone $z_n, Y_n(t)$, is needed. $Y_n(t)$ is the sum of two terms. The first term is the residual occupation time at zone z_i and the second term is the time to reach z_n upon departure from zone z_i. The distribution $R_i(x)$ of the first term is given by (7.10) whereas for the second term we have to consider the various paths taken upon departure from state z_i. Thus, if zone z_i neighbors N_i zones namely, $z_{k,}\ k = 1, \dots, N_i$, then the time to reach zone z_n upon departure is distributed according to

$$G_{in}(x) = \sum_{k=1}^{N_i} p_{ik}H_{kn}(x) \tag{7.17}$$

where $H_{kn}(x)$ is the distribution of the first passage from zone z_k to zone z_n. Pyke [42] and Mason [43], [44] provided solutions for the first passage distribution in a semi-Markov process. For example, Pyke's formula states that $H(s)$, the elementwise transform of the matrix $H(x) = \{H_{ij}(x)\}$, is given by

$$H(s) = T(s)[I - T(s)]^{-1}\{([I - T(s)]_d\}^{-1} \tag{7.18}$$

where $T(s)$ is the transmittance matrix with elements the transforms $T_{ij}(s)$ of the occupation time distribution $F_{ij}(x)$. The notation M_d denotes the matrix that is formed by the diagonal elements of M. A simplified version of (7.18) is obtained if we let $\Delta(s) = \det(I - T(s))$ and $\Delta_{ij=}(-1)^{i+j}\det(I - T(s))_{ij}$, the ijth cofactor of $I - T(s)$. Using this notation, for a semi-Markov process of n states we get

$$H_{1n}(s) = \frac{\Delta_{n1}(s)}{\Delta_{nn}(s)} \tag{7.19}$$

By relabeling the states $1, \ldots., n-1$ of the process we can find the transform of the first passage from any zone to zone z_n.

In summary,

$$F_{Y_n(t)}(s) = R_i(s) \cdot G_{in}(s) = R_i(s) \cdot \left(\sum_{k=1}^{N_i} p_{ik} H_{kn}(s)\right) \tag{7.20}$$

with $H_{kn}(s)$ computing using (7.19). Next, the saddlepoint approximation technique can be used to calculate the density $f_{Yn(t)}(x)$.

We have to mention that the process of estimating the first passage distributions needs to be performed only prior to the decision process. Thus, given the topology of the multi-zone system, we posit a parametric family for the occupation time distributions and we estimate the distributions' parameters from sample data. Then, the transition probabilities are estimated based on the data and the occupation mgf $F_{ij}(s)$ is obtained. Having in our disposal the transforms $F_{ij}(s)$ the transmittance matrix $T_{(s)}$ can be formed and be solved for the first passage transform $H_{ij}(s)$ using equation (7.19). Finally, numerical methods may be used to invert these transforms in order to obtain the necessary probability density functions.

7.3 Summary

In this chapter two HVAC control strategies were proposed focusing on the energy consumption control as well as the maintenance of the thermal comfort to satisfactory levels, by taking into account the occupancy of the zones. All strategies utilized a WSN network of temperature and occupancy sensors to control the zones' heating depending on the occupancy and the occupants' residence time (occupation time) into the zones.

The first method was an initial approach with the effort to reduce energy consumption while in the meantime preserving the comfort condition of the occupants. The proposed techniques were: the “1-hop”, the “2-hop” and the “Adaptive” algorithms. The first two algorithms utilized minimum occupancy information in the form of binary decisions. The “1-hop” algorithm provided a proactive heating of the adjacent zones when occupancy was detected into a zone, while the “2-hop” provided proactive heating to the directly adjacent zones as well as the neighbor to them, when occupancy was detected into a zone. Both algorithms were preliminary to the following more integrated algorithm.

The “Adaptive” algorithm required an additional parameter that was the expected residence time of the occupants for each zone (occupation time). The algorithm utilized the functionality of the above preliminary algorithms, as well as the two scenarios: the “full-proactive” (all zones heated when occupancy detected) and “full-reactive” (only the occupied zone heated), depending of the mean value of the occupation time of the zone.

The second strategy was a method where temperature and occupancy predictions were fused, in an effort to balance the thermal comfort condition and the consumed energy in a multi-zone HVAC system. The key point of the method was the decision process that relied on two kinds of predictions: the temperature-time prediction and the occupancy profile of the zones. Temperature predictions were based on a subspace identification technique that was used to model the thermal dynamics of each zone independently. A proactive heating of the zones was the task of the method, and to achieve that it proposed a computation of a risk of activating the heater. The computation of this risk was based on the estimation of the energy and discomfort costs, as these two parameters balance the total energy consumed and the total discomfort cost. Appropriate probability distributions and mathematical models were applied to model the occupation times of the zones, while a semi-Markov process was considered for the occupancy predictions with the logic that occupants were moving as a swarm from zone to zone by staying in each one for a random period of time.

Chapter 8

Results of the methods for energy efficiency in HVAC systems

8.1 Introduction

This Chapter contains the results of the methods presented in Chapter 7. In Section 8.1 the results of the first initial approach for energy efficiency are presented with the results of the evaluation of the proposed algorithms in contrast with the full-proactive and the full-reactive scenarios. In Section 8.2 the results of the second method for energy efficiency based on the SID model are presented including the results of the training (Subsection 8.2.1) and the decision (Subsection 8.2.2) phases.

8.2 Results of the initial approach

The same nine-zone model *(Figure 3.3 - Chapter 3)* was simulated with the model parameter values (Table 6.1) taken from [33]. The simulations had duration of 5 hours and external temperature set 5^{o}C. The target temperature (Tg ^{o}C) of the zones were set as in Table 8.1.

Table 8.1
Target temperatures of the zones

	Target temperatures								
Zone	**I**	**II**	**III**	**IV**	**V**	**VI**	**VII**	**VIII**	**IX**
(℃)	19	20	19	20	21	20	19	20	20

Initially, the algorithms "1-hop" and "2-hop" were simulated one at a time, by utilizing several (~50) mobility paths, through the nine zones. The same value of the mean occupants' residence time (t_m) has been set to all zones for each

simulation. The mobility paths were based on the probabilities of zone visits shown in Table 8.2 and they were the same for all simulations. Thus, the efficiency of the algorithms was evaluated, as far as the power consumption and the thermal discomfort time is concerned.

Table 8.2
Visitation probabilities of the adjacent zones (AZn) [46]

Occupied Zone	AZ 1	AZ 2	AZ 3	AZ 4	AZ 5	AZ 6	AZ 7	AZ 8	AZ 9
1		1/2		1/2					
2	1/3		1/3		1/3				
3		1/4				3/4			
4	1/6				2/3		1/6		
5		1/4		1/4		1/4		1/4	
6			1/4		1/2				1/4
7				1/2				1/2	
8					2/3		1/6		1/6
9						1/2		1/2	

The mean occupants' residence time (t_m) values used, have been quantized into four states: short time (st=250sec), medium-short time (mst=500sec), medium-long time (mlt=750sec), and long time (lt=1000sec). In order to create the random mobility paths, the first three zones (1,2&3) were initially used, one at a time, as the entrance zones. The simulation results of each entrance zone had no significant diversion and so, for the rest of the simulations, zone 1 has been used as the one and only entrance zone. Furthermore, the results of the above simulations were contrast with the "Full-proactive" and "Full-reactive" schemes, which they have had the form of algorithms in our simulation tool.

In the "Full-proactive" scheme, all the zones were equally heated. The heating starts when the very first occupancy entrance is detected in the entrance zone and stops when all zones are unoccupied.

"Full-proactive" Scheme

for *each* zone
  If zone occupied ***then***
  heat all zone
end

The "Full-reactive", is the scheme where each zone is heated only when occupancy is detected into it and heating continuously until the occupants exit the zone. Otherwise each zone remains unheated. Expected results were obtained, and consistent with the algorithms' rationale.

"Full-reactive" Scheme
for *each* zone
  If zone occupied ***then***
  heat only this zone
end

For all the above values of t_m, the "Full-proactive" scheme resulted with the greater energy consumption and this was totally expected due to the continuous equal heating of the zones. This scheme, instead, resulted with the less discomfort time (the time where the temperature is in the discomfort range) and this is reasonable, since none of the zones' temperature falls below the minimum comfort threshold. The "2-hop" algorithm has achieved the second greater energy consumption, while the third and the fourth greater energy consumption achieved from the "1-hop" and the "full-reactive" scheme respectively. The second best discomfort time (the shorter time that temperature is out of the comfort condition) has been achieved from the "2-hop" while the third and fourth achieved from the "1-hop" and "full-reactive" respectively. Indicatively, Table 3 shows the evaluation of the algorithms with t_m set to 500sec (≈8min) containing the values of simulation results.

Table 8.3
Evaluation of the algorithms with the same mean residence time of the occupants ($t_m = 500\ sec$)

Algorithm	Mean Energy Consumption (KWh)	Mean Discomfort Time (h)
Full-proactive	8.3	1.3
Full-reactive	3.6	12.0
1-hop	6.9	3.5
2-hop	7.8	1.9

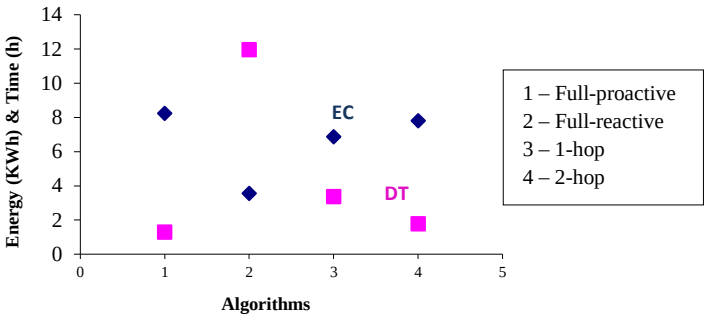

Figure 8.1 Mean value of Energy consumption (EC) and Discomfort time (DT) with the same occupants' residence time value (t_m = 500sec).

Similar, with different performance values, was the evaluation of the algorithms, with the t_m in all zones, set to each one of the remaining values (250, 750, 1000 sec). Our next step was the algorithms' (1-hop, 2-hop, Full-proactive, Full-reactive) simulation utilizing different t_m values for each zone.

Specifically, the t_m values set to the nine zones were: for zones I, VII & IX t_m=1000sec, for zone II t_m=500sec, for zones III, IV & VIII t_m=750sec and for zones V & VI t_m=250sec. Next, the "Adaptive" algorithm was simulated which combines all the above algorithms by maintaining the same t_m values in each zone. The "Adaptive" algorithm was the second better in energy save since the "Full-reactive" was the best. On the other hand, the "Adaptive" algorithm offered much less discomfort time than the "Full-reactive" one. The conclusion of the algorithms' evaluation is that the "Adaptive" achieved satisfactory energy consumption along with an equally satisfactory time where the zones are in a comfort condition. The rest of the algorithms "1-hop"and "2-hop" are evaluated as above [46].

Table 8.4
Evaluation of the algorithms with various mean of (t_m) [46]

Algorithm	Mean Energy Consumption (KWh)	Mean Discomfort Time (h)
Full-proactive	8.1	0.5
Full-reactive	3.1	10.3
1-hop	6.6	2.7
2-hop	7.6	1.1
Adaptive	6.5	2.3

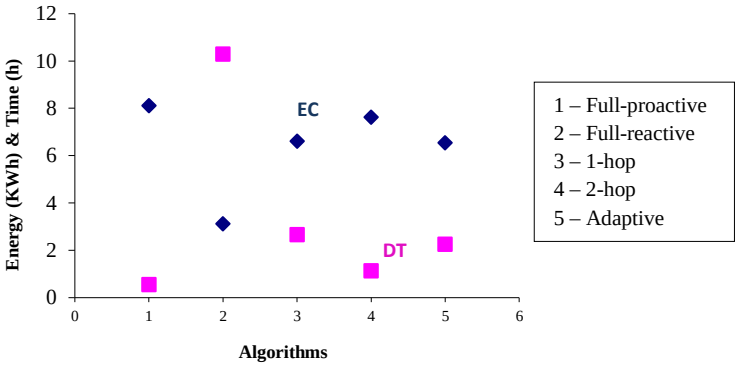

Figure 8.2 Mean value of Energy consumption (EC) and Discomfort time (DT) with occupants' residence time of I,VII&XI=1000, II=500, III,IV & VIII=750, V,VI = 250sec [46]

The resulting heating energy saving and the mean discomfort time difference, is shown in Table 8.5. They have been estimated in accordance with the values of Table 8.4, and in comparison with the full-proactive scheme where all zones are equally heated. The heating payback has been estimated in (KWh) and percentage (%) with negative values that emphasize the difference from the full-proactive scheme. The discomfort time difference is in (h) with positive values to emphasize the extra time where the space is in the discomfort condition [46].

Table 8.5
Energy saving of the algorithms and extra Discomfort
Time in comparison with the full-proactive scheme

Algorithm	Energy saving		Discomfort Time Difference (h)
	(KWh)	Percentage	
Full-reactive	-5	-61.7%	+9.8
1-hop	-1.5	-18.5%	+2.2
2-hop	-0.5	-6.1%	+0.6
Adaptive	-1.6	-19.7%	+1.8

8.3 Results of the method for energy efficiency based on the SID model

As before in Section 8.1, the same nine-zone system was simulated (Fig. 3.3), consisting of a squared arrangement of rooms (zones) where each room (zone) is equipped with a wireless sensor node, and the parameter values for this lumped capacity zone model have been taken from [33] as presented in Chapter 3.

The assumption is made that heat transfer takes place between room's air and the walls as well as between room's air and the roof. Furthermore, the effects of ground on the room temperature are neglected. North and south walls have the same effect on the room temperature and it's been assumed the same for the east and west walls. According to these assumptions, there is a symmetry in the dynamics of the zones. For example, zones I, III, VII and IX (Fig. 3.3) exhibit the same behaviour. Note that for the multi-zone system several state variables, such as wall temperatures, are common to the individual zone systems. In the simulations the nine-zone system is treated as a single system with 42 states and nine outputs (the temperature of the zones) as described in Chapter 3.

As it's been already mentioned, in Figure 3.3, T_o denotes the outside temperature which is assumed to be uniform with no loss of generality. For simulation purposes daily outside temprerature variations are obtained using the Walter's model [34] as presented in Chapter 3 *(Section 3.2)*. For this model, the maximum temperature of the day T_{max} , the minimum temperature of the day T_{min} and the mean of the 24 hourly temperature T_m need to be provided in order to estimate T_0.

8.3.1 Results of the "training phase"

For the deterministic subsystem identification we used 86400 samples with sampling period $T_s = 1sec$. For the outside temperature we used Walter's model with parameters given in the first row of table I and a heater gain equal to 600W. We set the zones' target temperatures T_{tg} to those

Table 8.6
Training and testing parameters for outer temperature model and heat gain

	Walter's model (℃)			**Heat gain (W)**
Phase	T_{max}	T_{min}	T_m	$q(t)$
Training	13	2	7	600
Testing	16	1	6	700

of Table 8.6 (first row) with a margin equal to $T_{mg} = 1^o C$. That is, for a specific zone the heater is on until temperature $T_{tg} + T_{mg}$ is reached. After this point the heater is turned off until temperature hits the lower threshold $T_{tg} - T_{mg}$ and the whole process is repeated.

Table 8.7
Training and Testing Zones' Target Temperature

	Target temperatures (℃)								
Zone	**I**	**II**	**III**	**IV**	**V**	**VI**	**VII**	**VIII**	**IX**
Training	16	18	16	15	14	13	12	16	14
Testing	17	20	17	17	17	14	18	19	21

Having collected the data over the period of 24 hours, the measurements of the zone's temperature, the outer temperature and the heat gains of each zone, are organized into input-output data for the subsystem identification process. For example, for zone I , the outer temperature, the heating gain of zone I, as well as the temperatures of zones II and IV, are the input data to the identification process whereas the temperature of the zone I itself is the output data. Note that the number of input signals differ from zone to zone. Zone I, III, VII and IX use 4 input signals whereas the rest of the zones use 5 input signals. Based on the input-output data the matrices *A, B, C* and *D* are identified for each zone as described in Section 3. During this process the order of the subsystems has to be decided. This is achieved by looking at the singular values of the SVD decomposition and deciding on the number of dominant ones. Figure 8.3 depicts the singular values for zones I, II and V. All subsystems exhibit similar behaviour regarding the profile of their singular values and therefore we set the

order of all subsystems equal to 2. Next we run a test on the obtained state-space models. We set the outer temperature parameters as in the second row of Table 8.6 and the target temperatures as in the second row of Table 8.7.

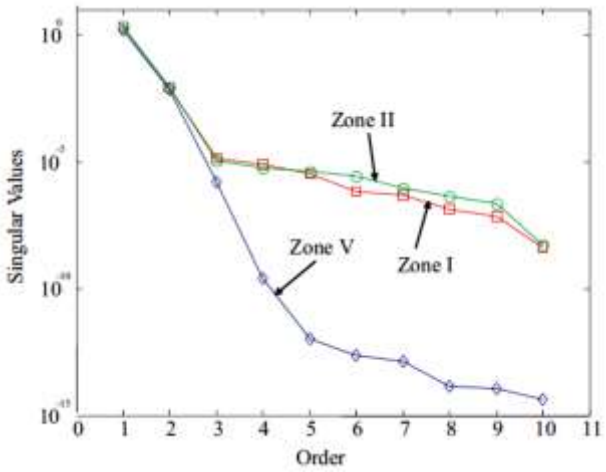

Figure 8.3 Singular values of zones I, II and V

The initial state of the subsystem model was set to [-10 0], whereas the elements of the 42 state vector of the multi-zone system were set equal to 3 (the initial output temperature). Figure 8.4 shows the evolution of the actual and predicted temperatures for Zone I and IV. For zone I the heater was on (heat again equal to 700) whereas the heater for zone IV was off. As it is observed, after 5000 samples (approx. 80 minutes period) the state of the subsystems has converged to one that produces almost the same output as the original system. After this point the WSN nodes can enter in the "decision phase".

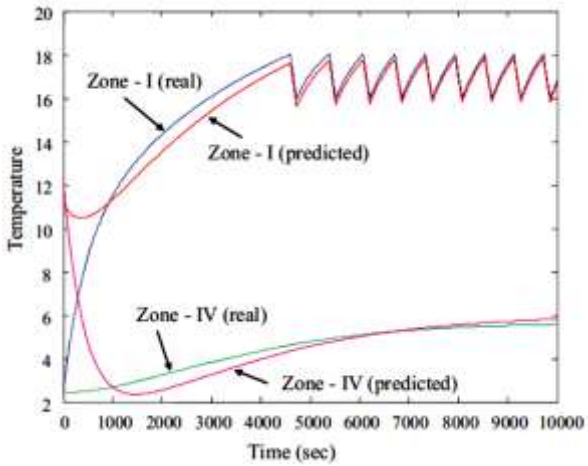

Figure 8.4 Real and Predicted temperature of zones I and IV

8.3.2 Results of the "decision phase"

It should be noticed at this point that the "original" simulated system (42 state-space model) is also linear and thus the use of linear subspace identification maybe questionable for more complex and possibly nonlinear systems. As the simulation results indicate, although the dynamics of each zone are more complex (including the roof temperature for example), a low dimensionality subsystem of order 2 can capture its behaviour. For more complex systems we can choose the order of the identified subsystem high enough. For nonlinear systems the identification of a time varying system is possible using a recursive update of the model.

Next the scenario of Figure 7.3 was simulated. The assumption is made that occupants enter zone I (at time instant 5000) and then after a random period of time they enter zone IV, where they remain for 3600 sec. Zone I is heated since the beginning of the process (heat gain 900 W) until the occupants leave the zone to enter zone IV. Zone IV uses a heater with gain 1200 W, which is turned on (or off) according to the decisions of its node. The target temperatures for zones I and IV are 17℃ and 16℃ respectively. For the first set of experiments, the occupation period of zone I is Gamma distributed, i.e.

$$f_X(x) = \frac{\beta^\alpha}{\Gamma(\alpha)} x^{a-1} e^{-\beta x} \tag{8.1}$$

with the shape parameter $\alpha = 5$ and β such that the expected value of X, $E[X] = \alpha/\beta$, is 3600 and 7200. Decisions were taken every $D = 67$ seconds. Figure 8.5 shows the total comfort cost achieved for various values of the comfort weight C_i. As "comfort cost" is defined the value that represents the loss of comfort per unit time and as "comfort weight" is defined the value that represents the thermal comfort per unit time. The results are averages over 200 runs of the simulation. The case of $C_i = 0$ is the full reactive case where heating of zone IV is postponed until occupants enter the zone. On the other extreme, for high values of C_i the decision process acts proactively by spending energy, in order to reduce the discomfort level. Figure 8.6 shows the total energy cost in

KWh for the two cases of Figure 8.5. As it is observed, the higher value of C_i the more energy is consumed since then heating of zone IV starts earlier. The difference between the two curves of Figure 8.6 is justified by the difference of the means of the occupation period, $E[X] = 3600$ and $E[X] = 7200$, for the two cases.

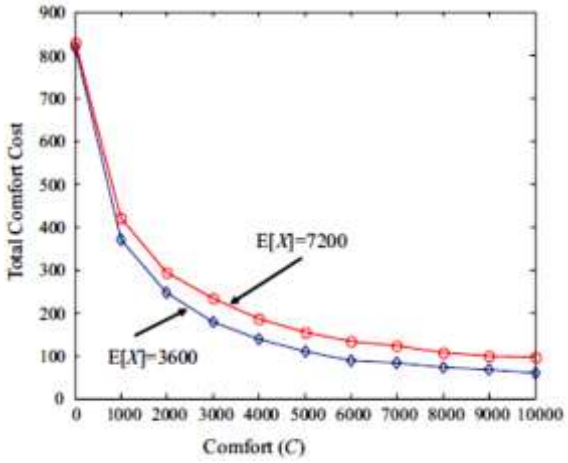

Figure 8.5 Total comfort cost vs. C_i. The occupation time of zone I Is Gamma distributed

In Figure 8.7 the temperature profiles for zones I, IV and for two different values of C is ploted. As it is observed the value of $C = 0$ corresponds to the reactive case, that is the heater of zone IV remains off until occupants are detected in the zone. On the other extreme a large value of C (10000) will force the heater of zone IV to be turned on as soon as possible in an effort to reduce the discomfort penalty.

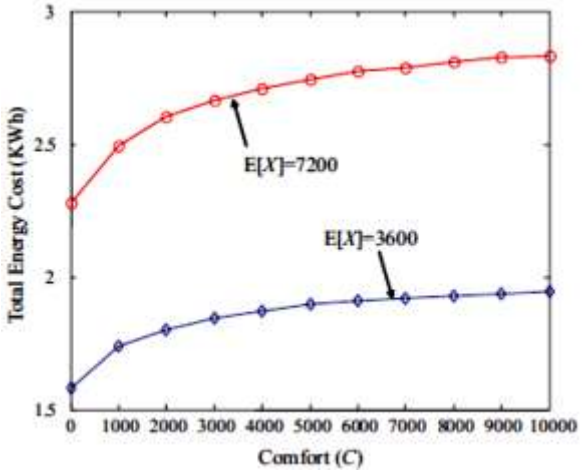

Figure 8.6 Total energy cost vs. C_i. The occupation time of zone I Is Gamma distributed

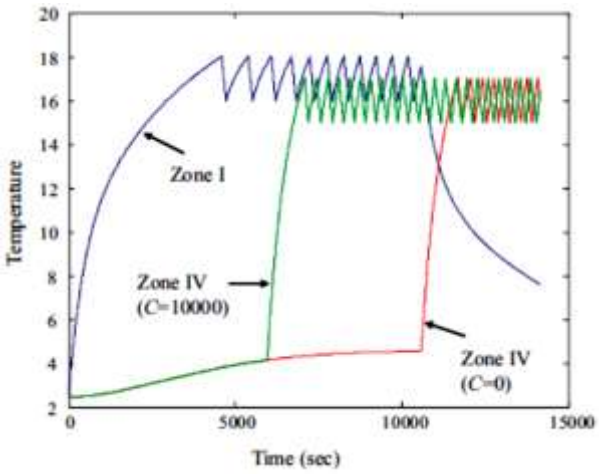

Figure 8.7 Temperature vs. time for $C = 10000$ and $C = 0$.

The scenario of Figure 7.3 *(two zone scenario)* was also simulated for Pareto distributed occupation times of zone I. The pdf for the Pareto distribution is

$$f_X(x) = \begin{cases} \frac{ax_m^a}{x^{a+1}}, & x \geq x_m \\ 0 & x < x_m \end{cases} \tag{8.2}$$

With expected value

$$E[X] = \begin{cases} \frac{ax_m}{a-1}, & a > 1 \\ \infty & a \leq 1 \end{cases} \tag{8.3}$$

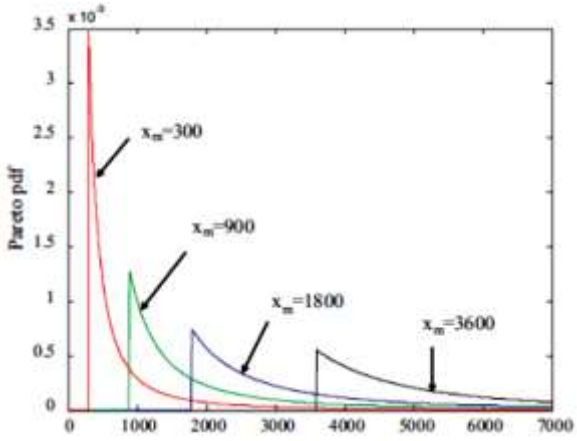

Figure 8.8 Pareto pdf for various values of x_m.

Figures 8.9 and 8.10 show the total comfort cost and the total energy consumed respectively for various values of the comfort gain C_i. As it is observed, a 50%

improvement on the comfort cost (compared to the reactive case) can be achieved for a value of C equal to 1000. However, there is a performance floor (this is evident for the case of $x_m = 300$), which is due to the nature of the Pareto distribution. Most of the samples for the occupation time period are concentrated close to x_m and therefore there is not enough time to preheat the next visiting zone, which in turn implies high discomfort costs. Moreover, the heavy tail of the Pareto distribution cause some extremely high values of the occupation period which result in an increase of the total consumed energy, as it can be observed clearly from figure 8.10.

Next, the scenario of figure 7.4 was simulated. The occupants move in cascade from zone to zone as it is depicted in Figure 8.11. The target temperatures for the zones are given in the first row of Table 8.8, whereas the heat gain of each zone is given in the second row of Table 8.8. For the occupancy time of each zone we considered an exponential random variable with mean provided in the last row of Table 8.8. Note that, this assumption is the least favorable for adjacent zones due to the memoryless property of the exponential distribution. The total comfort and energy costs for this scenario are plotted in Figure 8.12 for various values of the comfort weight C. The results are averages over 100 runs. The two curves for each cost correspond to $D = 67$ and $D = 167$ respectively. As it is observed, considerable comfort gains are achieved for a moderate increase of the consumed energy. In Figure 8.12 we also show the costs for a "fixed" proactive scenario in which the heating of a zone starts as soon as occupants are detected to its neighbor zone. For example, when occupants enter zone IV, the heater of zone V is turned on and so on.

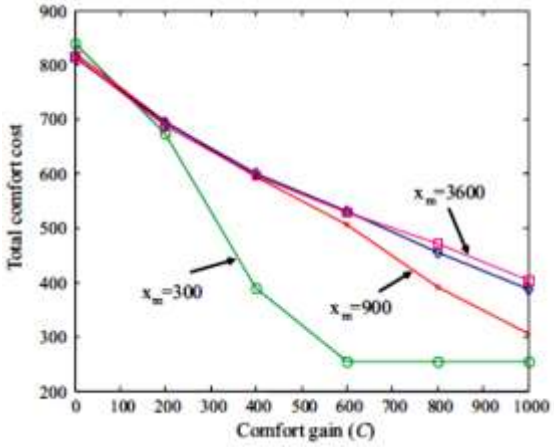

Figure 8.9 Total comfort cost for Pareto distributed occupation period

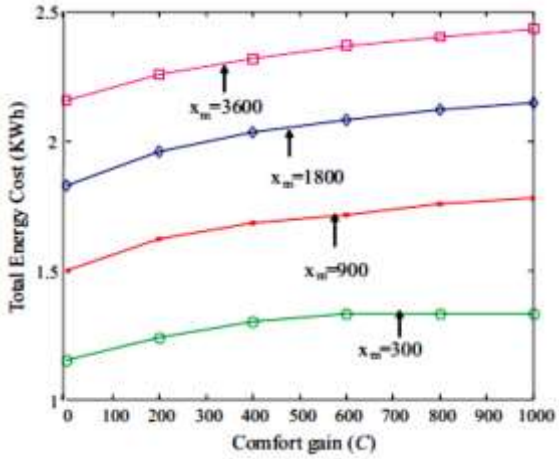

Figure 8.10 Total energy cost for Pareto distributed occupation period.

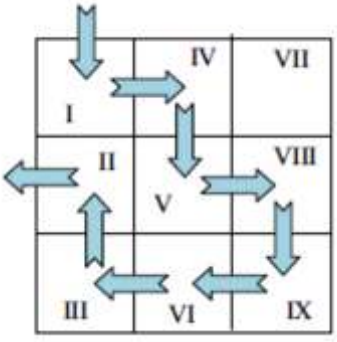

Figure 8.11 Movement of occupants in cascade (zones I, IV, V, VIII, IX, VI,III,II)

Table 8.8
Parameters used in cascade movement scenario

Zone	I	IV	V	VIII	IX	VII	III	II
Target ℃	**17**	**16**	**17**	**17**	**16**	**14**	**17**	**18**
Power (KW)	**0.9**	**1.2**	**0.9**	**0.9**	**0.9**	**1.2**	**0.9**	**1.2**
Mean Time x 10^2	**36**	**27**	**18**	**40**	**54**	**45**	**30**	**20**

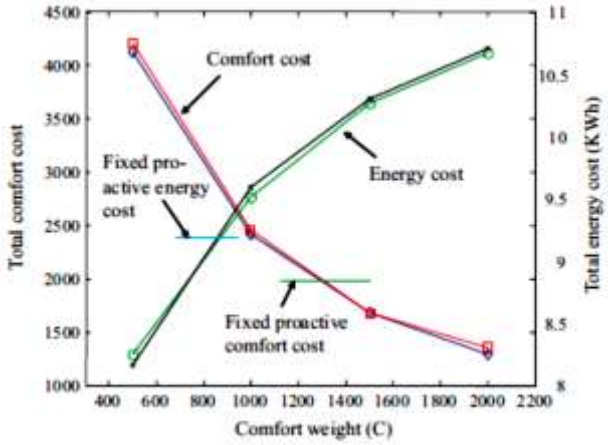

Figure 8.12 Total energy and comfort costs (cascade movement scenario)

Table 8.9 shows the comfort and energy costs obtained when there is no randomness on the occupancy times for various values of the comfort weight C and for two different values of D ($D = 67$ and 167). The occupancy times of the zones were set to the mean values provided in the last row of Table 8.8. As it is observed, extremely low comfort costs can be achieved in this case which implies that the right modeling of the occupancy times is of paramount importance to the process.

Table 8.9
Energy and Comfort costs for constant occupancy times

	Comfort weight C	**500**	**1000**	**1500**	**2000**
$\boldsymbol{D = 67}$	Comfort cost	2615	72	67	67
	Energy cost	7.15	9.02	9.73	10.20
$\boldsymbol{D = 167}$	Comfort cost	2856	72	71	64
	Energy cost	7.79	9.11	9.77	10.25

Finally, Figure 8.13 shows a sample of the zones' temperature profile. Note that, the temperature of zone II, although zone II is the last zone visited, starts increasing (at a slower rate) much earlier. This is because zone II neighbors zones I and V which are heated in earlier stages of the process.

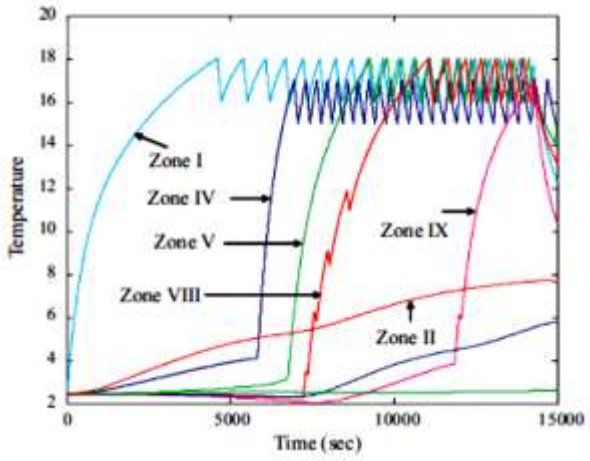

Figure 8.13 Temperature profiles of zones (cascade movement scenario)

8.4 Summary

The results of the two methods aimed to energy efficiency control concerning the energy consumption control as well as the maintenance of the thermal comfort were presented in this chapter.

8.4.1 Results of the initial approach to energy efficiency control

The initial approach which described in Section 7.2.2 consisting of three algorithms ("1-hop", "2-hop" and "Adaptive") of energy control, was first evaluated. The simulation was based on the aforementioned nine-zone model with certain target temperatures set to each zone and the random mobility of the occupants trough the nine zones had the following characteristics:

- The mean value of the residence time (t_m) of the occupants was quantized into four states with certain value each state and simulated one

at a time: short time (st=250sec), medium-short time (mst=500sec), medium-long time (mlt=750sec), and long time (lt=1000sec).

- For all zones the mobility paths of the occupants were based on certain probabilities of zone visits.
- Zone I, has been used as the only entrance zone for all simulations, since there was no significant diversion comparing with other any entrance zone.

The above algorithms and mobility characteristics were simulated and compared with the "Full-proactive" and "Full-reactive" schemes and the results were evaluated as follows:

- The "Full-proactive" scheme resulted with the greater energy consumption while instead, it resulted with the less discomfort time which was reasonable since all zones were heated even unoccupied and none of the zones' temperature was fallen below the minimum comfort threshold.
- The "2-hop" algorithm has achieved the second greater energy consumption, while the third and the fourth greater energy consumption achieved from the "1-hop" and the "full-reactive" scheme respectively.
- The second best discomfort time has been achieved from the "2-hop" while the third and fourth achieved from the "1-hop" and "full-reactive". respectively.

Subsequently, the algorithms were evaluated utilizing different t_m values for each zone, specifically: For zones $I, VII \& IX$ the t_m=1000sec, for zone II the t_m=500sec, for zones III, IV & VIII the t_m=750sec and finally for zones V & VI the t_m=250sec. The "Adaptive" algorithm which utilized a combination of all the above algorithms (1-hop, 2-hop, Full-proactive, Full-reactive) based on the logic of the short to long occupants' residence time was also evaluated and the results were as follows:

- The "Adaptive" algorithm was the second better in energy save since the "Full-reactive" was the best.

- On the other hand, the "Adaptive" algorithm offered much less discomfort time than the "Full-reactive" one.
- The conclusion of the algorithms' evaluation is that the "Adaptive" achieved satisfactory energy consumption along with an equally satisfactory time where the zones are in a comfort condition.

8.4.2 Results of the method based on the SID model

Next, the method of energy efficiency control based on the SID model was evaluated which consisted of two phases of operation: the Training phase and the Decision phase.

The evaluation of the training phase mechanism was the same as in Section 6.3.2. Subsequently, the "decision" phase of the WSN nodes was tested, by simulating two scenarios of occupants' movement: a) the movement between two adjacent zones (Figure7.3) and b) the movement in cascade from zone to zone following a certain path (Figure 7.4). For both scenarios the occupation time was simulated with two distribution types: a) Gamma distribution and b) Pareto distribution.

In the first scenario of movement (a), occupants enter the first zone (zone I) at time instant 5000 sec, where the heat gain was 900W and the target temperature was 17℃. After a random period of time they were entered the adjacent zone (zone IV), where the heat gain was 1200 W, the target temperature was 16℃ and they stayed for 3600 sec. The evaluation was as follows:

- This scenario, was first evaluated with Gamma distribution, where the shape parameters were: $\alpha = 5$ and β such that the expected value of X, $E[X] = \alpha/\beta$, was 3600 and 7200. The decision period $D = 67$ sec and 200 runs of simulation were implemented.
- The simulation of the temperature profiles of the two zones (I&IV) for two values of the total comfort weight C showed a reasonable behaviour. For $C = 0$, which was the case of the full reactive heating of zone IV, the heater was remaining off until the detection of the first entrance of the occupants. For a larger value of C ($C = 10000$), the heater was forced to be turned on in an effort to reduce the discomfort penalty.

- Then, C_i had been taken values in the range of [0 – 10000] with a step of 1000 and as it was observed the higher value of C_i the more energy was consumed with the highest energy value when C_i=0 (full reactive heating).
- As it was observed for the total energy cost (in KWh) for both cases (3600 & 7200), the higher value of C_i the more energy is consumed.
- The same scenario was then simulated for Pareto distributed occupation times of zone I [equations (8.2) and (8.3)] and at first stage the pdf of the Pareto distribution was simulated, for four values of x_m ($x_m = 300, 900, 1800, 3600$) with a suitable value of α so that the mean value of the occupation period was 7200.
- As it was observed, the total comfort cost for various values of the comfort gain C_i was improved for a 50% compared to the full reactive case and this was achieved for $C = 1000$ and x_m*=300*.
- The heavy tail of Pareto distribution caused some extremely high values of the occupation period which resulted to an increase of the total consumed energy.

Next, the second scenario of movement (b) was simulated where the occupants were moving in cascade from zone to zone following a certain path. In each visited zone a target temperature as well as a heating gain had been set. The occupancy time of each zone was considered as an exponential random variable with certain mean value and this assumption was the least favorable due the memoryless property of the exponential distribution. The results were averages over 100 runs for $D = 67$ and $D = 167$ and they have been evaluated as follows:

- As it was observed, considerable comfort gains achieved for a moderate increase of the consumed energy.
- Also, non random occupancy times were tested for various values of comfort weight C and for $D = 67$ and $D = 167$. Extremely low comfort costs were observed in this case and this implies that the right modeling of the occupancy times is very important.

Chapter 9

Conclusions and future work

9.1 Summary and Conclusions

Two main functions concerning the control of the energy spend for heating in HVAC systems, which include novel proposed methods, constituted the content of this thesis. All proposed methods aimed at a serious scientific contribution to the total effort for a more sophisticated energy consumption control in the HVAC systems technology. Methods for detection of abnormal behaviour concerning the unexpected power consumption were included in the first control function, while the second control function contained methods for an improved energy efficiency control.

All the proposed methods were integrated simulation works based on a multi-zone space model of nine zones with certain arrangement and dimensions, equipted with a wireless sensor network that was consisted of wireless nodes of temperature and occupancy sensors.

The first contribution of this thesis is the utilization of the WSN in a HVAC system that bases the development of more sophisticated control teqniques. In this reasearch the implementation of the WSN had the following form: All wireless nodes were scatered in the nine zones, one in each zone and the WSN was capable to operate in centralized mode when the nodes were sending their readings to a central computer unit, or in dicentrlized mode when all nodes were comunicating their readings with each other.

The outside temerature was based on the Walter's model which provided the temperature variations during the day period while the dynamics and uniformity of the zones's temperature were baded on a lumpted capacity model.

In Chapter 2 the evolution of the HVAC systems with the most important features of their current technology related to this work, as well as the state of the art technology of the HVAC control systems were presented. The proposed methods relied on the capability and efficiency of the current technology of the

HVAC control systems to provide inovative mechanisms (algorithms) of energy control. Further in the same Chapter, recent valuable related research works of both directions were presented showing different research approaches, so as the uniqueness and innovation of the proposed methods to be distinguished.

In Chapters 3 the fundamental elements: the single- zone, the multi-zone space model and the weather model were analyticaly presented while in Chapter 4 the detection algorithm (CUSUM) and the system identification model (SID) were also presented. The CUSUM algorithm was imlemented as the basic detection technique in both methods for the accurate detection of abnormal situations (first and second objective), while the SID model was utilized as the basic predictive model of the temperature behaviour of the zones, in the detection method of the second objective as well as in the method of the fourth objective.

In Chapter 5 the methodology of the first control function concerning the detection of abnormal sistuations in HVAC systems were presented. Both methods achieved to detect abnormal behaviour concering the power consumption, each one with different apprach. The first method successfully detected divergences of the power consumption than the anticipated, while the second method succesfully detected temperature deviations due to the higher infiltration gain as well as the higher heat gain that may cause unexpected and continues power consumption.

The points of the total contribution of the first control function and the achievement of the first and second objective were as follows:

- The utilization of the deterministic SID as a temperature predictive model. The stong potential of it formed the basis and supported the idea for the prediction of the temperature behaviour of each zone in the multi-zone model. The functionality of the SID that requires the given inputs and the observed outputs in order to predict the system states and the parameter matrices, allowed the temperature measurements of the surrounding zones (or the outside temperature) as well as the power of the heater to be entered as inputs, while the temperature of the zone itself to be entered as the output. This situation produced an obvious logic for

collecting the dynamics (temperature and heat power measurements) of all zones for a certain period of time in order to be utilized appropriately by the SID model. According to the rationale of the methods, the time period that was decided for the collection of the dynamics was the period of the day (24h). Thereafter, with the data arrangement in input/output form, the relevant parametric matrices *A,B,C,* and *D* of the state space model of each zone were identified by the SID. Thus, the temperature of each zone was predicted successfully, with convergence to the real temperature in short period of time. This process called the "training phase" was utilized both by the method for second odjective for detection of abnormal situations, as well as by the method of the fourth objective concerning the energy efficiency control.

- The detection mechanism that was based on predicted temperature deviations and the accuracy of the CUSUM change detection algorithm. The mechanism provided reliable and accurate detection of the high infiltration gain as well as th high heat gain.

  The data of the dynamics collected during the training phase. The state space model of each node was predicting the temperature of each zone by using the parametric matrices of the SID, and any change in the dynamics the system resulted to a deviation of the predicted temperature from the real one. Significant supporting mechanism was the CUSUM algorithm. The algorithm in the presented method was utilized to detect changes in the mean of the rate change of the prediction error. Thus, the algorithm provided accurate and reliable detection of temperature deviations.

- As an initial approach for the above novel mechanism was the method of the first objective, which utilized a WSN on a decentralized mode of operation in a multi-zone space with the task to evalute the accuracy of the CUSUM algorithm for the detection of power divergencies. The method succecfully detected the change in the distribution of the power

profile when a heat leackage and a heat gain were applied in the zone's temperature. Each wireless node was capable to control the heating source which was located into the zone with a PI controller and also had the functionality to detect possible higher power consumption than the anticipated one. A state space model was running in each node where according to the input vector (surrounding temperature values), the temperature of the zone and the target temperature, the node was able to specify the ideal power profile. By comparing the real and the hypothetical power profile during operation, the node was able to detect possible deviations

In Chapter 7 the methods of the second control function of this thesis concerning the energy efficiency control, were presented. Both methods were aimed to control the energy consumption for heating in HVAC systems, while concurrently maintain the thermal comfort to satisfactory levels.

The basic concept that characterize the logic of the proposed merthods is the proactive heating the unoccupied zone in the multi-zone space. The parameters taken into account in these methods were: the occupancy of the zones, the mobility of the occupants, the occupation time of the zones as well as the temperature prediction. The points of the total contribution of the second control function and the achievement of the third and fourth objective were as follows:

- The method of the fourth objective for the energy efficiency control, managed to apply proactive heating to unoccupied zones according to the proposed risk criterion and achieve satisfactory results in balancing the energy cost and the discomfort cost. The method required two kinds of prediction: the temperature prediction and the occupancy prediction. As mentioned before, the potential and effectiveness of the SID has been also utilized in this method. The "training phase" has been also applied just as in the method of the second objective for the detection of abnormal situations. This mechanism formed the temperature prediction as required by the method. Furthermore, the wireless nodes of temperature and

occupancy sensors of each zone were exchanging the temperature and occupancy information between them and the neighboring nodes. The proposed mechanism aimed to a proactive heating of the zones or not, by implementing a periodical computation of the risk of activating the heater or not. The computation of the risks was relied on the relative weights of the energy and discomfort costs, by managing the balance between the total energy consumed and the total discomfort cost. Two scenarios were examined in this method: the two adjacent zone scenario where one zone was occupied and the other not, and the multi-zone scenario where the occupants were moving in a cascade mode following a certain path. The method was framed by the appropriate mathematical models for the above scenarios, as well as the probability distributions to model the occupation times according to rationale as presented in the evaluation of the results of this method.

- An initial approach for the above novel method was the method of the third objective concerning the energy efficiency control. The method achieved a satisfactory balance between enery consumption and comfort while the occupation time of the zones was exponentially distributed. Three algorithms were proposed, two of which were preliminary to the third one. The preliminary algorithms were the "1-hop" and the "2-hop" which aimed to provide proactive heating to the neighbor zones while the third one namely "Adaptive" combines the functionality of the preliminary ones with the knowledge of the occupation times and applied their functionality appropriately. The Adaptive algorithm also applied the "full-proactive" an "full-reactive" schemes appropriately.

The results of the proposed methods of both directions were presented in Chapters 6 and 8, the abnormal situations detection and the energy efficiency control respectively. All methods exhibited satisfactory results, which verified and supported their contribution. Concisely, the results of the methods of both directions were evaluated as follows:

The results of the methods of the first direction:

- The first method as an initial approach to the detection of abnormal situations exhibited satisfactory results. Initially, the experimental environment was created with regard to temperature behaviour and power profile of each zone of the multi-zone space model, which showed the desired behaviour. Thereafter, the mechanism of detection of unnecessary power consumption was evaluated. An infiltration gain due to an exogenous factor i.e. an open window was added to the dynamics of the system and by implementing the CUSUM sequential detection algorithm, the detection was successfully made within a reasonable time period.

- The second method of the same direction also exhibited the desired results of detection. First, the training phase was implemented where the data of the dynamics of the zones were collected over a period of 24h. Thereafter, the appropriate arrangement to input/output form was made with the logic that the temperature measurements of the neighbor zones and the outside temperature, as well as the heating power were the inputs, while the temperature of the zone was the output. Based on this arrangement the SID model identified the matrices A, B, C and D which they were communicated to the wireless nodes and the temperature prediction of the zones was made accurately. Subsequently, when a hypothetical heat leakage was added into a zone by increasing the infiltration gain, a change in the dynamics of the zone occurred. The same situation occurred (change in the dynamics) when the opposite of the heat leakage was created, by adding a hypothetical extra source with 100W power. The CUSUM algorithm was implemented at a certain time instant in both the above scenarios and the change in the mean of the prediction error was detected successfully. The method finally was evaluated with the presence of an exogenous heat noise with power in the range of [50,

100] watt uniformly distributed and with time exponentially distributed with a mean of 180 sec. The temperature deviation was again clearly showed.

The results of the methods of the second direction:

- The first method as an initial approach to the energy efficiency control aimed to control the energy waste while maintaining the thermal comfort to a satisfactory level. As mentioned above the method proposed three algorithms ("1-hop", '2-hop" and "Adaptive") that provided proactive heating to the adjacent zones or in addition to the neighbor of them, when occupancy was detected into a zone, each one with different aspect. The first two preliminary algorithms were evaluated one at a time, with four state values of the mean of the residence time (250, 500, 750, 1000 sec) of the occupants into the zones of the multi-zone model. The evaluation results were compared with the "Full-proactive" and the "Full-reactive" schemes, which were: all zones were heated when occupancy was detected to one zone of the space and only the occupied zone was heated, respectively. Reasonable and expected results came out of the above comparison. The "Adaptive" algorithm utilized the functionality of the preliminary algorithms together with the "Full-proactive' and "Full-reactive" schemes in an integrated unique mechanism with the logic to implement each one according to the mean value of the occupation time of the zones from the shortest to the longest. The "Adaptive" algorithm was the second better in energy save since the "Full-reactive" was the best. In conclusion the "Adaptive" achieved the most satisfactory energy consumption along with equally satisfactory comfort time of the zones, than the other algorithms.
- The second method for energy efficiency control aimed to balance the energy cost with the comfort cost and it was based on the SID predictive model. The method was consisted of two phases of operation: the "training phase" and the "decision phase".

The “training phase”, where all data with the dynamics of the zones were collected was applied exactly as in the second method for anomaly detection which was described in Section 6.3.2. Thereafter, the “decision phase” that was implemented by the WSN nodes was evaluated, with the application of two scenarios of the occupants' movement: a) the movement between two adjacent zones and b) the movement in cascade from zone to zone following a certain path. The occupation time for both scenarios was simulated with Gamma and Pareto distributions.

The first movement scenario was initially simulated for 200 runs, with Gamma distribution with certain values of the shape parameters *(α & β)* such that the expected value ($E[X]$) was 3600 and 7200, and also with certain value of the decision period D. The total comfort weight was taken values in the range of [0 – 10000].

The evaluation of this scenario came out with a reasonable conclusion that the higher was the value of the comfort weight C_i, the more energy was consumed with the highest energy value when $C_i = 0$ (full reactive heating).

The evaluation of the same scenario that was simulated with Pareto distributed occupation time was that, the total comfort cost for various values of the comfort gain C_i was improved for a 50% compared to the full reactive case and this was achieved for $C = 1000$ and x_m=300.

Note that the pdf of the Pareto distribution was simulated for four values of x_m ($x_m = 300, 900, 1800, 3600$) and mean occupation period of 7200. Extremely high values of occupation period were observed due to the heavy tail of the Pareto distribution and this caused an increase of the total consumed energy.

Subsequently, the second scenario of the occupants’ movement was evaluated, where the occupants were moving from zone to zone in cascade, following a certain path. The occupation time was exponentially distributed and this was the least favorable assumption for adjacent zones, due the memoryless property of the exponential distribution.

Considerable comfort gains were achieved for a moderate increase of the consumed energy, and extremely low comfort costs were observed when there was no randomness on the occupancy times implying the importance of the right modeling of it.

9.2 Future work

First action of the future work will be the validation of the proposed methods. Further to the work for detection of abnormal situations, the utilisation of sophisticated classifiers such as support vector machines (SVM) may be investigated. As supervised learning models with associated learning algorithms by recognizing patterns and analyzing data, may be utilized for classification and regression. Moreover, neural networks may also be investigated that incorporate more features of the reference signals in the decision process for the early detection of abnormal behaviour.

Several extensions and modifications of the proposed method for energy efficiency are possible. The comfort parameter C_i may depend on the zone, the number of occupants and the current status of the zones. Moreover, this parameter may be time variable, i.e. different values may be used for day and night hours. Regarding the decision process itself, there is no need to be executed at regular time epochs. If the energy consumed by the wireless sensor nodes is an issue, we may take decisions at irregular time epochs, depending on the occupancy predictions of the zones. The computation of the risks, used by the decision process, may take into consideration additional parameters that affect energy consumption and/or the thermal comfort of the occupants. For example, an open windows situation may be easily detected and incorporated suitably in the decision process. Moreover the method will be evaluated with Particle swarm optimization (PSO) stochastic technique for the best possible solution for balancing the energy and the discomfort costs.

References

[1] U.S. Energy Information administration “Annual Energy Outlook 2015”

[2] U.S. Energy Information administration http://www.eia.gov/tools/faqs/faq.cfm?id=86&t=1 (June 2015)

[3] ”Fundamentals of HVAC Systems: SI Edition”, R. McDowall, ISBN-13:978-0123739988

[4] Richard J de Dear, Gail S. Brager. Thermal comfort in naturally entilated buildings: revisions to ASHRAE Standard 55, Energy and buildings, Volume 34, Issue 6, July 2002.

[5] Aqeel H. Kazmi, Michael J. O’Grady, Declant T. Delaney, AntonioG. Ruzzelli,and Gregory M. P. O’Hare, “A Review of Wireless-Sensor-Network-Enabled Building Energy Management Systems”, ACM Transactions on Sensor Networks, Vol. 10, No. 4, Article 66, Publication date: June 2014.

[6] http://www.spluss.eu/7-radio-sensor/20-wireless-radio-sensor-transmitter/en (5/6/2015)

[7] http://www.ecolodgix-hosted.com/EcoLodgix%20Product%20Submittal%20WIRELESS.pdf (5/6/2015)

[8] https://nest.com (5/6/2015)

[9] http://www.distech-controls.com/en/us/ (5/6/2015)

[10] G Liu, J Zhang, A Dasu, “Review of Literature on Terminal Box Control, Occupancy Sensing Technology and Multi-zone Demand Control Ventilation (DCV)”, Pacific Northwest National Laboratory, March 2012

[11] Chenyan Song , Yavari, E. ; Singh, A. ; Boric-Lubecke, O., “Detection sensitivity and Power consumption vs. operation modes using system-on-chip based Doppler radar Occupancy sensor”, 15-18 Jan. 2012 , Page(s): 17 – 20, Santa Clara, CA, IEEE

[12] Tomastik, R., Lin, Y., and Banaszuk, A. (2008), “Video-based estimation of building Occupancy during emergency egress”, American Control Conference,Seattle, WA, June 11-13.

[13] S. Wang, and F. Xiao,Detection and diagnosis of AHU sensor faults using principal component analysis method Energy Conversion and Management 45, 26672686, 2004

[14] J. E. Seem, Using Intelligent Data Analysis to Detect Abnormal Energy Consumption in Buildings Energy and Buildings, 39 (2007), 52-58.

[15] C. Huang, Y. Tsao and J. Yung-jen Hsu, Abnormality Detection by Model-based Estimation of Power Consumption, Fifth IEEE International Conference on Service-Oriented Computing and Applications (SOCA), ISBN 1467347736, pp. 1 - 6, 2012.

[16] J.A. Clarke, J. Cockroft, S. Conner, J. W. Hand, N. J. Kelly, R. Moore, T. OBrien, and P. Strachan, Simulation-Assisted Control in Building Energy Management Systems. Energy and Buildings, 34(9), 933-940, 2002.

[17] D. Sklavounos, E. Zervas, O. Tsakiridis and J. Stonham, “A Wireless Sensor Network Approach for the control of a multizone HVAC system”, International Conference on Power, Energy and Control (ICPEC) 978-1-4673-6030, IEEE, 2013

[18] S. Wu and J.-Q. Sun, Multilevel Fault Detection and Diagnosis on Office Building HVAC Systems ACEEE Summer Study on Energy Efficiency in Buildings, 2010

[19] J. Weimer, S. Alizera, J. Araujo, F. Madia Mele, D. Papale, I. Shames, H. Sandberg and K. H. Johanson, Active Actuator Fault Detection and Diagnosis in HVAC Systems Buildsys12, Torondo, ON, Canada. ACM 978-1-4503-1170-0, Nov 6, 2012.

[20] J. Cigler and S. Prvara, Subspace Identification and Model Predictive Control for Buildings, 11th Int. Conf. Control, Automation, Robotics and Vision Singapore, 7-10th Dec. 2010

[21] S. Wang, Q. Zhou and F. Xiao, A system-level fault detection and diagnosis strategy for HVAC systems involving sensor faults, Energy and Buildings 42 , 477490, 2010

[22] S. Privara, Z. Vana, J. Cigler and L. Ferkl, Predictive Control Oriented Subspace Identification Based on Building Energy Simulatio Tools, 20th Mediterranean Conference on Control & Automation (MED) Barcelona, Spain, July 3-6, 2012.

[23] J. Liang and R. Du Model-based Fault Detection and Diagnosis of HVAC systems using Support Vector Machine method International Journal of Refrigeration 30, 2007.

[24] James Scott, A.J. Bernheim Brush, John Ktumm, Brian Meyers, Mike Hazas, Steve Hodges, Nicolas Villar, “PreHeat: Controlling Home Heating Using Occupancy Prediction, UbiComp’11, September 17-21, 2011, Beijing, China.

[25] Yahia Tachwali, Hazem Refai, John E. Fagan, “Minimizing HVAC Energy Consumption Using a Wireless Sensor Network”, The 33rd Annual Conference of the IEEE Industrial Electronics Society (IECON), Nov. 5-8 2007, Taipei, Taiwan.

[26] Seungwoo Lee, Yohan Chon, Yunjong Kim, Rhan Ha, and Hojung Cha, “Occupancy Prediction Algorithms for Thermostat Control Systems Using Mobile Devices” IEEE TRANSACTIONS ON SMART GRID, VOL. 4, NO. 3, SEPTEMBER 2013.

[27] Varick L. Erickson, Stefan Achleitner, Alberto E. Cerpa, “POEM: Power-efficient Occupancy-Based Energy Management System”, IPSN’13, April 8–11, 2013, Philadelphia, Pennsylvania, USA.

[28] Varick L. Erickson, Miguel Á. Carreira-Perpiñán and Alberto E.Cerpa, “OBSERVE: Occupancy- Based System for Efficient Reduction of HVAC Energy”, IPSN’11, April 12–14, 2011, Chicago, Illinois

[29] Bharathan Balaji, Jian Xuy, Anthony Nwokafory, Rajesh Guptay, Yuvraj Agarwal, “Sentinel: Occupancy Based HVAC Actuation using Existing WiFi Infrastructure within Commercial Buildings” SenSys ’13 Rome, Italy Copyright 2013 ACM 978-1-4503-2027-6/13/11

[30] Bing Dong, Khee Poh Lam, “A real-time model predictive control for building heating and Cooling systems based on the occupancy behaviour pattern detection and local weather forecasting” BUILD SIMUL (2014) 7: 89–106 DOI 10.1007/s12273-013-0142-7

[31] Justin R. Dobbs and Brandon M. Hencey, Member, IEEE, “Predictive HVAC Control Using a Markov Occupancy Model” 2014 American Control Conference (ACC) June 4-6, 2014. Portland, Oregon, USA

[32] Jonathan Brooks, Saket Kumar, Siddharth Goyal, Rahul Subramany, Prabir Barooah, "Energy-efficient control of under-actuated HVAC zones in commercial buildings", Energy and Buildings 93 (2015) 160–168

[33] B. Tashtoush, M. Melhim and M. Al-Rousan, "Dynamic Model of an HVAC System for Control Analysis", Energy, Elsecier, Journal, Vol. 30, pp. 1729-1745, 2005.

[34] A. Walter, "Notes on the Utilization of Records from Third Order Climatological Stations for Agricultural Purposes", Ag. Met. Journ, Vol. 4, pp. 137-143, 1967

[35] S. E. Page, "Continuous Inspection Schemes," Biometrika 41: 100-114, 1954.

[36] Mich`ele Basseville, Igor V. Nikiforov, "Detection of Abrupt Changes:Theory and Application", ISBN:0-13-126780-9

[37] E. Gombay and D. Serban, "An Adaptation of Page's CUSUM test for Change Detection", Period. Math Hungarica, Vol. 50, pp. 135-147, 2005

[38] Darling and Erdos, "A Limit Theorem for the Maximum of Normalized Sums of Independent Random Variables", Duke Math Journal, Vol. 23, pp. 143-145, 1956.

[39] P. Van Overschee and B. De Moor, "Subspace Identification for Linear Systems, Theory-Implementation-Applications", Kluwer Academic Publishers, 1996

[40] A. W. Shewhart, "Quality Control Charts," Bell System Technical Journal 5: 593-603, 1926

[41] H. E. Daniels, "Saddlepoint approximations in statistics, " Ann. Math. Statist. 25, pp. 631-650, 1954.

[42] R. Pyke, "Markov renewal processes with finitely many states", Ann. Math. Statist. 32, pp. 1243-1259, 1961

[43] S. J. Mason, "Feedback theory- Some properties of signal flow graphs," Proceedings of Institute of Radio Engineers, 41, pp. 1144-1156, 1953

[44] S. J. Mason, "Feedback theory- Further properties of signal flow graphs," Proceedings of Institute of Radio Engineers, 44, pp. 920-926, 1956.

[45] Dimitris Sklavounos, Evangelos Zervas, Odysseas Tsakiridis and John Stonham, "A Subspace Identification Method for Detecting Abnormal Behaviour in HVAC systems", Journal of Energy, Volume 2015, Article ID 693749, Hindawi Publishing Corporation

[46] D. Sklavounos, E. Zervas, O. Tsakiridis and J. Stonham, "Energy Control Algorithms for HVAC Systems", ENERGYCON-2014, May 13-16, 2014, Dubrovnik, Croatia (IEEE publication) 10.1109/ENERGYCON.2014.6850583

[47] Tsakiridis Odysseas, Dimitris Sklavounos, Evangelos Zervas, John Stonham, "A Comfort-Aware Energy Efficient HVAC System based on the Subspace Identification Method ", Journal of Energy, Volume 2016, Article ID 5074846, Hindawi Publishing Corporation

[48] http://www.arca53.dsl.pipex.com/index_files/hgain2.htm (5/6/2015)

[49] Joern Ploennigs, Bei Chen, Anika Schumann, Niall Brady," Exploiting Generalized Additive Models for Diagnosing Abnormal Energy Use in Buildings", Buildsys'13, November 13 - 14 2013, Roma, Italy. Copyrightc 2013 ACM 978-1-4503-2431-1/13/11

[50] Guanjing Lin, David E. Claridge, “A temperature-based approach to detect abnormal buildingenergy consumption”, Energy and Buildings 93 (2015) 110–118

[51] Jianjun HU, Panagiota KARAVA “A State-Space Modeling Approach and Subspace Identification Method for Predictive Control of Multi-Zone Buildings with Mixed-Mode Cooling”, 3rd International High Performance Buildings Conference at Purdue, July 14-17, 2014

[52] Siyu Wu, Jian-Qiao Sun, “Cross-level fault detection and diagnosis of building HVAC systems”, Building and Environment 46 (2011) 1558-1566

Appendix

Published Papers

Conference papers

[1] D. Sklavounos, E. Zervas, O. Tsakiridis and J. Stonham, "A Wireless Sensor Network Approach for the control of a multizone HVAC system", International Conference on Power, Energy and Control (ICPEC) 978-1-4673-6030, IEEE, 2013

[2] D. Sklavounos, E. Zervas, O. Tsakiridis and J. Stonham, "Energy Control Algorithms for HVAC Systems", ENERGYCON-2014, May 13-16, 2014, Dubrovnik, Croatia (IEEE publication) 10.1109/ENERGYCON.2014.6850583

Journal papers

[3] Dimitris Sklavounos, Evangelos Zervas, Odysseas Tsakiridis and John Stonham, "A Subspace Identification Method for Detecting Abnormal Behaviour in HVAC systems", Journal of Energy, Volume 2015, Article ID 693749, Hindawi Publishing Corporation

[4] Tsakiridis Odysseas, Dimitris Sklavounos, Evangelos Zervas, John Stonham, "A Comfort- Aware Energy Efficient HVAC System based on the Subspace Identification Method ", Journal of Energy, Volume 2016, Article ID 5074846, Hindawi Publishing Corporation